

Molecular Fate Determinants
in Embryonic and Adult Neural Stem Cells

DISSERTATION

ZUR ERLANGUNG DES DOKTORGRADES
DER NATURWISSENSCHAFTEN (DR.RER.NAT)
DER FAKULTÄT FÜR BIOLOGIE
DER LUDWIG-MAXIMILIANS UNIVERSITÄT MÜNCHEN

ANGEFERTIGT AM MAX-PLANCK-INSTITUT FÜR NEUROBIOLOGIE
IN DER ARBEITSGRUPPE NEURONALE SPEZIFIZIERUNG UND AN DER GSF;
INSTITUT FÜR STAMMZELLFORSCHUNG

Michael Anton Hack

eingereicht am 10. März 2005

1. Gutachter: Prof. Dr. Magdalena Götz
2. Gutachter: Prof. Dr. Benedikt Grothe
3. Gutachter: Prof. Dr. Rüdiger Klein
4. Gutachter: Prof. Dr. Rainer Uhl

Tag der mündlichen Prüfung: 29.6.1005

1 Table of content

1	TABLE OF CONTENT	3
2	ABSTRACT	7
3	ZUSAMMENFASSUNG	8
4	INTRODUCTION	9
4.1	Cell fate in the developing CNS	9
4.2	Lineage restriction in the adult CNS	10
4.3	Isolation of multipotent precursors in the neurosphere culture system	12
4.4	Isolation of functionally distinct precursor populations by FACS	13
4.5	Candidate genes	15
4.6	Tools for manipulating gene expression	16
5	ABBREVIATIONS	19
6	MATERIALS AND METHODS	23
6.1	Animals	23
6.2	Genotyping	23
6.3	In vivo injections	24
6.3.1	Anesthesia.....	24
6.3.2	Stereotaxic injections in adult mice.....	24
6.3.3	Stereotaxic injections in pups.....	25
6.3.4	In utero injections in E14 embryos.....	25
6.4	Tissue culture	26
6.4.1	Cultures of primary dissociated neural precursors.....	26
6.4.2	Neurosphere cultures.....	27
6.4.2.1	Embryonic neurospheres.....	27
6.4.2.2	Adult neurospheres.....	27
6.4.2.3	Differentiation of neurosphere cultures.....	28
6.4.2.4	Transduction of cultured cells.....	28
6.5	Tracing	28

6.6	Fluorescence-activated cell sorting analysis and cell lineage analysis	29
6.7	BrdU administration and Histology	29
6.8	Immunostaining	30
6.8.1	Immunocytochemistry	30
6.8.2	X-Gal cytochemistry	31
6.8.3	Immunohistochemistry	32
6.8.4	Tunel staining.....	32
6.9	Retroviruses.....	32
6.9.1	Retroviral vectors	32
6.9.2	Retrovirus production	33
6.10	RNA extraction and LightCycler RT-PCR analysis	34
6.11	RNAi.....	35
6.11.1	Construction of the RNAi	35
6.11.2	Labeling of the RNAi.....	36
6.12	Microarray analysis.....	36
6.13	Data analysis.....	37
6.13.1	Quantification of fluorescent cells at the confocal	37
6.13.2	Clonal analysis	37
6.14	Statistics	38
7	RESULTS	39
7.1	Selective enrichment of functionally distinct precursor (stem cells, neurogenic and gliogenic precursors)	39
7.1.1	Selective enrichment of functionally distinct precursor subsets from different regions of the embryonic CNS by means of GFP intensity in the hGFAPeGFP transgenic mouse model.....	39
7.1.2	Subdissection	41
7.1.3	Selective enrichment of functionally distinct precursor subsets from the cortex by means of GFP intensity in the hGFAPeGFP transgenic mouse model.....	42
7.1.4	Neurosphere cultures to enrich a population of multipotent precursors	44
7.2	Gene expression analysis of functionally distinct precursors (stem cell, neurogenic and gliogenic precursors)	45
7.2.1	Candidate transcription factor analysis of functionally distinct precursor subsets as a test for microarray analysis.....	45
7.2.2	Regulation of transcription factors upon growth factor exposure	47
7.2.3	Transcription factor analysis in neurosphere cultures in differentiation conditions.....	48

7.3	Microarray analysis of differential gene expression in functionally distinct precursor subtypes	49
7.4	Functional analysis of Pax6 and Olig2 for fate specification	51
7.4.1	Functional analysis of Pax6 and Olig2 in vitro	51
7.4.1.1	Functional analysis of Pax6 in neurosphere cells	51
7.4.1.2	Functional analysis of Olig2 in neurosphere cells	52
7.4.2	Functional analysis of Pax6 and Olig2 in vivo	54
7.4.2.1	Functional analysis of Olig2 in vivo during embryonic development.....	54
7.4.2.2	Functional analysis of Olig2 and Pax6 in vivo in adult neural stem cells	56
7.4.2.2.1	Expression analysis of the transcription factors Pax6 and Olig2 in adult neural stem cells and their progeny in vivo	56
7.4.2.2.2	Expression pattern of Pax6 in adult neurogenesis	56
7.4.2.2.3	Expression pattern of Olig2 in adult neurogenesis	57
7.4.2.2.4	The role of Pax6 and Olig2 in adult neural precursors	59
7.4.2.2.5	Olig2 promotes adult oligodendrogenesis	62
7.4.2.2.6	RMS precursors are further restricted towards the neuronal fate	62
7.4.2.2.7	The role of Pax6 for the specification of dopaminergic periglomerular neurons	63
7.4.2.3	Overexpression of Pax6 in non neurogenic astrocytes in vivo	65
8	DISCUSSION	68
8.1	Regional heterogeneity of radial glial cells	68
8.2	Radial glial cells from the cortex are heterogeneous	71
8.3	Changes of gene expression patterns upon EGF and FGF2 in neurosphere cultures	73
8.4	Transcriptom analysis	76
8.5	The role of Pax6 in neurogenic precursors.....	78
8.5.1	Role of Pax6 in vitro in neurosphere cultures.....	78
8.5.2	Role of Pax6 in vivo	80
8.5.2.1	Pax6 in adult neurogenesis.....	80
8.5.2.2	Neural subtype specification by Pax6.....	82
8.5.2.3	Pax6 in non neurogenic astrocytes.....	83
8.6	The role of Olig2 in multipotent precursors.....	86
8.6.1	Olig2 in vitro in neurosphere cells.....	86
8.6.2	Olig2 in vivo in adult neurogenesis	87
8.6.3	Are Olig2-positive precursors in the adult SEZ neuron-oligodendrocyte precursors (NOPs) or glial restricted precursors (GRPs)?.....	91

8.7	Patterning of the SEZ/RMS system.....	92
8.8	Cell therapy for human neurodegenerative disorders	94
9	FIGURES.....	95
10	REFERENCES.....	134
11	ACKNOWLEDGMENTS	149
12	CURRICULUM VITAE.....	150

2 ABSTRACT

The molecular signals specifying neuronal, glial or multipotent precursors in the developing and adult central nervous system (CNS) are largely unknown. Radial glial cells have recently been discovered as major precursor population generating neurons or glial cells in separate lineages in the developing CNS. Towards this aim to identify the key molecular determinants for neurogenic versus gliogenic fate in radial glial cells I used a novel method to selectively enrich neurogenic or non-neurogenic radial glia and compared their gene expression to adult subependymal zone (SEZ) precursors in vitro and in vivo. The expression profile of the transcription factors Olig2 and Pax6 were particularly intriguing. Olig2 was 67 fold higher in multipotent compared to neuronal or glial precursors, while Pax6 showed strongest expression in neuronal precursors. I therefore focused further on the functional analysis of Pax6 and Olig2 in neural stem cell in vitro and in vivo. Interference with Olig2 in neural stem cells in vitro revealed its role in self-renewal. In adult neural stem cells of the SEZ overexpression of Olig2 promoted oligodendrocyte formation. Pax6, in contrast, proved to be a very potent neurogenic determinant since neurogenesis is not only Pax6-dependent in neural stem cells in vitro, but also in adult neural stem cell in vivo.

Taken together, these results demonstrate a pathway combining transcription factors of dorsal and ventral regions that is activated in a specific lineage progression of adult neural stem cells in vitro and in vivo. Most importantly also in regard to therapeutic approaches, this work revealed the molecular mechanisms to direct adult neural stem cells towards a specific cell fate, neuronal or oligodendroglial.

3 ZUSAMMENFASSUNG

Sowohl während der Entwicklung, als auch im adulten Gehirn in jenen Regionen, in denen Neurogenese zeitlebens fortgesetzt wird, erfolgt eine hierarchische Spezifizierung von Vorläuferzellen. Multipotente Stammzellen generieren schnell proliferierende bi- oder multipotente Vorläuferzellen, die dann neurogene und gliogene Vorläuferzellen bilden. Die molekularen Mechanismen dieser Zellschicksalspezifizierung zu ergründen, war Ziel dieser Arbeit. Es gelang mir mittels Fluoreszenz-aktivierter Zellsortierung radiale Gliazellen, die auf die Bildung von Neuronen festgelegt sind, selektiv anzureichern. Deren spezifische Genexpression wurde mit jener von nicht neurogenen radialen Gliazellen verglichen. In dieser vergleichenden Expressionsanalyse war das Expressionsprofil der Transkriptionsfaktoren Olig2 und Pax6 besonders bemerkenswert. Olig2 ist in multipotenten Vorläuferzellen 67-fach höher exprimiert als in neuronalen oder glialen Vorläufern, während Pax6 43-fach in neuronalen Vorläufern angereichert war. Ich konnte Pax6 immunhistochemisch in neuronalen Vorläuferzellen der Subependymalzone (SEZ) des lateralen Ventrikels und des rostralen migratorischen Stromes (RMS) lokalisieren. Im Gegensatz dazu war Olig2 ausschliesslich in bi- oder multipotenten Vorläuferzellen *in vivo* und *in vitro* nachweisbar. Deshalb konzentrierte ich mich in meiner weiteren Arbeit auf die funktionelle Analyse von Pax6 und Olig2 in neuralen Stammzellen *in vitro* und *in vivo*. Experimente in denen die der Expression von Olig2 in neuralen Stammzellen *in vitro* behindert wurde, demonstrierten seine Rolle in Selbsterneuerung undifferenzierter Stammzellen und deren Fähigkeit, Neurone und Oligodendrozyten zu bilden. Pax6, hingegen, offenbarte sich als starker neurogener Faktor, da Pax6 notwendig und hinreichend für die Neurogenese nicht nur aus Stammzellen in Zellkultur, sondern auch aus adulten Stammzellen *in vivo* ist. In diesen Versuchen zeigte sich zudem eine völlig neue Rolle des Transkriptionsfaktors Pax6 auf die Differenzierung von dopaminergen Neuronen in der adulten Neurogenese. Meine Arbeit konnte daher die Schlüsselrolle von zwei Transkriptionsfaktoren bei der Zellschicksalsbestimmung neuraler Stammzellen aufzeigen.

INTRODUCTION

3.1 Cell fate in the developing CNS

A central question in neural development is how different precursor populations differ on a molecular level. The adult central nervous system is composed of different neuronal and glial cell types that are generated during development. Different lines of evidence show a hierarchical fate restriction as depicted in **Fig. 1**.

In most CNS regions multipotent precursors are sequentially more and more restricted during development to generate a specific cell type (**Fig. 1**). Early neuroepithelial precursors throughout the CNS are multipotent and can generate undifferentiated precursors, astrocytes, oligodendrocytes and neurons (McCarthy et al., 2000). However, during development, they do not generate these diverse cell types directly, but rather via precursors that are more restricted in their potential, i.e. generate exclusively a single cell type. This restriction occurs around the onset of neurogenesis when most progenitor cells in the cerebral cortex and striatum generate a single cell type, even though some precursors give rise to large and wide-spread clones containing multiple cell types (Grove et al., 1993; Luskin et al., 1993; Luskin et al., 1988; Price and Thurlow, 1988; Reid and Walsh, 2002; Walsh and Cepko, 1993).

This fate restriction might occur step-wise with intermediate precursors that are not anymore multipotent, but only oligo- or bi-potent (see e.g. Williams et al., 1991; Mizuguchi et al., 2001; Novitch et al., 2001; Gregori et al., 2002). Neuronal progenitors are hence restricted to the generation of neurons but still proliferate and generate further neuron-restricted progenitors. It is conceivable that this amplification phase is also accompanied by further differentiation of the precursors so they can then generate the finally differentiating cells (**Fig. 1**). In contrast, the progeny of a single precursor in the retina frequently generates neurons and glia (Turner and Cepko, 1987), suggesting that fate specification occurs differently in these regions of the CNS.

The intrinsic lineage bias of telencephalic precursors was confirmed when single cells were isolated in vitro and most of them also generated exclusively a single cell type (Qian et al., 1997), with approximately 15% of these being multipotent stem cells that generate both neurons and glia, while the remainder being restricted neuroblasts that

generate only neurons (Qian et al., 1997). Likewise, the addition of growth factors favoring either the neuronal lineage, such as the platelet derived growth factor (PDGF), or the glial lineage, such as ciliary neurotrophic factor (CNTF) can no longer affect the progeny of precursors isolated during neurogenesis from the cerebral cortex. Nevertheless these factors still can influence fate decisions of neuroepithelial cells isolated at earlier stages (Götz et al., 2002; Williams and Price, 1995; Williams et al., 1991). Similarly fate-restricted precursors have been isolated from the developing spinal cord (Kalyani et al., 1998; Mayer-Proschel et al., 1997). In these studies so-called neuronal-restricted precursor (NRP) cells have been found that express E-NCAM (high polysialic-acid NCAM) and are morphologically distinct from neuroepithelial cells (Kalyani et al., 1997) and spinal cord glial progenitors (Rao and Mayer-Proschel, 1997). Taken together, these experiments suggest a progressive fate restriction of precursors in some CNS regions during development by intrinsic fate determinants (Eklund and Jessell, 1999) whose molecular nature, however, is still largely unknown (**Fig. 1**).

3.2 Lineage restriction in the adult CNS

For a long time, it had been the dogma that most neurons are generated during the development and there is no neurogenesis in the adult mammalian brain (Rakic, 1985). However, in the non-mammalian vertebrate adult brains, such as fish, amphibians, reptiles, and birds, widespread neurogenesis had reported (for review, see Doetsch et al., 2002). For example, in the telencephalon of song birds there are hot spots of adult neurogenesis (Alvarez-Buylla and Nottebohm, 1988; Belluzzi et al., 2003). Newly generated neurons are important to learn songs for birds and actually those cells are generated from radial glia that persist throughout life in the hot spot.

In contrast to these lower vertebrate classes, there are only two neurogenic sites in the adult mammalian brain including. One is the subependymal zone (SEZ) in the lateral wall of the lateral ventricle of the brain and another is the subgranular layer (SGL) of the dentate gyrus of the hippocampus (Doetsch et al., 1999; Seri et al., 2004; Seri et al., 2001). The SEZ and SGL are responsible for the adult neurogenesis of olfactory bulb interneurons and hippocampus granule neurons respectively (**Fig. 2a**).

The adult olfactory bulb (OB) is supplied lifelong distinct types of interneurons are continuously generated throughout adulthood (Altman, 1969; Lois and Alvarez-Buylla, 1994; Luskin, 1993), the GABAergic interneurons located in the granule cell layer (GCL) and glomerular layer (GL) as well as the dopaminergic interneurons in the GL (Carleton et al., 2003; Kosaka et al., 1998; Kosaka et al., 1985). The newborn neurons originate from astroglia-like stem cells immunoreactive for the glia-fibrillary acidic protein GFAP (type B cells) lining the lateral wall of the lateral ventricle (SEZ; **Fig. 2a,b**; Doetsch et al., 1999). The adult neural stem cells divide slowly, while their progeny, the transit-amplifying precursors (type C cells; Capela and Temple, 2002; Doetsch et al., 1999; Doetsch et al., 2002), divide fast and generate neuroblasts (type A cells) that already express neuronal traits (PSA-NCAM or doublecortin) and migrate via the rostral migratory stream (RMS) towards the OB (Lois and Alvarez-Buylla, 1994; Luskin, 1993; **Fig. 2a,b**).

This proposed lineage progression seems to resemble the progressive fate restriction as present during development observed (described above). Indirect evidence suggests that the type C cells are not yet irreversibly restricted to a certain lineage since they can still give rise to several cell types upon isolation in the neurosphere culture conditions (Capela and Temple, 2002; Doetsch et al., 2002; Imura et al., 2003; Morshead et al., 2003) and they can alter their progeny in response to certain lesion paradigms in vivo (Arvidsson et al., 2002; Decker et al., 2002). In contrast, the progeny of type C cells, the type A cells, express neuronal characteristics and seem to be specified to the neuronal fate (Doetsch et al., 1999; Menezes et al., 1995).

Important progress has been made in the identification of factors regulating stem or transit-amplifying cell fate as well as asymmetric cell division (Doetsch et al., 2002; Molofsky et al., 2003; Shi et al., 2004). Dlx2 expression has been detected in transit-amplifying cells (Doetsch et al., 2002), reminiscent of transcription factors specific for the ventral telencephalon during development, but its role for fate specification has so far only been examined in the developing telencephalon (Anderson et al., 1997a; Anderson et al., 1997b). Molofsky et al. showed that Bmi-1, a polycomb family transcriptional repressor, is required for adult neural stem cells to maintain their self renewal ability mainly by repressing the expression of p16^{Ink4a} encoding a cyclin-dependent kinase

inhibitor (Molofsky et al., 2003). Polycomb family proteins are supposed to silence their target gene by binding DNA and modifying chromatin structure (Peterson et al., 1997). In addition, the transcriptional repressor, Tlx, was also shown to be crucial for adult neural stem cells (Shi et al., 2004) Tlx belongs to the nuclear orphan receptor and function as a transcription repressor (Yu et al., 2000). Shi et al. showed that in the adult Tlx deficient mice, neurosphere forming cells were greatly reduced and they differentiated into astrocyte spontaneously *in vitro*. Indeed, and also *in vivo* in the SEZ and SGL the absence of Tlx resulted in a reduction of the number of proliferating cells (Shi et al., 2004). However, little is known about the molecular determinants of this sequential fate restriction and about the mechanisms directing cell progenitors towards specific neuronal or glial subtypes in the adult brain.

3.3 Isolation of multipotent precursors in the neurosphere culture system

The identification of such intrinsic fate determinants might be important to direct precursors of the adult telencephalon towards desired phenotypes. Notably, because of their role in neurogenesis *in vivo*, the isolation of multipotent cells from the adult CNS (Kilpatrick and Bartlett, 1995; Reynolds and Weiss, 1996) has prompted great hopes for reconstitution of degenerating neurons or oligodendrocytes in neuropathological conditions. The neurosphere culture system serves as a technique to expand precursors with a bi- or multipotent fate (Reynolds et al., 1992). The neurosphere model was previously used to characterize gene expression of multipotent and self-renewing precursors in comparison to stem cells of other organs (Ivanova et al., 2002; Ramalho-Santos et al., 2002). Interestingly, a surprising similarity in gene expression was detected between cells cultured as neurospheres and undifferentiated embryonic stem cells (Ramalho-Santos et al., 2002).

This might be due to alterations of the precursors induced by the neurosphere culture system. Are the same region-specific fate determinants acting normally in the ventral telencephalon important in neurospheres from the ventral, but not the dorsal telencephalon? Is patterning information in these precursors maintained? Indeed, region-

specific differences between neurosphere cultures originating from different regions have been reported (Hitoshi et al., 2002b; Ostenfeld et al., 2002; Parmar et al., 2002), but others found significant changes in region-specific features after expansion in neurosphere cultures (Gabay et al., 2003; Santa-Olalla et al., 2003). Moreover, little is known about the differences or similarities of neurospheres derived from the adult subependymal zone to those from different embryonic regions.

However, precursors isolated from the adult telencephalon and propagated as neurospheres generate disappointingly few neurons, both in transplantation paradigms as well as in differentiating conditions *in vitro* (Fricker et al., 1999; Herrera et al., 1999; Song et al., 2002; Winkler et al., 1998). Thus, the identification of fate determinants that direct the progeny of adult precursors towards the generation of neurons or oligodendrocytes will be very valuable for reconstitutive approaches.

3.4 Isolation of functionally distinct precursor populations by FACS

To identify intrinsic fate determinants directing distinct subsets of precursors towards a specific fate, I aimed to separate functionally distinct precursor populations from the developing telencephalon. Mayer-Pröschel and colleagues (1997) succeeded to isolate a neuron-restricted precursor cell from the developing spinal cord by immunopanning with an antibody directed against the embryonic form of the neural cell adhesion molecule (E-NCAM). However, isolation of precursors by the same antigen from the developing telencephalon resulted in a mixed population of precursors with only 50-60% neuronal precursors (Blass-Kampmann et al., 1994), similar to the proportion of neurogenic cells in un-sorted cells at this stage (Götz, 1995; Heins et al., 2002; Williams et al., 1991). Another approach to isolate neuronal precursors was the use of the *Talpha1*-promoter active in neurons and their immediate precursors (Bamji and Miller, 1996; Wang et al., 1998b). However, most of the cells isolated by this promoter are already postmitotic and double labeling with a nestin-enhancer driven transgene reveals co-localization only in 1% of all cortical cells (Sawamoto et al., 2001). At this stage, about 40% of all cells in the developing cortex are neurogenic precursors (Hartfuss et al., 2001; Malatesta et al.,

2000), suggesting that only a small subpopulation of these can be isolated by this dual-promoter strategy. Finally, quintuple fluorescent activated cell sorting (FACS) analysis proved to be more efficient in selecting of neurogenic, gliogenic or immature precursors (Maric et al., 2000; Maric et al., 2003). Maric et al. used surface immunolabeling against the fibroblast growth factor receptor 1 (FGFR-1) and the epidermal growth factor receptor (EGFR) together with membrane potential and Ca^{2+} indicator dyes to characterize physiological properties emerging among precursors, neuroglial progenitors and differentiating neurons during neurogenesis of embryonic rat neocortex (Maric et al., 2000; Maric et al., 2003).

Here I focused on radial glial cells since they have been shown to constitute the majority of precursors in the ventricular zone (Hartfuss et al., 2003; Hartfuss et al., 2001; Noctor et al., 2002). Therefore these lineage data described above directly apply to radial glia, and suggest that they consist of different sublineages, some of which are specialized to generate neurons, and others to generate glial cells. Therefore, I choose the selection of radial glial cells by the green fluorescent protein (GFP) under control of the human glial-fibrillary acidic protein (hGFAP) promoter (Nolte et al., 2001; Zhuo et al., 1997) because I suspected that their fate regulation might be similar to the hGFAP-GFP-positive adult neural stem cells that also exhibit astroglial features (Doetsch et al., 1999; Seri et al., 2001). Specifically, hGFAP-GFP-positive radial glial cells isolated from the cortex at mid-neurogenesis contain three major lineages: precursors that generate only neurons, precursors that generate exclusively non-neuronal progeny (nestin- and GFAP-positive cells) and a small subset of precursors that generate neurons and glial cells (Götz et al., 2002; Heins et al., 2002; Malatesta et al., 2003; Malatesta et al., 2000). Here, I attempted to separate these functionally distinct precursors by selecting for precursors expressing different levels of the transgene.

Notably, however, radial glial cells do not only differ within a brain region, such as described above for the cerebral cortex, but also between regions of the developing CNS. This regional heterogeneity of radial glial cells is apparent at the molecular level, and translates into pronounced differences in cell fate. For example, radial glial cells of the lateral ganglionic eminence (LGE), the anlage of the striatum (Olsson et al., 1998), contain the retinol-binding protein 1 (RBP-1), which is not detectable in the medial

ganglionic eminence (MGE) or cortex (Toresson et al., 1999). Indeed, retinoid signaling seems important for the development of neurons in the striatum, but not in adjacent regions (Toresson et al., 1999). To determine whether the neurogenic lineage of radial glia observed in the cerebral cortex is an exception or the rule in the developing CNS I isolated in a second approach radial glia from different regions of the developing CNS, namely the ganglionic eminence (GE) and the spinal cord. To address this issue the progeny of radial glial cells was analyzed in vivo by Cre recombinase based fate-mapping (Malatesta et al., 2003) and in vitro by FACS. Also in this second approach I took advantage of the transgenic mouse line expressing eGFP under the control of the hGFAP promoter since I found the transgene expressed in all three regions in radial glial cells.

These different approaches allowed us to separate distinct precursor populations, the multipotent neurosphere cells and radial glial cells that are enriched for precursors that are firmly restricted to the neurogenic or the gliogenic lineage respectively (**Fig. 3**).

3.5 Candidate genes

In the developing CNS, some intrinsic fate determinants have been already identified. For example, our lab has recently characterized the transcription factor Pax6 as a potent neurogenic determinant in precursors of the dorsal telencephalon, the anlage of the cerebral cortex (Götz et al., 1998; Heins et al., 2002). The loss of Pax6 reduces the number of neurogenic radial glia cells in the cerebral cortex, resulting in a prominent reduction of neurons in a region-specific manner (Heins et al., 2002).

Similarly, members of the basic helix loop helix (bHLH) transcription factor family also play important roles in the specification of neurons and oligodendrocytes, but they also act in a tight region-specific and cell-type specific context (Bertrand et al., 2002). Yang and colleagues have recently suggested that the local influence of sonic hedgehog (Shh) induces the expression of the transcription factor Olig2 and thereby instructs precursors to generate GABAergic neurons and oligodendrocytes (Yung et al., 2002). These data are therefore further in line with the suggestion that the Olig2-positive cells in the MGE generate GABAergic neurons and oligodendrocytes. Notably, however,

Mash1 seems to be additionally required for the lineage of GABAergic neurons (Yung et al., 2002), but only very few radial glial cells in the GE contain Mash1 (Hartfuss et al., 2001; Malatesta et al., 2003). Taken together, these data would support a view that most radial glial cells of the MGE generate oligodendrocytes. Indeed, the loss of Olig2 in radial glial cells of the ventral telencephalon results in a lack of oligodendrocytes in the forebrain (Lu et al., 2002; Zhou and Anderson, 2002), the loss of Gsh2 in radial glia of the LGE leads to defects in olfactory bulb and striatal neurogenesis (Corbin et al., 2000; Toresson and Campbell, 2001; Yun et al., 2001) and the loss of Pax6 in cortical radial glia results in a reduction of cortical neurons (Heins et al., 2002). These results highlight the importance of patterning in CNS development and the close link between patterning and fate determination (Bertrand et al., 2002; Campbell and Götz, 2002; Götz et al., 1998) and raise the question about these mechanisms in neurosphere cultures.

To gain some insights into the molecular mechanisms of fate specification I first examined the expression of candidate fate determinants in neurospheres derived from different regions of the developing CNS and the adult SEZ before and after differentiation, and of the lineage restricted FACS sorted precursor populations (**Fig. 3**). These results showed a pan-regional downregulation of most transcription factors in the expansion phase of neurospheres with the exception of the Olig genes. Interestingly, a similar downregulation of most region-specific transcription factors except the Olig genes was also observed when adherent cells were exposed to the epidermal growth factor (EGF) or the fibroblast growth factor (FGF2). When neurosphere cells were exposed to differentiation conditions and in the FACS sorted neurogenic precursors, only Pax6 was upregulated.

3.6 Tools for manipulating gene expression

Therefore, I mainly concentrated on Olig2 and Pax6 and evaluated their role in loss-of-function and gain-of-function experiments in neurosphere cultures and in vivo in adult neurogenesis. The gain of function experiments were performed with retroviral vectors containing the wildtype form of the Pax6 or Olig2 resulting in a strongly enhanced

expression of the respective gene (**Fig. 4**). However, gain-of-function approaches alone are not useful to fully determine the function of a gene of interest.

To block the function of these endogenous transcription factors I used different approaches to validate the results observed with one approach. First, I used the knock down approach with small interfering RNA (siRNA) to block the transcription. These siRNA molecules are recruited by a protein complex, RNA-induced silencing complex (RISC) that recognizes and destroys complementary mRNAs, thereby preventing generation of the gene product. However, the knock down approach does only interfere with the production of new protein, but can not hinder the function of already expressed proteins.

Therefore I used second approach, and exchanged the transactivating or repressor domain of the respective transcription factor. For example, the transactivating domain of Pax6 was replaced by a repressor domain of Engrailed (Pax6-engrailed; Yamasaki et al., 2001) whereas the repressor domain of Olig2 was removed or replaced with the transactivator VP16 (Mizuguchi et al., 2001; **Fig. 4**). These recombinant proteins then interfere directly with the endogenous wildtype protein and compete with them for DNA-binding. However, the replacement of a repressing domain by an activating domain, might not result in the same phenotype as it would be observed with a true loss of function.

For that reason and to confirm the specificity of the observed results I took, lastly, advantage of the Cre-lox system (Dymecki and Tomasiewicz, 1998; Zinyk et al., 1998). By using mice in which an exon of the gene to be analyzed was replaced by a modified exon flanked by two *lox* sequences, the endogenous transcription factors could then be eliminated from cells by recombination performed by the Cre recombinase. By transducing few cells retroviral vectors the consequences of the inactivation of the target gene could be observed. Importantly, the combination of these distinct approaches makes me confident about the results obtained.

The results of this PhD work have been published in part:

Hack, M. A., Saghatelian, A., de Chevigny, A., Lledo, P. M., Götz, M. (2005). Neuronal fate determinants of adult olfactory bulb neurogenesis. (*under revision Nat Neurosci*)

Koutmani, Y., Hurel, C., Patsavoudi, E., **Hack, M.**, Götz, M., Thomaidou, D. and Matsas, R. (2004). BM88 is an early marker of proliferating precursor cells that will differentiate into the neuronal lineage. *Eur J Neurosci* **20**, 2509-23.

Hack, M. A., Sugimori, M., Lundberg, C., Nakafuku, M. and Götz, M. (2004). Regionalization and fate specification in neurospheres: the role of Olig2 and Pax6. *Mol Cell Neurosci* **25**, 664-78.

Hartfuss, E., Forster, E., Bock, H. H., **Hack, M. A.**, LePrince, P., Luque, J. M., Herz, J., Frotscher, M. and Götz, M. (2003). Reelin signaling directly affects radial glia morphology and biochemical maturation. *Development* **130**, 4597-609.

Malatesta, P., **Hack, M. A.**, Hartfuss, E., Kettenmann, H., Klinkert, W., Kirchhoff, F. and Götz, M. (2003). Neuronal or glial progeny: regional differences in radial glia fate. *Neuron* **37**, 751-64.

Heins, N., Malatesta, P., Cecconi, F., Nakafuku, M., Tucker, K. L., **Hack, M. A.**, Chapouton, P., Barde, Y. A. and Götz, M. (2002). Glial cells generate neurons: the role of the transcription factor Pax6. *Nat Neurosci* **5**, 308-15.

4 Abbreviations

AB	Antibody
Ara-C	β -D-arabinofuranoside
bFGF	Basic fibroblast growth factor
bHLH	Basic helix-loop-helix
BLBP	Brain lipid binding protein
BMP	Bone morphogenic protein
bp	Base pairs
BLBP	Brain lipid-binding protein
BrdU	5-bromo-2'deoxy-uridine
cDNA	Complementary DNA
CDS	Coding sequence
CNS	Central nervous system
CNTF	Ciliary neurotrophic factor
CP	Cortical plate
Ctx	Cortex
DAPI	4'-6-Diamidino-2-phenylindole
DCX	Doublecortin
dd1	Differentiated for 1 day
dd3	Differentiated for 3 days
DIV	Days in vitro
DNA	Desoxyribonucleic acid
DNase	Desoxyribonuclease
dNTP	Deoxynucleotides
dsRNA	Double-stranded RNA
E	Embryonic day
ECM	Extracellular matrix
EGF	Epidermal growth factor

EGFR	Epidermal growth factor receptor
eGFP	Enhanced green fluorescent protein
eng	Engrailed repressor domain
ES cells	Embryonic stem cells
EtOH	Ethanol
FACS	Fluorescent activated cell sorting
FCS	Fetal calf serum
FGF	Fibroblast growth factor
FGFR	Fibroblast growth factor receptor
Fig	Figure
GABA	Gamma-aminobutyric acid
GAPDH	Glyceraldehyde-3-phosphate dehydrogenase
GCL	Granule cell layer
GE	Ganglionic eminence
GFAP	Glial fibrillary acidic protein
GFP	Green fluorescent protein
GL	Glomerular layer
GLAST	Glutamate astrocyte-specific transporter
GN	Granule neuron
GRP	Glial restricted precursor
GS	Glutamin synthase
HC	Hippocampus
hGFAP	Human Glial fibrillary acidic protein
HPRT	Hypoxanthine guanine phosphoribosyl transferase
HRP	Horse radish peroxidase
Ig	Immunoglobulin
IRES	Internal ribosome entry site
IZ	Intermediate zone
LGE	Lateral ganglionic eminence
LI	Labelling index

LTR	Long terminal repeat
LV	Lateral ventricle
mAB	Monoclonal antibody
MGE	Medial ganglionic eminence
MI	Maximum intensity
M-phase	Mitosis phase of the cell cycle
mRNA	Messenger ribonucleic acid
n	Sample number
Ngn	Neurogenin
NGS	Normal goat serum
NOP	Neuron-oligodendrocyte precursor
NRP	Neuron restricted precursor
NS	neurospheres
OB	Olfactory bulb
P	Postnatal day
pAB	Polyclonal antibody
Pax6eng	Pax6 full length cDNA fused to the repressor domain of engrailed
PBS	Phosphate buffered saline
PCR	Polymerase chain reaction
PDL	Poly-D-lysine
PDGF	Platelet derived growth factor
PDGFR	Platelet derived growth factor receptor
PFA	Paraformaldehyde
PGN	Periglomerular neuron
PSANCAM	Polysialylated neural cell adhesion molecule
RA	Retinoic Acid
RBP-1	Retinol-binding protein 1
RC2	Radial cell 2
RMS	Rostral migratory stream

RNA	Ribonucleic acid
RNase	Ribonuclease
RNAi	Inhibitory RNA
rpm	Rounds per minute
RT	Room temperature
RT-PCR	Realtime- polymerase chain reaction
SEM	Standard error of the mean
Sey	Small eye mutant
SEZ	Subependymal zone
Shh	Sonic Hedghog
siRNA	Short inhibitory RNA
STDEV	Standard deviation
SVZ	Subventricular zone
TH	Tyrosine hydroxylase
TSA	Tyramid signal amplification
U	Uridine
ud	undifferentiated
UTR	Untranslated region
VZ	Ventricular zone
WT	Wildtype

5 MATERIALS AND METHODS

5.1 Animals

The experiments of this work were performed with time-mated Wistar rats, C57/Bl6 and FVB/N mice, the Pax6-mutant allele Small-eye (Sey/Sey; Heins et al., 2002; Hill et al., 1991) and the hGFAP-eGFP transgenic mouse line (background FVB/N; Malatesta et al., 2003; Nolte et al., 2001). Embryos were collected from time-mated mice or rats (mice: day of plug=E0; rats: day of sperm detection=E1).

The Pax6 mutant mouse carries the Sey allele on a C56BL6/6J x DBA/2J background. This naturally occurring point mutation leads to non-functional truncated proteins (Haubst et al., 2004; Hill et al., 1991). Heterozygous Sey mice were recognized by their eye-phenotype and were crossed to obtain homozygous and WT mice in a litter. WT and Sey/Sey mice were mainly used in the experiments. Sey/Sey embryos were recognized by the lack of eyes. Heterozygous (Sey/+) mice were recognized by their reduced eye size (Hill et al., 1991). The hGFAPeGFP mouse embryos were identified by visualization of green fluorescence at the fluorescent stereo microscope. The Pax6^{flox/flox} mouse line contained two loxP sites in the region encoding the amino terminus of Pax6, including the initiator methionine and most of the paired domain (Ashery-Padan et al., 2000). These mice were kept in a homozygous colony.

5.2 Genotyping

For maintenance of the colony hGFAPeGFP mice were genotyped by PCR on tail DNA. DNA was obtained following the protocol from Laird et al. (Laird et al., 1991): Tail biopsies of less than 5mm length were transferred in 0.5ml lysis buffer and incubated rotating for several hours or overnight at 55°C in a modified hybridization oven. Following complete lysis, hairs and tissue residues were removed by centrifugation in an Eppendorf centrifuge at maximal speed (13.1 x 103g~ 16.000 rpm) for 10-20 minutes. The supernatant was poured into 0.5ml isopropanol and mixed well. DNA-precipitates

were transferred in 300-500µl TE-buffer. To solve the DNA, tubes were again rotated at 55°C for several hours.

The PCR protocol for genotyping of the hGFAP-GFP(94-4) and the hGFAP-eGFP mouse line was adapted from previous publications (Nolte et al., 2001; Zhuo et al., 1997). PCR was carried out using about 40ng of genomic DNA (~1µl) and 0.4µM of the primers GFAP-LZ: 5'-ACTCCTTCATAAAgCCCTCg-3' and GFP-2 5'-AAgTCgATgCCCTTCAgCTC-3'. in a 30µl reaction volume containing 0.2mM dNTPs, 1.5 U of Taq-DNA-polymerase, 3µl 10xPCR-buffer and 3µl 5xQ-solution. Cycling conditions were: 4 minutes at 94°C, followed by 30 cycles at 94°C for 30 seconds, at 61.5°C for 30 seconds and at 72°C for 1 minute. Finally, amplicons were extended at 72°C for 5 minutes. 15µl of each PCR-product was analyzed on a 1 % agarose-TBE-gel. The amplicon obtained from transgenic animals is 498bp long.

5.3 In vivo injections

5.3.1 Anesthesia

For the in utero injections mice were anesthetized by intraperitoneal injection of Medetomidine (Domitor, 0.5 mg per kg body weight), Midazolam (Dormicum, 5 mg per kg body weight), and Fentanyl (Fentanyl Hexal, 0.05 mg per kg body weight). The anesthesia was antagonized by intraperitoneal injection of Atipamezol (Antisedan, 5 mg per kg body weight), Flumacenil (Anexate, 0.5 mg per kg body weight) and Naloxon (Narcanti-vet, 1.2 mg per kg body weight) were used.

For the adult injections animals were anesthetized by intraperitoneal injection of ketamin (Ketaminhydrochlorid, 100mg per kg of body weight) and rompun (Xylazinhydrochlorid, 0.6mg per kg of body weight).

5.3.2 Stereotaxic injections in adult mice.

Injections of retroviral particles were done stereotactically on 9-10 weeks old male mice (C57BL/6J) as described (Carleton et al., 2003). Briefly, the adult mice were fixed in a

stereotactic apparatus (Kopf). The head was shaved and a 1 cm midline cut was performed. The skull was opened at the anterior-posterior and medio-lateral coordinates (see below) using a drill (Multipro395PR, Dremel). About 500 nl of virus were injected at both sites of each hemisphere by means of a glass micropipette prepared as described above. An oil microinjector (Narashige) was used to inject the solution with viral particles very slowly (100 nl/ min). I used the following coordinates for virus injections (relative to bregma): for the subependymal zone (SEZ), anterior-posterior = 0.75; medio-lateral = 1.2; dorso-ventral = 1.7 and anterior-posterior = 1.0; medio-lateral = 1.0; dorso-ventral = 1.9 and for the rostral migratory stream (RMS), anterior-posterior = 3.3; medio-lateral = 0.82; dorso-ventral = 2.9.

5.3.3 Stereotaxic injections in pups

For injections into the cortex of 8-11 day old male mice (CD-1) I used the following coordinates: anterior-posterior = 1; medio-lateral = 1; dorso-ventral = 0.7. The injections were performed as described above (Stereotaxic injections in adult mice.). After injection, animals were returned to their mother and monitored every 10 min until they resumed nursing.

5.3.4 In utero injections in E14 embryos

Timed pregnant CD1 mice (Charles River) with embryos at a gestational age of embryonic day 14 (E14) were used for these experiments. Injection needles were made from glass micropipettes pulled to produce a long taper and broken under a dissection microscope at an inner diameter of 10–20 μm . The glass microcapillaries were sharpened with sharpener (Model EG44, Narishige) to produce a bevel angle between 25° and 35° as described previously (Olsson et al., 1995). The abdomen was wet shaved and a 2 cm midline laparotomy was performed. Each uterine horn was carefully taken out individually and kept wet with sterile saline. Embryos located on both sides were injected by positioning the uterine horns on a swan neck lamp to illuminate the uterus and to visualize the embryo. After positive identification of the forebrain the glass microcapillary was inserted in the uterine wall, and 500 nl–1 μl of virus solution was

injected into each site. The successful injection of the virus solution in the ventricles could be verified by the darkening of the ventricles by Fast Green (0.1%, Sigma) which was added to the virus suspension. Between four and ten embryos were injected in every pregnant mouse, and surgery was limited to half an hour for each to optimize survival. After injections, the uterine horn was washed again with sterile saline, placed back into the abdomen and the skin was sutured. The injected pups were sacrificed 2 or 21 days after birth.

5.4 Tissue culture

5.4.1 Cultures of primary dissociated neural precursors

Embryos (E12– E14) were removed by caesarean section from time-pregnant mice anesthetized by an overdose of diethylether (Sigma). The meninges were removed, the telencephalic hemispheres separated, the hippocampi and the olfactory bulbi removed. The cortex and the ganglionic eminence (GE) were dissected and collected in separate tubes under sterile conditions in HBSS (GIBCO) containing 10 mM HEPES (GIBCO) on ice (Götz et al., 1998). The tissue was then allowed to settle, and the balanced salt solution was removed and replaced by trypsin-EDTA (0.05 % [w/v] in HBSS (without Ca²⁺, Mg²⁺ with 0.02 [w/v] EDTA (GIBCO)) and incubated for 15 min at 37°C. The enzyme activity was stopped by the addition of twice the volume of Dulbecco's modified eagle medium (DMEM; GIBCO) supplemented with 10 % fetal calf serum (FCS; Sigma) and penicillin/streptomycin (100 units/ml penicillin, 100 units/ml streptomycin (GIBCO)). The tissues were mechanically dissociated with a fire-polished Pasteur pipette coated with serum, twice pelleted for 5 min at 172 x g and resuspended in FCS containing medium. Cells were plated at 10⁶ cells/ml in DMEM/FCS (0.5ml/well) in a 24-well plate on poly-D-lysine (PDL) coated coverslips and incubated at 37°C and 5 % CO₂. Acutely dissociated cells were fixed after 2 hours with 4% PFA for 15 minutes. Long-term cell cultures were maintained in SATO-medium (DMEM, 1g/l Glucose, 2mM Glutamine, 10µg/ml Insulin (bovine), 100µg/ml Transferrin (human), 0.0286% BSA-pathocyte, 0.2µM Progesterone, 0.1mM Putrescine, 0.45µM Thyroxine, 0.224µM Selenite, 0.5µM

Tri-iodo-thyronine), which was changed every second day and then fixed after 5-7 days in vitro (DIV) with 4% PFA for 15 minutes. After three washes with PBS at room temperature (RT), cells were processed for immunocytochemistry. In some experiments cells from E14 mouse cortex were plated without sorting and cultured for 2 days with or without 20 ng/ml fibroblast growth factor-2 (FGF2, human recombinant; Sigma) and/or 20ng/ml epidermal growth factor (EGF, human recombinant; Sigma).

For some experiments I established a method to separate ventricular from subventricular zone cells. Slices were cut at 300 μm thickness using a McIlwain tissue chopper from mouse E14 telencephalon, and the respective regions were then dissected in each slice as depicted in **Figure 8b**.

5.4.2 Neurosphere cultures

5.4.2.1 Embryonic neurospheres

Embryonic neurosphere cultures were prepared from the cortex or ganglionic eminence (GE) of C57/Bl6 mice or Sey/Sey and wildtype littermates at E14 as described above with the exception that these cells were dissociated mechanically without enzymatic digestion, then pelleted and cultured after dissociation at clonal density (10 cells/ μl) in a T75 flask in 15 ml serum-free DMEM/Nut.Mix.F-12 medium (GIBCO) containing B-27 supplement (concentration 1:50 in F-12 medium; GIBCO), additional 3.5mM glucose, 20ng/ml EGF and FGF2. Cells were passaged once a week by centrifugation at 172g for 10 min, followed by mechanical redissociation and replating in 50% neurosphere-conditioned medium and 50% fresh medium. Cells were frozen for RNA extraction and fixed for immunostaining 7 days after passage 4. This ensures that contaminating aggregates of cells that are not neurospheres are removed efficiently from the culture

5.4.2.2 Adult neurospheres

Adult neurospheres were obtained from the lateral wall of the lateral ventricle of adult (about 10 week old) mice. The SEZ was prepared after sagittal sectioning of the brain. The SEZ was cut in pieces and these pieces were incubated in a dissociation solution

containing 0.7 mg/ml hyaluronic acid, 0.2 mg/ml kynurenic acid, and 1.33 mg/ml trypsin in HBSS with 2 mM glucose at 37°C for 30 min and gently triturated. The cells were centrifuged at 200 g for 5 min, resuspended in 0.9 M sucrose in 0.5× HBSS, and centrifuged for 10 min at 750 g. The cell pellet was resuspended in 2 ml of culture medium, placed on top of 10 ml 4% BSA in EBSS solution, and centrifuged at 200 g for 7 min, followed by washing in DMEM/F12. The culture conditions were identical to those described above for neurospheres from embryonic brains.

5.4.2.3 Differentiation of neurosphere cultures

For differentiation of cells from adult and embryonic neurospheres, spheres were spun down 7 days after the fourth passage, trypsinized at 37°C for 3 min and dissociated. Dissociated cells were plated on PDL-coated glass coverslips at a density of 2×10^5 cells/ml and cultured for 1 day in the medium described above followed by 7 days in the same medium without growth factors.

5.4.2.4 Transduction of cultured cells

Cultured cells were infected with retroviral vectors 2h after plating or transfected 24h after plating using 50nM of RNAi constructs and the Effectene Transfection Reagent (Qiagen). Then the cells were cultured as described above for 2-7 days.

5.5 Tracing

For the labelling of precursors with radial morphology from the pial surface, the meninges were removed from telencephali (Voigt 1998, Goetz 1998) and placed into a solution of green fluorescent beads (Lumafluor 50 nm; ventral side down for GE labeling, see **Figure 8a** and (Malatesta et al., 2000)). Briefly, the green fluorescent beads were diluted 1:1 in Hanks-balanced salt solution (HBSS, Gibco) and 5µl of this solution were used per brain. Brains were incubated for 10 minutes, transferred to fresh HBSS and incubated for further 15 min before dissection to allow sufficient time for transport of the fluorescent beads, as demonstrated previously (Malatesta et al., 2000).

5.6 Fluorescence-activated cell sorting (FACS) analysis and cell lineage analysis

Cortex (Ctx), ganglionic eminence (GE) and spinal cord (SC) were dissected from hGFAP-EGFP mice (Nolte et al., 2001) at embryonic day (E) 12 (SC) and 14 (Ctx, GE). Fluorescent cells were isolated using a FACSort or FACSVantage (Becton Dickinson). By reanalysis a purity of 95% was confirmed. A negative control of non-fluorescent cells was used to determine the background fluorescence such that less than 1% of non-fluorescent cells were included in the sort gate. Sorted cells were plated on PDL coated coverslips, in presence of a feeder layer derived either from the same or from different CNS region of rat embryos at the same developmental stage.(Malatesta et al., 2003; Malatesta et al., 2000). To analyze the composition of the cells, they were fixed as soon as they were adherent (2h).

For cell lineage analysis, not more than 50 sorted cells were plated per coverslip to minimize the likelihood of clonal superimposition (see Williams et al., 1991) and cultured for 6-7 days in chemically defined medium (SATO) as described above (see also Götz et al., 1998; Williams and Price, 1995). To detect dividing cells, 5-bromo-2'-deoxyuridine (BrdU; Sigma) was added to the culture medium at a final concentration of 10 μ M.

5.7 BrdU administration and Histology

For some experiments two to three months old FVB/N, C57/Bl6 or hGFAPeGFP mice were injected intraperitoneally with a DNA synthesis marker, 5-bromo-2'-deoxyuridine (BrdU; 50 mg/kg of body weight, dissolved in 0.9% NaCl with 0.4 N NaOH). After different survival times following a single BrdU pulse, the mice were anesthetized with 3% chloralhydrat and perfused with 4% paraformaldehyde (PFA) in 0.1M phosphate-buffered saline, pH 7.5, (PBS). After overnight post-fixation at 4°C in the same fixative, the tissue was incubated for 24hr in 30% sucrose in PBS and embedded in Tissue Tek

and stored at -20°C. Cryosections (15-20 µm thick) were cut sagittally and collected on Superfrost glass slides (Fischer Scientific) and processed for immunohistochemistry.

5.8 Immunostaining

5.8.1 Immunocytochemistry

As primary antibodies I used anti-BrdU (Bio-Science, mouse IgG1), 1:10; anti-CC1 (Oncogene, IgG2b), 1:200; anti-DCX (Chemicon, guinea pig), 1:2000; anti-Dlx (Hevner et al., 2003; rabbit) 1:75; anti-Emx1 (Briata et al., 1996; rabbit) 1:1000; anti-β-galactosidase (IgG2b), 1:500; anti-GFAP (Sigma, mouse IgG1), 1:200; anti-GFP (Clontech, rabbit), 1:1000; anti glutamine synthase (Becton Dickinson, IgG2a), 1:500; anti-Gsh2 (Toresson et al., 2000; rabbit) 1:1000; anti-LewisX (Becton Dickinson, mouse IgM), 1:10; M2 and M6 (rat),1:200; anti-Mash1 (provided by D. Anderson; Lo et al., 1998; IgG1) 1:2; anti-NeuN (Chemicon, IgG1), 1:50; anti-NG2 (Chemicon, rabbit), 1:300; anti-nestin (Dev. Hybridoma Bank, mouse IgG1) 1:4; O4 (J. Price, mouse IgM), 1:100; anti-Olig2 (Takebayashi et al., 2000; rabbit) 1:400; anti-Pax6 (BABCO, rabbit) 1:500; anti-PSA-NCAM (kindly provided by P. Durbec, IgM) 1:500; RC2 (P. Leprince, mouse IgM) 1:500; anti-S100β (Sigma, IgG1), 1:1000; anti-Sox10 (kindly provided by M. Wegener, guinea pig), 1:1000; anti-β-III-tubulin (Sigma, mouse IgG2b), 1:100; anti-TH (Pel-Freez, rabbit), 1:500. Usually the antibody mix was applied and incubated overnight at 4°C in a humid chamber, but for some antibodies special pretreatments were necessary.

For BrdU immunostaining the sections and cell cultures were pretreated with 0.2 % Triton X-100 for 2 hrs, and DNA was denatured with 2N HCl for 30 min at 37°C followed by two washing steps of 15 min with 0.1M Sodium-tetra-borat (pH 8.5). Overnight incubation with the anti-BrdU antibody at 4°C was followed by 2 hrs of incubation at room temperature with the secondary antibody.

Intermediate filament stainings like anti-nestin-, anti-β-tubulin-III- and anti-GFAP-staining required a special pre-treatment for better visualization of intermediate filaments before application of the primary antibodies. Therefore, cells were incubated in EtOH-

glacial acetic acid for 15 minutes at -20°C followed by three washes in PBS for 10 minutes at. Acutely dissociated cells and long term cell cultures were incubated in the primary antibody at the appropriate dilution. After several washes in PBS cells were incubated in the secondary antibody for 45 minutes at room temperature.

The primary antibodies were then detected by subclass specific secondary antibodies coupled to FITC- or TRITC at a dilution of 1:50, or Cy2- or Cy3-coupled antisera at 1:100. For triple-stainings, I used biotinylated secondary antibodies (dilution 1:50) followed by incubation in Streptavidin-AMCA at a 1:50 dilution. After three further washes, the glass coverslips were mounted in Aqua Poly/Mount, a glycerol-based mounting medium. To rule out any unspecific binding of the secondary antisera, control experiments were performed by either leaving out the primary antibody or by using a primary antibody against an antigen that is not present in the respective tissue or at the respective developmental stage. The following secondary antibodies were used: anti-rabbit Ig FITC / TRIC / biotinylated, anti-rabbit Ig Cy2 / Cy3, Streptavidin AMCA (Boehringer Ingelheim, Vector Laboratories), anti-mouse IgG+M Cy3, anti-mouse IgG1 FITC / TRIC / biotinylated, anti-mouse IgG2b FITC / TRIC / biotinylated, anti-mouse IgM FITC / TRIC / biotinylated (EuroPath Ltd., Southern Biotechnology Associates), anti-guinea pig Ig Cy2 / Cy3, anti-rat FITC / TRIC Dianova Immundiagnosics, Jackson ImmunoResearch).

5.8.2 X-Gal cytochemistry

For X-Gal cytochemistry dissociated cell cultures were fixed for 15 min at RT or 30 min at 4°C . The fixative contained 0.5 % Glutaraldehyde, 2 mM MgCl_2 and 1.25 mM EGTA. The cells were washed twice in PBS and incubated for 1 hour at 37°C in X-Gal staining solution, containing 4 mM $\text{K}_3\text{Fe}(\text{CN})_6$, 4 mM $\text{K}_4\text{Fe}(\text{CN})_6$, 1 mM MgCl_2 , 0.01 % sodium desoxycholate and 0.02 % NP-40. The X-Gal (5-Bromo-4-chloro-3-indolyl- β -D-galactopyranoside) was added to a final concentration of 0.04 mg/ml in PBS.

5.8.3 Immunohistochemistry

Cryostat sections were incubated free floating in primary antibody always containing 0.5% Triton X-100 and 10% normal goat serum (NGS) overnight at 4°C. Special pre-treatment as for anti-nestin, anti- β -tubulin-III or anti-GFAP was omitted for better preservation of the slices. Some stainings were enhanced using the tyramide amplification kit (Perkin Elmer) as described in the tyramide signal amplification (TSA) handbook (Perkin Elmer). Briefly, the TSA system uses horse radish peroxidase coupled to a secondary antibody to catalyze the deposition of fluorescein labeled tyramide amplification reagent onto tissue sections that have been previously blocked with proteins (e.g. NGS). This reaction results in the deposition of numerous fluorescein labels immediately adjacent to the immobilized HRP enzyme. Since this techniques result in a significant enhancement of the signal, it was used for antibodies with low affinity. Sections were then counter-stained with 4'-6-Diamidino-2-phenylindole (DAPI) and stainings were analyzed at a confocal microscope with 10x or 40x objectives (Leica).

5.8.4 Tunel staining

Tunel staining was carried out using the cell death kit (Roche) following manufacturer's instructions. Briefly, sections were incubated for two min in 0.1% Triton X-100, 0.1% sodium citrate on ice. The slides were incubated with the Tunel reaction mixture (Roche) containing the fluorescein labeled nucleotides binding to double stranded low molecular weight DNA fragments occurring during apoptosis for 60 min at 37°C. The samples were directly analyzed by fluorescence microscopy. Apoptotic TUNEL-positive cells were detected in the green (515-565nm) wavelength spectrum.

5.9 Retroviruses

5.9.1 Retroviral vectors (Fig. 4)

A 1873-bp fragment containing the entire coding sequence of Pax6 was inserted in the sense orientation into the BglII unique restriction site of the retroviral vector 1704 (gift of

J.E. Majors), between the upstream LTR and the IRES sequence followed by the lacZ gene (Ghattas et al., 1991; Heins et al., 2002). For co-expression with eGFP a 2050 bp fragment containing the entire coding region of Pax6 and parts of 5'UTR and 3'UTR was inserted in the sense orientation into the EcoRI unique restriction site of the retroviral vector pMXIG (Nosaka et al., 1999) between the upstream LTR and the IRES sequence. Similarly, the Pax6-EnR fusion construct described in (Yamasaki et al., 2001) was subcloned from pMES (consists of the chimeric CMV enhancer/ β -actin promoter and the Pax6-enR construct, followed by an internal ribosome entry site (IRES) and the EGFP coding sequences) and inserted in sense orientation into the EcoRI unique restriction site of the retroviral vector pMXIG (Nosaka et al., 1999) between the upstream LTR and the IRES sequence. The entire coding sequence of Olig2 and a fusion construct of the entire coding sequence of Olig2 with a 675-bp fragment encoding for VP16 were inserted into the same site (Olig2-virus, Olig2VP16 virus). BAG (Price, 1987) or the CMMP (the transgene in the plasmid described by Klein et al (Klein et al., 2000) was replaced by eGFP to generate a control virus to express GFP under control of LTR) virus were used as controls.

5.9.2 Retrovirus production with the 293gpg retrovirus producing cell line

Gpg cells (Ory et al., 1996) were cultured in DMEM (Gibco) containing 10% (v/v) FCS (heat inactivated 30 min. at 56°C; Gibco), 1% (v/v) Penicillin-Streptomycin in DMEM (Gibco), 1 μ g/ml tetracycline (Sigma), 2 μ g/ml puromycin (Sigma) and 0.3 mg/ml G418 (Gibco). Cells were passaged 1/week with PBS and trypsin containing 1ug/ml tetracycline. These cells allow for the production of high titer amphotropic retrovirus. Many retrovirus packaging cell lines lose packaging efficiency as they are cultured due to the gradual loss of expression of the packaging genes. The packaging plasmids introduced into this cell line were introduced using different selection markers (gentamycin (G418), puromycin). Therefore, expression of packaging proteins can be fairly well maintained by culturing the cells continuously in media containing the corresponding antibiotics. In addition, the vesicular stomatitis virus G (VSV-G) protein is toxic to gpg293 cells so expression of this gene is controlled by tetracycline. Therefore,

these cells are maintained in tetracycline, puromycin, and G418 containing medium (described above). Retroviral vectors pseudotyped with VSV-G differ from standard murine retroviruses by their very broad tropism and the capacity to be concentrated by ultracentrifugation without loss of activity (Galipeau et al., 1999).

Gpg helper-free packaging cells were used for viral production (Pear et al., 1993; Yee et al., 1994). For retrovirus production 90-95% confluent gpg cells were transfected using Lipofectamine 2000 (Invitrogen) and Opti-MEM I reduced-Serum Medium (Invitrogen) as described in the Lipofectamin 2000 transfection protocol for adherent cells (Invitrogen). Transfection medium was replaced after 8-10 hours, and gpg cells were further cultured in DMEM containing 10% (v/v) FCS (heat inactivated 30 min. at 56°C; Gibco), 1% (v/v) Penicillin-Streptomycin in DMEM (Gibco). After 48h the virus-containing-medium was combined and filtered through a 0.4 um filter (Becton Dickinson) and centrifuged at 50000 x g for 90 minutes at 4°C. The virus pellet was resuspended in TNE (50mM Tris-HCl (pH7.8), 130MM NaCl, 1mM EDTA) and aliquoted. Virus aliquots were stored at -80°C. Virus titres (viral particals/ml) were measured by transduction of primary cell cultures in a serial dilution. Cells were cultured for 2 days to allow expression of the transgene and then number of infected clones was counted (see below). The number of infected clones corresponds to the viral particals used for transduction of the primary cells. Viral titers typically were about 10⁷ viral particals/ml. Reliable coexpression of GFP and Olig2 or Pax6 was observed 3, 7 and 21 days after viral transduction with exception of neurons in the OB that had downregulated Olig2 14 days after transduction.

5.10 RNA extraction and LightCycler RT-PCR analysis

Total RNA was extracted using RNeasy kits (Qiagen), treated with DNase I and quantified by optical density. 1µg of total RNA was used to synthesize cDNA with oligo(dT)₁₂₋₁₈ primers and MoMLV reverse transcriptase (Superscript II; Roche). As negative controls, the reverse transcriptase was omitted at the cDNA synthesis step. RT-PCR was performed with a LightCycler instrument (Roche) with 2µl of cDNA (40ng) and the primers listed in **Table 1**. The protocol consists of two programs: amplification of

cDNA and melting curve analysis for product identification and the LightCycler analysis software was used for quantitative analysis consisting of the specificity control of the amplification reaction using the melting curve program, followed by use of the quantification program. The SYBR Green I signal (included in the PCR reaction) of each sample is plotted versus the number of cycles and the background fluorescence is removed by setting a noise band. This fluorescence threshold is used to determine cycle numbers that correlate inversely with the log of the initial template concentration. The crossing points (CP) are the intersections between the best fit lines of the log-linear region and the noise band and correlate inversely with the log of the initial template concentration (LightCycler Operator's Manual, Version 3.3, April 2000, Roche). The CP determined for the candidate mRNA were normalized to those of GAPDH to compensate for variability in RNA amount and for exclusion of general transcriptional effects. I calculated fold reduction (FR): $FR = 2^{(CP1-CP2)}$ with CP1 as the CP of GAPDH; CP2 as the CP of the gene of interest. The mRNA levels of GAPDH in each tissue sample were set to 1. To test whether the expression of GAPDH remains constant, I quantified the expression levels of hypoxanthine phosphoribosyltransferase (HPRT). The differences in gene expression between these two genes remained similar in all of the examined mRNA samples from different cell types at different developmental stages.

5.11RNAi

5.11.1 Construction of the RNAi

The Olig2RNAi constructs including the scrambled controls were designed as described on Ambion webpage (see also **Fig. 5a,b**). Briefly, 29-mer-DNA-oligonucleotides (siRNA oligonucleotide templates) with 21 nucleotides encoding the siRNA and 8 nucleotides complementary to the T7 promotor sequence were designed and ordered at TibMolBiol (Berlin). The siRNA templates were hybridized to a T7 Promotor primer and the 3' ends of the hybridized oligonucleotides were extended by the Klenow fragment (Ambion). The sense and the antisense siRNA templates were then transcribed by T7 RNA polymerase (Ambion) and the resulting RNA transcripts are hybridized to create dsRNA. The dsRNA

consists of 5'terminal single-stranded leader sequences, a 19 nucleotide target specific dsRNA and 3'terminal UUs. The leader sequence is removed by digesting the dsRNA with a single-strand specific ribonuclease. Overhanging UU dinucleotide will remain because the RNase does not cleave U residues. The DNA template is removed at the same time by a deoxyribonuclease. The resulting siRNA is purified by glass fiber binding and elution which removes excess nucleotides, short oligomers, proteins, and salts in the reaction. The following primers were used for Olig2RNAi synthesis: Olig2RNAi#19: 5'-AATGCGGCTGCCGACGGTGACCCTGTCTC-3', scrambled Olig2RNAi: 5'-AAGATAACGACGAAGTACGAACCTGTCTC -3'. The 21-nucleotide-long target sequence for Olig2 was chosen because it had no significant homology with other known genes, including the other members of the Olig family (Takebayashi et al., 2000).

5.11.2 Labeling of the RNAi

The Olig2RNAi constructs including the scrambled controls were fluorescently labeled as described on the Ambion webpage (see also **Fig. 5b**). Briefly, Cy3 was covalently attached to the synthesized RNAi molecules in a one step labeling reaction. The labeled RNAi molecules are then precipitated and resuspended in nuclease-free water (Ambion) and ready to be transfected. The labeled strands retain complete functionality and can therefore be used to reduce the expression of the corresponding target gene (Byrom et al., 2002), own observations.

5.12 Microarray analysis

Total RNA was extracted using RNeasy kits (Qiagen), treated with DNase I and quantified by optical density as described above. Total RNA was processed and hybridized to the murine expression array 430A (Affymetrix) according to the manufacturer's protocols. After hybridization, the gene chips were automatically washed and stained with streptavidin-phycoerythrin by using a fluidics station. Microarrays were scanned and analyzed using Affymetrix Microarray Suite v5.0 software (MAS 5.0). Output from the microarray analysis was annotated to the RefSeq or GenBank descriptor,

exported as an Excel data spreadsheet and stored as CEL files. Cells from 7 independent FACS experiments were pooled to obtain 10 μ g of total RNA for one microarray hybridization. Undifferentiated neurospheres and neurospheres differentiated for 1 day were pooled from 3 independent experiments to obtain 10 μ g of total RNA for the microarray hybridization.

The probe sets were filtered with mean expression levels ≥ 1 and then selected all probe sets with a ratio smaller than 0.25 or larger 4

5.13 Data analysis

5.13.1 Quantification of fluorescent cells at the confocal

Sections were optically sliced in the Z plane by using a 0.7 to 1 μ m interval, and cells were rotated in orthogonal planes to verify double labeling.

5.13.2 Clonal analysis

For cell fate analysis in FACS- or retrovirus-experiments, clones were analyzed for their composition of neurons, astrocytes, oligodendrocytes and precursor cells. Clones are discrete clusters of cells, derived from a single progenitor. The percentage of pure neuronal, pure non-neuronal and mixed clones was calculated per coverslip. Clones from sorted cells were detected by labeling with the antibodies M2 (mouse precursors and glial cells) and M6 (mouse neurons), detecting all mouse cells on the rat feeder layer (Malatesta et al., 2000). Control-infected clones were detected by anti- β -gal and anti-GFP immunohistochemistry (see above). M2M6 or anti- β -gal respectively were combined with cell type specific markers like anti- β -tubulin-III for neurons, anti-GFAP for astrocytes or anti-nestin for precursor cells. Clones were analyzed at 40x magnification (Zeiss Fluorescent Microscope). The probability of clonal superimposition was calculated as described in (Williams et al., 1991), e.g. for coverslips containing a maximum of 65 clones the probability was calculated to be 0.07, for those with 25 clones 0.02. The mean number of clones per coverslip obtained in my experiments was 32 ± 2 .

5.14 Statistics

For all data sets, the arithmetic average $\bar{x} = \frac{1}{n} \sum_{i=1}^n x_i$ was calculated and the standard

deviation $s = \sqrt{\frac{\sum_{i=1}^n (x_i - \bar{x})^2}{n-1}}$ and the standard error of the mean $SEM = \frac{s}{\sqrt{n}}$ were

computed. Error bars depict the SEM. The unpaired Student's t-test was used to examine whether data sets differed significantly. Data were considered as significant with $p < 0.05$ and as highly significant with $p < 0.01$. Calculations of the arithmetic average, the standard deviation, the standard error of the mean were performed with Microsoft Excel. The significance of the obtained data was tested using unpaired student's T-test.

6 RESULTS

6.1 Selective enrichment of functionally distinct precursor (stem cells, neurogenic and gliogenic precursors)

6.1.1 Selective enrichment of functionally distinct precursor subsets from different regions of the embryonic CNS by means of GFP intensity in the hGFAPeGFP transgenic mouse model.

As a first approach I examined whether radial glia isolated from different CNS regions, might differ in their intrinsic lineage restrictions. I concentrated on the developing telencephalon which is divided in two dorso ventral domains, namely the ventral domain (pallidum, ganglionic eminence, GE) and the dorsal domain (pallium, cortex) and the developing spinal cord (SC). In these regions it is known that radial glial cells act as precursors (Hartfuss et al., 2001; Haubst et al., 2004; Malatesta et al., 2000; McMahon and McDermott, 2001). To test the lineage restriction of radial glial cells from different CNS regions, I examined the progeny of individual radial glial cells, a clone, in vitro. Green fluorescent cells were isolated from three regions of the CNS (GE, cortex, SC) by FACS from a transgenic mouse line expressing eGFP (enhanced GFP) under the hGFAP-promoter (Nolte et al., 2001). I first established whether the hGFAP promoter directs eGFP to radial glial cells also in this mouse line, as shown previously in a different hGFAP-GFP mouse line (Malatesta et al., 2000) and for the hGFAP-Cre line (Malatesta et al., 2003) Indeed, the hGFAP-promoter directs eGFP to radial glial cells in all CNS regions analyzed (**Fig. 6a-e**). GFP labelling was observed in the somata of the radial glial cells in the ventricular zone (VZ) and in the typical radial processes. After isolation of green fluorescent cells by FACS the majority of sorted cells express the radial glial markers GLAST and RC2 (**Fig. 6e**, Malatesta et al., 2000). Almost all of these cells were RC2 and GLAST positive (68±3% RC2-positive cells, $n=288$; 60±4% GLAST-positive cells, $n=236$). Taken together these data indicate that the sorting of eGFP-positive cells

from the cortex of hGFAP-eGFP transgenic mice therefore selectively enriches for radial glial cells and more specifically for precursor cells expressing GLAST.

I then cultured the sorted cells on a feeder layer from either the same brain region of rat embryos at corresponding ages. The use of the mouse neural-specific antibodies M2M6 allows visualization of the sorted cells from mouse CNS and their progeny on the immunonegative rat feeder layer (**Fig. 7a',b',c'**, see also Malatesta et al., 2000). Since fate changes require in most cases cell cycle progression (McConnell and Kaznowski, 1991). I examined exclusively the progeny generated from sorted cells undergoing at least one cell cycle in vitro, detected by 5-bromo-2'deoxy-uridine (BrdU) incorporation (see Materials and Methods). BrdU is a DNA-base analogue that is incorporated into the DNA of dividing cells (Nowakowski et al., 1989), and can be therefore used to distinguish between cells that had divided in culture and cells that are already postmitotic. In vitro radial glia isolated from the GE and cultured in their normal environment did not generate neurons, in contrast to radial glia from the cortex or the spinal cord (**Fig. 7a-d**). Notably, radial glial cells from the cortex or the spinal cord generated significantly more neuronal progeny ($p < 0.005$, **Fig.7b-d**).

These profound lineage differences observed between cortical and GE radial glia might be instructed by the local environment or rely on intrinsic lineage differences. To allow manipulation of the in vitro environment, I cultured the sorted cells on a feeder layer not only from the same, but also from a different brain region of rat embryos at corresponding ages. Importantly, GE radial glia did not change their fate when plated on a cortex layer and still generated almost exclusively non-neuronal cell (nestin and/or GFAP positive precursors and astrocytes, **Fig. 7a',d**) In contrast cortical radial glia still generated neurons on a feeder layer from the GE (**Fig. 7d**). Thus, the lineage differences of radial glial cells from different CNS regions persist in radial glia undergoing cell division in a different environment in vitro and hence seem to be cell-autonomous. Therefore, by isolating radial glial populations from different CNS regions I could separate intrinsically different precursor populations that are firmly restricted in the lineage decision.

6.1.2 Subdissection

So far, my analysis *in vivo* (Malatesta et al., 2003) and *in vitro* (see above) relied on the hGFAP promoter-mediated targeting of the glutamate astrocyte-specific transporter (GLAST)-positive cells located in the ventricular zone (VZ). To confirm the result obtained in the FACS analysis, that the radial glial cells from the GE are mostly gliogenic precursors, I decided to employ two more independent techniques to isolate the radial glial cells and to isolate them from the potential neurogenic precursors located in the subventricular zone (SVZ) of the GE. I used first a previously established method to back-label precursors with long radial processes by application of fluorescent beads on the pial surface (see Malatesta et al., 2000). Since the radial processes of cells in the GE are curved ventrally, the fluorescent beads were applied by placing the brain on the beads-containing solution (**Fig. 8a**) with our previous data obtained in the cortex, this incubation labels only a few percent of all cells in this region (4.5%, **Fig. 8a**) that are mostly neurons (86% \pm 1%) but that also comprise a small number of RC2-positive cells (14% \pm 2%, $n = 179$) as detected shortly after the sort. Therefore, in accordance to our previous data, the radial cells isolated by their morphology comprise not only GLAST-positive but also a small population of RC2-only-positive precursors [($p < 0.005$, see also (Malatesta et al., 2003; Malatesta et al., 2000)]. The progeny of proliferating precursors was then examined by the selective analysis of clones that had incorporated BrdU during the 5–7 days *in vitro*, thereby excluding the postmitotic neurons that were included among the sorted cells. Notably, hardly any neurons were generated from precursors of the GE that had been labeled from the pial surface (4%, **Fig. 8c**) in pronounced contrast to precursors labeled by the same procedure in the cortex (42%, Malatesta et al., 2000). These experiments therefore support the region-specific difference of radial glial cells from the cortex and the GE in their neurogenic potential.

To further confirm this region-specific difference, I took a second approach to separate VZ and SVZ precursors by surgical dissection, since the radial glial cells are exclusively located in the ventricular zone of the GE. Telencephalic slices were cut at 300 μ m thickness, and in each slice, a small stripe of the GE adjacent to the ventricle as well as a larger piece comprising the SVZ was isolated as depicted in **Figure 8b**. Indeed, I succeeded to largely deplete the SVZ fraction from VZ precursors, since only 11% of

the SVZ fraction were RC2 immunoreactive (n =121), an antigen not present on SVZ precursors (Hartfuss et al., 2001). These mechanically separated fractions of GE precursors were then cultured at clonal density in BrdU on a rat feeder layer identical to the conditions of cells isolated by FACS. After 1 week in vitro, VZ cells enriched by dissection also generated hardly any neuronal clones, while many more were generated by the SVZ fraction (**Fig. 8c**). There was no difference in the size of the clones generated by VZ ($3.1\% \pm 0.2\%$) or SVZ ($3.6\% \pm 0.8\%$) precursors, nor in the proportion of neurons contained in mixed clones (VZ, 24% neurons; SVZ, 22%). Thus, three independent means of labeling VZ cells in the GE show consistently these precursors generate very few neurons and suggest that cortical and GE radial glia cell differ profoundly in their neurogenic potential. GE radial glia generate very few neurons and therefore these data suggest that the majority of neurons in the GE arise from the SVZ precursor pool (Miyata et al., 2004; Noctor et al., 2004).

6.1.3 Selective enrichment of functionally distinct precursor subsets from the cortex by means of GFP intensity in the hGFAPeGFP transgenic mouse model.

With the aim to separate neurogenic from gliogenic radial glial cells for a comparative gene expression analysis of neurogenic *versus* gliogenic radial glial cells, I examined whether these populations may differ in their GFP intensity in the same brain region. The rationale of this approach is that the GFAP promoter is turned off in neurons and hence may be already down-regulated in neuronal precursors, while it should still be active in glial precursors. I therefore divided the GFP-positive cells from the cortex of hGFAP-eGFP mice at embryonic day 14 (E14; **Fig. 6a,b**) in half to selectively enrich strongly and weakly GFP-positive precursors. The sorting gate was set such that about half of the GFP-positive cells with lower GFP intensity (=GFP+; but above negative control, see red in **Fig. 9a,b**) were separated by a small gap from the sorting gate selecting the strongest GFP-positive cells (=GFP++; **Fig. 9a,b**). Both gates sorted about 30% of all cells. To identify the nature of the sorted cells, they were immunostained shortly after plating (see Materials and Methods for details). Notably, both populations contained a similar number

of precursors immunopositive for RC2 (65% (GFP+), n = 110, 64% (GFP++), n = 102) and the remaining cells (33% ± 3% (GFP+)/ 33% ± 2% (GFP++); (n = 216 (GFP+)/ n = 181 (GFP++)) were β -III-tubulin-positive postmitotic neurons (Malatesta et al., 2000) with no overlap between these antigens. This high percentage of neurons in the GFP+ - sorted cell population can be explained by neurons that had shortly before sorting differentiated from GFP+ precursors, and therefore still contain endogenous GFP levels that can be detected by the detectors of FACS sorter.

Despite this relative high degree of contaminating neurons in the sort, the progeny of the weakly and the strongly GFP-positive cells isolated from E14 cortex differed markedly after 1 week in vitro. Most of the clones, i.e. the cells generated by a single sorted precursor detected by M2M6 and cell type specific antibodies (see Materials and Methods), derived from weakly GFP-positive cells contained only neurons (77%), while only 43% neuronal clones were observed in cultures of strongly GFP-positive radial glia. However, as described above for the analysis 2 hours after sorting, about 30% of all cells are already postmitotic neurons in both fractions. Therefore, the number of newly formed neuronal clones is 44% in the weakly GFP-positive fraction, but only 10% in the strongly GFP-positive fraction. This proportion of neurogenic precursors was directly assessed by addition of BrdU to the culture medium. While 54% ± 9% (n = 31) of BrdU-containing clones were purely neuronal in the GFP+ fraction, the precursors isolated by their strong GFP signal generated hardly any neurons (9% ± 10, n = 34). Taken together, these results show that the GFP intensity driven by hGFAP allows enriching populations of neurogenic and non-neurogenic precursors, respectively, about 2-fold. Under these culture conditions, most of the sorted precursors generated only a single cell type (GFP+: 92.4%, GFP++: 92% of all clones). To determine whether these cells are truly restricted in their fate, I challenged the potential of these cells in the neurosphere culture conditions. Notably, the GFP+ precursors generated only 53% of the number of neurospheres formed by the GFP++ fraction (6000 GFP+ cells: 100 ± 8 neurospheres; 6000GFP++ cells: 170±18 neurospheres). Thus, only a small fraction of the sorted precursors (1.6%/3%) can be expanded in neurosphere culture conditions, consistent with the predominant fate restriction in these precursors.

6.1.4 Neurosphere cultures to enrich a population of multipotent precursors

To complement these models of different fate-restricted precursors, I used the neurosphere assay as an in vitro model for bi- or multipotent precursors. In this assay cells are cultured in non-adherent conditions at clonal density in the presence of mitogens such as epidermal growth factor (EGF) and fibroblast growth factor-2 (FGF2; Reynolds and Weiss, 1992). Under these conditions the neural stem cells generate clonal aggregates called neurospheres. The multipotency of the neural stem cell can then be assessed by allowing cells derived from a single sphere to differentiate. If progeny of all three neural cell types, i.e. astrocytes, oligodendrocytes and neurons, is produced, this is taken as direct evidence for multipotency of the founder stem cell. Likewise, when a neurosphere can give rise to secondary neurospheres upon dissociation, this is taken as proof of self-renewal capacity of the cell of origin of the primary neurosphere. Consistent with this, cells from the adult subependymal zone (SEZ), E14 cortex and GE were cultured at clonal density (10cell/ μ l; Morshead et al., 2003) for 4 passages as neurospheres (NS, **Fig. 10**, see Materials and Methods) and then plated in differentiating conditions (see Materials and Methods for details). Consistent with previous data the progeny of neurospheres included few neurons (adult NS: $12\% \pm 5\%$, $n = 75$; E14 ctx: $9\% \pm 5\%$, $n = 199$; E14 GE: $9\% \pm 4\%$, $n = 140$) and oligodendrocytes (adult NS: $3\% \pm 1\%$, $n = 45$; E14 ctx: $5\% \pm 1\%$, $n = 257$; E14 GE: $5\% \pm 2\%$, $n = 201$), but many astrocytes (adult NS: $50\% \pm 13\%$, $n = 112$; E14 ctx: $47\% \pm 15\%$, $n = 232$; E14 GE: $40\% \pm 10\%$, $n = 214$) 7 days after exposure to differentiation conditions. Thus, these techniques provide model systems for populations of enriched in neurogenic, non-neurogenic and less fate restricted precursors (**Fig. 10**).

6.2 Gene expression analysis of functionally distinct precursors (stem cell, neurogenic and gliogenic precursors)

6.2.1 Candidate transcription factor analysis of functionally distinct precursor subsets as a test for microarray analysis

Next, I examined the expression of candidate genes to evaluate whether differential expression can be detected. I chose transcription factors expressed in subsets of telencephalic precursors, such as Pax6, Emx1, Emx2, Ngn2 and Olig1/2, Dlx1, Dlx2, Gsh2, and Mash1. During midneurogenesis (E14) Pax6, Emx1, Emx2 and Ngn2 are expressed in the dorsal telencephalon (cortex), while Dlx1, Dlx2, Mash1, Gsh2 and Olig1/2 are expressed in the GE (Götz et al., 1998; Rubenstein and Puelles, 1994; Stoykova et al., 1997; Toresson et al., 2000). I used this region-specific difference in expression levels during development to evaluate the accuracy of the real time RT-PCR method. Indeed, all of the dorsally expressed genes showed 7-36 fold higher expression (all normalized to GAPDH, see Materials and Methods) in tissue from dorsal compared to ventral telencephalon (**Fig. 11a**), consistent with their well known region specific expression. Conversely, Olig1/2, Dlx1/2, Mash1 and Gsh2 were enriched 9-40 fold in the tissue from the ventral compared to the dorsal telencephalon (**Fig. 11a, Table 2**). These data show that differential expression levels of 7 fold reflect prominent differences in gene expression. For example Emx1 is expressed 7 fold higher in the dorsal than ventral telencephalon and is in fact not detectable by in situ or antibody staining in the latter region (Briata et al., 1996; Stoykova et al., 2000). This method therefore allows assessing reliably the expression levels of one gene in different conditions (tissues or cell culture). However, the comparison of absolute mRNA levels of different genes in the same condition is not possible, since the measured expression levels of Olig2 in the GE are similar to the ones of Pax6 in the GE. Nevertheless Olig2 can be detected on protein level in the GE (Tekki-Kessarlis et al., 2001), but not Pax6 (Gulisano et al., 1996; Stoykova et al., 2000), **Fig. 11a**). Only the high expression levels of Pax6 such as present in the cortex are functionally relevant and detectable on protein level. These difficulties to

compare absolute mRNA levels may be due to differences in the rate of reverse transcription of different mRNAs or the binding site of different primer sets.

When I isolated RNA from the cortical precursors sorted on the basis of their GFP content from the cortex of E14 hGFAP-eGFP mice, I observed that the population enriched two fold in neurogenic precursors (GFP⁺) expressed 4.6x higher levels of Pax6 compared to the more non-neurogenic population (GFP⁺⁺; **Fig. 11b**), consistent with its previously described neurogenic role in cortical progenitors (Heins et al., 2002). Olig2 (4,5x) and Emx2 (6,4x), however, are enriched in the less neurogenic population (GFP⁺⁺) that was also enriched in neurosphere-forming cells (**Fig. 11b**). No significant differences were detected in the expression of the other genes examined (Emx1, Ngn2, Mash1, and Dlx1/2). Gsh2 is expressed at higher levels in the neurogenic precursors, but the expression levels are below the level detectable by antibody staining (data not shown). Thus, the precursors isolated by FACS from the dorsal telencephalon maintained their region specific expression and Pax6 was specifically enriched in neurogenic, whereas Olig2 and Emx2 were enriched in non-neurogenic precursors. Thus, this enrichment is sufficient to detect differences in genes expression and hence these populations were further processed for microarray analysis.

As mentioned above, cells cultured as neurospheres were used as model for multipotent precursors in comparison to the fate restricted precursor populations isolated by FACS. I therefore examined the expression levels of candidate genes listed above also in this model. Strikingly, cells isolated from the dorsal or ventral telencephalon that had cultured as neurospheres for 4 passages exhibited hardly region-specific differences in the expression level of Pax6, Ngn2, Emx1, Emx2, Dlx1/2, Mash1, Gsh2 and Olig1/2 anymore (**Fig. 11c**). Cortical neurospheres reduced the normally high levels of Emx1, 2, Pax6 and Ngn2 even below the low expression levels of these genes in the E14 GE. Similarly, neurospheres derived from the E14 GE reduced gene expression of Dlx1, 2, Gsh2, Vax1, Islet1 and Nkx2.2 to or below the low level of expression of these genes in the dorsal telencephalon (**Fig. 11a and Table 2**). However, independent of their region of origin, the expression levels of Olig1 and Olig2 were very high, even exceeding the levels seen in the E14 GE in situ (**Fig. 11a,c and Table 2**). Mash1 and Prox1, were detected at levels intermediate between cortex and GE in neurospheres, i.e. they were up-

regulated in neurospheres derived from the E14 cortex and down-regulated in neurospheres from the GE (**Fig. 11a,c and Table 2**). Thus, quantitative mRNA analysis of 14 transcription factors with distinct expression in dorsal and ventral regions in vivo revealed a prominent reduction in region-specific differences under neurosphere culture conditions. Notably, even neurospheres from adult SEZ contained the same expression levels of these transcription factors as seen in neurospheres from the embryonic dorsal or ventral telencephalon (**Fig. 11c and Table 2**). Only the expression of *Emx2* and *Islet1* was slightly higher in adult neurospheres compared to those from embryonic stages. Thus, neurospheres from adult and embryonic telencephalon exhibit similar patterns of gene expression with particularly high levels of *Olig1* and *Olig2*.

To confirm these data obtained on mRNA level I performed immunocytochemistry on single neurospheres after the fourth passage (**Fig. 13**). Consistent with the real-time PCR data, 97% (n = 316) of all cells in a single neurosphere were *Olig2* immunopositive, while *Mash1* was detected in about 30% of neurosphere cells (n = 187; **Fig. 13**). *Pax6* and *Ngn2* were undetectable at the protein level in neurospheres, in agreement with their low amount of mRNA.

Taken together, this candidate gene approach revealed the highest expression levels of *Olig2* in a culture system enriched in bi- or multipotent precursors, while *Pax6* expression was strongly enriched in neuronal precursors (**Fig. 12**). Moreover it demonstrated a deregulation of region specific gene expression in neurosphere cells. Is this part of the dedifferentiation process? To identify the mechanisms for this I examined the influence of the growth factors EGF and FGF2 on the expression of these candidates

6.2.2 Regulation of transcription factors upon growth factor exposure

Since neurosphere cultures are maintained in high concentrations of FGF2 and EGF, I examined the influence of these potent growth factors after short-term exposure (48 hours) in adherent dissociated cell cultures by immunostaining for the dorsal transcription factors *Pax6* and *Emx1*, and the ventral transcription factors *Olig2*, *Mash1*, pan-*Dlx* and *Gsh2*. Importantly, the regionalization of the precursors is maintained in this cell culture

model (e.g. Pax6: cortex $21 \pm 3\%$; GE $2 \pm 1\%$; **Fig. 14, Fig. 15**). However, upon exposition of cortical cultures to EGF and FGF2 the number of Pax6- and Emx1-immunopositive cells was down-regulated in cultures, while the number of Mash1- and Olig2-immunopositive cells increased in either of the growth factor treated compared to control cultures (**Fig. 14**). In cultures from E14 GE the number of Olig2-positive cells was doubled after 2 days and increased to $88\% \pm 7\%$ of cells ($n = 64$) after 7 days exposure to FGF2 or EGF ($90\% \pm 7\%$, $n = 52$). No further increase, however, was observed in the number of Mash1-, Dlx- or Gsh2-positive cells upon growth factor exposure (**Fig. 15**). Taken together, these data suggest that FGF2 and EGF are responsible for the loss of dorsal identity in neurosphere cultures, since Pax6 and Emx1 were reduced, but do not account for the partial loss of ventral identity since the number of Dlx- or Gsh2-immunopositive cells were not influenced by exposure to these growth factors.

Thus, this cell culture system allowed me to isolate multipotent precursor cells, and hence these neurosphere cultures were further processed for microarray analysis. However, one has to keep in mind that these cells are deregulated by EGF and FGF2.

6.2.3 Transcription factor analysis in neurosphere cultures in differentiation conditions

To analyze the consequences of this observed deregulation of genes in the neurosphere cultures and the loss of regional specificity I exposed the neurospheres to differentiation condition. Under these conditions the neurosphere cells are forced to differentiate due to the withdrawal of the growth factors. Since Pax6 expression was strongly enriched in neuronal precursors of the E14 cortex, one would predict its upregulation at least during differentiation of the cortical neurosphere cultures. Indeed, when I exposed neurosphere cells to differentiation conditions (see Materials and Methods), the number of Pax6-immunopositive cells increased to $7\% \pm 3\%$ (Ctx NS, $n = 30$). Surprisingly this was also observed in the GE, where $8\% \pm 3\%$ (GE NS, $n = 26$) were observed 3 days after plating. In contrast, Olig2-immunoreactivity decreased to $74\% \pm 7\%$ (Ctx NS, $n = 51$) or $73\% \pm 6\%$ (GE NS, $n = 45$) immunoreactive cells 3 days after plating. Notably, the upregulation of Pax6 and downregulation of Olig2 was also observed at mRNA level (**Fig. 16a,b**). The

expression levels of Emx1, Emx2, Ngn2 and Mash1 were all increased in differentiation conditions, while Olig2 and Dlx1 decreased. However, the increase or decrease in expression levels was very similar for neurospheres derived from E14 cortex and GE (**Fig. 16a,b**). One exception was Dlx2 mRNA that increased only in differentiating neurospheres derived from the GE, suggesting some remnants of regional specification. It is important to realize, however, that the Dlx2-expression levels after differentiation of neurospheres from the GE were still 3 orders of magnitude (1000x) below the levels seen in the GE during development. Taken together, this candidate gene approach revealed that the regionalization is still lost after differentiation. Moreover, it demonstrated that the highest expression levels of Olig2 in expansion conditions of neurosphere cells, while Pax6 was most prominently up-regulated in differentiation conditions (**Fig. 16a,b**).

6.3 Microarray analysis of differential gene expression in functionally distinct precursor subtypes

The gene expression data obtained in the candidate gene approach with the different precursor populations (the neurogenic precursors (GFP+) and the more non-neurogenic population (GFP++) from E14 hGFAP-eGFP mice or the neurosphere cells isolated from different regions and or differentiated for 1 and 3 days showed that these cell types are not only functionally different, but that some differences can also be detected on the gene expression level. These results encouraged me to evaluate global differences in gene expression of these functionally distinct precursor populations by oligonucleotide microarrays (Affymetrix). More specifically I selected for the microarray study the neurogenic precursors (GFP+) and the more non-neurogenic precursor population (GFP++) from E14 hGFAP-eGFP mice as model for neuronal and glial fate restricted precursors and the neurosphere cells isolated from the E14 cortex undifferentiated as model for multipotent precursors. Neurospheres that had been differentiated for 1 day represent again the progression to more fate-restricted precursors.

10µg total RNA were collected from these cells and purified as described in the Materials and Methods. The probe sets were filtered with mean expression levels ≥ 1 and then all probe sets with a ratio smaller than 0.25 or larger 4 were selected. For neurosphere cells isolated from the E14 cortex undifferentiated and differentiated for 1 days (dd1) this resulted in a set of 1354 probe sets (down in dd1: 617, up in dd1: 737; see **Table 3**). Interestingly, for the neurogenic precursors (GFP+) and the more non-neurogenic population (GFP++) from E14 hGFAP-eGFP mice this resulted in a set of 4398 probe sets with a majority of probe sets upregulated in the GFP++ , i.e. the more gliogenic precursors (down in GFP++: 189, up in dd1: 4109; see **Table 4**)

To verify the data obtained by microarray analysis, I performed RT-PCR with RNA from either the microarray experiments or from independent RNA preparations. The genes of interest (**Fig. 17**) were chosen because of their expression profile apparently correlated with cell fate according to the following categories:

- 1) Genes expressed in multipotent stem cells: high expression in undifferentiated neurosphere cells, medium expression in differentiated neurospheres and GFP++ gliogenic precursors, lowest expression in the GFP+ neurogenic precursors (**Fig. 17a**, *tweety* (Suzuki and Mizuno, 2004), yellow bars; *sirtuin2* (Fulco et al., 2003), dark orange bars and *FABP7* (Veerkamp and Zimmerman, 2001), light orange bars).
- 2) Genes expressed in neurogenic precursors: lowest expression levels in undifferentiated neurosphere cells, low expression in differentiated neurospheres and GFP++ gliogenic precursors, highest expression in the GFP+ neurogenic precursors (**Fig. 17c**, *LMO1* (Hinks et al., 1997), dark blue bars and *Sox4* (Cheung et al., 2000), light blue bars).
- 3) Genes expressed in gliogenic precursors: medium expression in undifferentiated neurosphere cells, highest expression in differentiated neurospheres and GFP++ precursors, low expression in the GFP+ neurogenic precursors (**Fig. 17b**, *Sox9* (Stolt et al., 2003), brown bars and *Klf9* (Zhang et al., 2003), red bars).

Not surprisingly the expression profiles of *Pax6* and *Olig2* in these 4 functionally distinct populations (**Fig. 12, 16**), strikingly fit into the expression profiles of group 2 (for *Pax6*) and group 1 (for *Olig2*), respectively. Seven of nine (78%) of the selected genes from the

MAS5.0 probe summary reproduced the data collected by the microarrays over a broad spectrum (**Fig. 17a,b,c**). I thus concluded that the microarray data are relatively reproducible and reliably reflect both cellular RNA content as well as the difference of gene expression in distinct precursor subsets.

6.4 Functional analysis of Pax6 and Olig2 for fate specification

6.4.1 Functional analysis of Pax6 and Olig2 in vitro

6.4.1.1 Functional analysis of Pax6 in neurosphere cells

Since I observed upregulation of Pax6 in a subset of neurosphere cells exposed to differentiating conditions and enhanced expression in neurogenic precursors from the E14 cortex (**Fig. 16a,b, Fig. 11c and Fig. 12**), I tested whether I could boost neurogenesis by forcing Pax6 expression in cells differentiating from neurosphere cultures of the adult telencephalon. Towards this end I used different replication-incompetent retroviral vectors containing full-length Pax6 cDNA and either the marker gene lacZ or GFP (Heins et al., 2002; **Fig. 4a,f**). Neurosphere cells dissociated after 4 passages were infected shortly after plating and analyzed the fate of infected cells by double immunocytochemistry for cell type specific antigens 5-7 days after infection and culturing under differentiating conditions. Amongst the control infected cells (n = 122) 25% ± 8% turned into β-III-tubulin-positive neurons, whereas significantly more β-III-tubulin-positive neurons (87% ± 6%) were detected amongst the Pax6-infected cells (n = 143; **Fig. 18a,b,c**). Thus, Pax6 is sufficient to direct almost all precursors from adult neurospheres towards neurogenesis. This is to my knowledge the highest amount of neuronal differentiation achieved in cultures of adult neurospheres and is highly relevant for attempts to regenerate dying neurons by transplantation of neurosphere cells [see for example (Li et al., 2003)].

In order to assess whether adult neurospheres are particularly amenable to Pax6, I also examined its effect in neurosphere cultures from E14 cortex or GE. In neurospheres from the cortex I observed 72% ± 7% of the cells infected with Pax6-encoding virus (n = 234)

had generated neurons compared to $11\% \pm 5\%$ of the control infected cells ($n = 496$; **Fig. 19a**). Surprisingly, also neurospheres from the embryonic GE could be induced to differentiate into neurons by Pax6 overexpression (Pax6: $79\% \pm 10\%$, $n = 353$; control: $10\% \pm 7\%$, $n = 366$; **Fig. 19a**). This is in pronounced contrast to primary cells from the GE cultured without growth factors that are resistant to effects mediated by Pax6 (**Fig. 19c,d**; Heins et al., 2002). Interestingly, even neurosphere cultures from the E14 midbrain that were infected with Pax6-encoding retrovirus generated significantly more β -III-tubulin-positive neurons compared to control infected cultures (Pax6: $64\% \pm 8\%$, $n = 205$, control: $19\% \pm 2\%$, $n = 103$). Thus, culturing cells from different brain regions as neurospheres not only abolishes their region-specific expression profile, but also renders them susceptible to Pax6 overexpression.

To evaluate whether neurogenesis in neurosphere cells also becomes Pax6 dependent, I examined the cell fate of neurosphere cells generated from the Pax6 mutant (Sey/Sey) cortex (Heins et al., 2002; Hill et al., 1991) after 4 passages. Interestingly, cells from Pax6 deficient neurospheres were not able to generate neurons, while neurospheres from wildtype (WT) littermates generated the normal low percentage of neurons in the same culture batch (**Fig. 19b**). Thus, the alterations in regionalisation of neurosphere cells seemingly activate a Pax6 dependent mode of neurogenesis.

Taken together these results confirm at a functional level the role of Pax6 in directing stem cells towards a neurogenic lineage (**Fig. 3**)

6.4.1.2 Functional analysis of Olig2 in neurosphere cells

Since the above analysis showed Olig2 expression in fast proliferating, not lineage restricted precursors, I next examined its role in self-renewal and fate specification in the neurosphere cultures by RNA interference with Olig2 expression levels. I first tested several 21 nucleotide double stranded siRNAs in their effectiveness to reduce the Olig2 protein. Neurospheres were plated after 4 passages, transfected with different siRNA and control constructs and immunostained for Olig2 2 days later. Different target sequences proved to be more (reduction by 41%, Olig2 RNAi#19) or less (reduction by 14%, Olig2 RNAi#1) effective in their reduction of Olig2 protein. Consistently, there was no

significant reduction in the number of Olig2-immunoreactive cells when cells were treated with each of these constructs containing the same sequence in a scrambled manner (**Fig. 20a**). For all constructs the percentage of transfected cells was similarly high (80% of cells) as detected by labeling the siRNA constructs with Cy3 (see Materials and Methods).

Then, I examined the effect of Olig2 reduction on self-renewal of neurosphere cells by transfection of Olig2RNAi#19 and its scrambled RNAi control 1 day after dissociation of the spheres into single cell suspension and quantification of the newly formed neurospheres 6 days later. Notably, only about half the number of neurospheres was generated by cells transfected with Olig2 RNAi compared to the control transfected cultures (**Fig. 20b**). I also noted that Olig2 RNAi treated neurospheres were smaller than neurospheres observed under control conditions. Since the remaining 40% neurospheres may still be Olig2-positive as they correspond in number to the cells not affected by the Olig2-knock down, I conclude that Olig2 is required for the generation of neurosphere cells and may act as an essential mediator of EGF and FGF2 signaling in this system.

Next, I studied the influence of Olig2 on cell fate by transfecting the neurosphere cells 1 day after plating in differentiating conditions. In cultures examined 7 days after transfection, the number of neurons and oligodendrocytes generated from Olig2RNAi transfected cells was reduced to a third of the control treated cells (**Fig. 20c**). To further ensure the specificity of the observed effects I used a replication-incompetent retroviral vector containing full-length Olig2 cDNA fused to the herpes simplex virion protein VP16 in front of an IRES sequence and GFP (Olig2VP16; **Fig. 4d**). As reported previously, Olig2 acts normally as a repressor (Novitch et al., 2001; Zhou et al., 2001), but is converted into an activator by fusion to VP16 (Sadowski et al., 1988). This construct therefore interferes with the normal function of Olig2 (Novitch et al., 2001). When cultures were examined 7 days after viral infection a similar reduction in the number of neurons and oligodendrocytes as detected by RNAi was observed (**Fig. 21a,b**). Notably, cells infected with Olig2VP16 differentiated almost exclusively into GFAP-positive astrocytes (CTX NS: $88 \pm 5\%$, $n = 969$; GE NS: $88\% \pm 2\%$, $n = 874$). Consistent with the high expression of Olig2 right after plating of the dissociated neurosphere cultures the effect of Olig2 overexpression was very mild showing a slight increase in the

number of neurons (β -III-tubulin, $11\% \pm 1\%$; $n = 595$ compared to $9\% \pm 1\%$ in the WT; $n = 813$) and oligodendrocytes (O4, $13\% \pm 1\%$; $n = 595$ compared to $8\% \pm 1\%$ in the WT; $n = 813$). However, the number of GFAP-positive astrocytes was fully suppressed after Olig2 transduction (0% , $n=355$, consistent with Gabay et al., 2003). Taken together the high levels of Olig2 in neurosphere cells play a role in self-renewal as well as neurogenesis and oligodendrogenesis from neural stem cells. Thus, Olig2 favors a stem cell fate with self renewal and bi-/multipotency.

Since Olig2 seems to promote neural stem cell fate, I examined whether it may be sufficient to convert fate-restricted into multipotent precursors. Towards this end I overexpressed Olig2 for 7 days in cell prepared from the cortex at E14 and cultured as high density adhesive cultures without or with factors. Also in this experimental system I found an increase in the number of oligodendrocytes (O4, $10\% \pm 1\%$; $n = 204$ compared to $3\% \pm 1\%$ in the control; $n = 317$) and a decrease in the number of mature neurons (NeuN, $52\% \pm 5\%$; $n = 204$ compared to $44\% \pm 2\%$ in the WT; $n = 317$). Thus, Olig2 seems to act in a context dependant way by promoting bi-/multipotency in neurosphere cells and by promoting oligodendrogenesis in more restricted precursors.

6.4.2 Functional analysis of Pax6 and Olig2 in vivo

6.4.2.1 Functional analysis of Olig2 in vivo during embryonic development

So far I could show that Olig2 acts in a strong context dependant manner and therefore I decided to compare this observed effect in precursors in vitro to precursors in vivo during embryonic development. By injecting an Olig2 containing retroviral expression vector into mouse forebrain ventricles at midneurogenesis (E14), I achieved focal misexpression of Olig2 in cortical progenitor cells that do not normally express Olig2. Injected embryos developed to term and were harvested at two different postnatal time points, namely at postnatal day 2 (P2) and postnatal day 21 (P21). Infected cells were identified by staining for GFP encoded by the pMXIG retroviral vector or CMMP (see Materials and Methods for details, **Fig. 4**). Cell types of the retroviral-infected cells were assigned on the basis of

immunostaining with cell type specific markers (**Fig. 22c-f**) and morphology of the GFP positive cells (**Fig. 22b**). When examined at P21, cells infected with the control retrovirus CMMP were mainly neurons; only few astrocytes and few oligodendrocytes were noted. In contrast, cells infected with the Olig2 retrovirus were exclusively glia. A high percentage of these glia were astrocytes (S100 β -immunoreactive, **Fig. 22d**) and oligodendrocytes (data not shown), which were found in all brain regions analyzed (cortex, corpus callosum, **Fig. 22b-d**). However the astrocytes were GFAP negative consistent with previous results that had shown the Olig2 potently suppresses GFAP expression (**Fig. 22c**; Gabay et al., 2003). To determine whether Olig2 misexpression affects formation or survival of neurons, I examined the brains of Olig2 infected animals at an earlier postnatal time point, P2. Cortical cells that were infected with the control virus had a constant ratio of neurons to glia from P2 to P21 (33%, n=613). In contrast, cortical cells that were infected with the Olig2 retrovirus had a much reduced ratio (**Fig. 22e,f**). These data indicate that Olig2 has similar effects on cortical development as other bHLH genes tested to date. Previous misexpression studies have identified a wide range of positive regulatory bHLH genes (including Olig1, Mash 1, Math 2, Math 3, Ngn 1, Ngn 2, NeuroD and NeuroD2) that are deleterious to the survival of neurons in the developing mouse cortex (Gangemi et al., 2001). These same bHLH proteins permit, and perhaps even promote, the formation and survival of astrocytes (Cai et al., 2000; Gangemi et al., 2001).

Consistent with my observation that high levels of Olig2 are deleterious for neuronal differentiation and survival, endogenous Olig2 protein in the adult (P22) mouse cortex is exclusively detectable in CC1-positive oligodendrocytes (**Fig. 23b**) and a subset of glutamine synthase (GS)-positive (**Fig. 23c**) or S100 β -positive astrocytes (**Fig. 23d**). Notably, Olig2-immunoreactivity was never detectable in neurons labeled with antibodies directed against β -III-tubulin or NeuN.

Taken together, these data indicate that overexpression of Olig2 induces oligodendrocyte and neuronal differentiation in both, the neurosphere cultures and precursors of the dorsal telencephalon in vivo and in vitro. However, these data further suggest, that Olig2, such as other bHLH transcription factors, induces apoptosis in

neurons when high expression levels persist during terminal differentiation of postmitotic neurons.

6.4.2.2 Functional analysis of Olig2 and Pax6 in vivo in adult neural stem cells

6.4.2.2.1 Expression analysis of the transcription factors Pax6 and Olig2 in adult neural stem cells and their progeny in vivo

In order to further evaluate the correlation of Pax6 to neurogenesis, and Olig2 to fast proliferating precursors, neurogenesis and oligodendrogenesis, I examined Pax6 and Olig2 in the adult SEZ in vivo, where multipotent and fate-restricted precursors can nicely be discriminated as described in the introduction (**Fig. 24a**; Doetsch et al., 1999; Doetsch et al., 2002).

6.4.2.2.2 Expression pattern of Pax6 in adult neurogenesis

Notably, however, a prominent gradient of Pax6-immunopositive cells was observed along the rostro-caudal extension of the SEZ/RMS system that had previously not been noticed. The number of Pax6-immunostained cells was lowest in the region lining the ventricle, where only $7\pm 3\%$ of DAPI-labeled cells were Pax6-positive ($n = 223$, 3 animals; **Fig. 25b**). Already in the caudal RMS immediately adjacent to the SEZ the proportion of Pax6-immunopositive cells increased to $42\pm 6\%$ ($n = 126$, 1 animal; **Fig. 25c**) with a further increase to $61\pm 5\%$ ($n = 221$, 3 animals; **Fig. 25d**), where the descending limb of the RMS intersects with the horizontal limb.

Interestingly, the number of Pax6-positive cells then decreases when cells reach the OB ($26\pm 4\%$ of DAPI-labeled nuclei are Pax6-positive in the RMS in the OB; $n = 131$, 1 animal; **Fig. 25e**) and only few Pax6-immunopositive cells were scattered throughout the OB (**Fig. 26d**). Most of these were migrating neuroblasts as detected by PSA-NCAM- or doublecortin (DCX)-immunoreactivity ($76\pm 6\%$, $n = 131$, 1 animal, **Fig. 25g**) as observed throughout the SEZ/RMS (SEZ: $74\pm 4\%$ of Pax6-positive cells were DCX-

positive, $n = 235$, 2 animals; RMS: $67\pm 5\%$, $n = 563$, 2 animals), and virtually no colocalization of Pax6 and GFAP could be detected ($<1\%$, $n = 112$, 1 animal). Interestingly, Pax6 immunoreactive cells with weak levels of GFP were observed in the RMS (**Fig. 25f**) consistent with the idea that the Pax6-positive neuroblasts derive from hGFAPeGFP-positive astrocytes (Doetsch et al., 1999; **Fig. 24b**). Thus, about two thirds of Pax6-positive cells are neuroblasts, and one third is precursors at a less committed stage throughout the SEZ/RMS system.

A notable accumulation of Pax6-positive cells was then again apparent in the glomerular layer (GL; **Fig. 26d**), where most Pax6-immunoreactive cells had differentiated into postmitotic NeuN-positive neurons ($81\pm 3\%$ of Pax6-positive cells were NeuN-positive, $n = 126$, 1 animal). In contrast, hardly any of the few Pax6-positive cells in the GCL were NeuN-positive ($9\pm 1\%$, $n = 186$, 1 animal), suggesting that Pax6 is downregulated in granule cells, but not periglomerular cells during neuronal differentiation.

Next, I identified the subtype of neurons in the glomerular layer. I observed that Pax6 was contained mostly in tyrosine hydroxylase (TH)-positive neurons of the GL (78% of Pax6-positive cells in GL were TH-positive and 95% of TH-positive neurons were Pax6-positive, $n=683$, 3 animals, **Fig. 26e**). Almost no Pax6/calretinin double positive cells was observed ($1,5\pm 0.4\%$; $n = 361$ cells, 1 animal), while $9,8\pm 0,9\%$ ($n = 437$ cells, 2 animals) were co-labeled for Pax6 and calbindin. Taken together, these data suggest that Pax6-expression is mostly maintained in the dopaminergic subset of periglomerular neurons [(Gall et al., 1987; Kosaka et al., 1998; Kosaka et al., 1985), see also (Dellovade et al., 1998; Vitalis et al., 2000)]. These data demonstrate an intriguingly dynamic regulation of Pax6 in adult neurogenesis: first, Pax6 is up-regulated in almost all neuroblasts along the RMS, but down-regulated during neuronal differentiation in most neurons except those of the GL.

6.4.2.2.3 Expression pattern of Olig2 in adult neurogenesis

In contrast to Pax6, Olig2 did not double-stain for PSA-NCAM or DCX (SEZ: 0% , $n = 123$; RMS: 2% , $n = 111$, **Fig. 27d**) or for GFAP (0% in SEZ, $n = 120$, or RMS, $n = 100$,

Fig. 27e). To further elucidate the identity of Olig2-immunopositive precursors, I employed different BrdU-labeling paradigms. When BrdU was continuously supplied in the drinking water for 14 days all proliferating cells are labeled, and according to their higher incidence the majority of BrdU-positive cells are fast proliferating cells, type C or type A. In this paradigm many BrdU-positive cells also contained Olig2 (**Fig. 27f**). Next, I used a single BrdU-pulse and examined colocalization 45 minutes after this pulse, a paradigm that should exclusively label fast proliferating cells in S-phase. **Fig. 27g** depicts an example of an Olig2- and BrdU-double-labeled cell, demonstrating that Olig2 is contained in fast proliferating precursors in the adult SEZ.

Indeed, the localization of Olig2 in fast proliferating precursors, is further confirmed by the 6-fold higher labeling index (LI) as determined with a short BrdU-pulse (1 hour) of Olig2-positive precursors (LI (%BrdU-positive cells amongst all Olig2-positive cells) = 0.3) compared to Pax6-positive precursors (LI = 0.05). This suggests that it is mostly contained in the transient-amplifying precursors which are negative for GFAP, as well as GFAP. Consistent with this I detected some co-localization within Lewis X antigen, a proposed marker for type C cells (Capela and Temple, 2002; arrows in **Fig. 27c**). Note however, that not all Olig2-positive cells co-localize Lewis X (arrowheads in **Fig. 27c**), nor all Lewis X-positive cells contain Olig2 (arrowhead with asterisk in **Fig. 27c**). Since Lewis X was shown to contain type C and supposedly also some type B cells (Capela and Temple, 2002), this cell type analysis would suggest that Olig2 is contained in some or most type C cells.

Interestingly, the transcription factor Olig2 exhibited the opposite gradient with $18 \pm 4\%$ Olig2-immunopositive amongst all DAPI-positive cells in the SEZ ($n = 341$, 2 animals), while only $2 \pm 1\%$ ($n = 412$, 2 animals; **Fig. 27b,b'**) Olig2-positive cells were detectable within the RMS. In contrast to Pax6, the number of Olig2-positive cells did not increase again and no Olig2-immunopositive neurons could be detected within the OB ($n = 196$, 1 animal).

Thus, Olig2-positive adult neural precursors are fast-proliferating type C cells with their highest density in the SEZ and decreasing numbers within the RMS. Notably, no co-localization of Pax6- and Olig2-immunoreactivity could be detected ($n = 186$)

suggesting that these transcription factors are contained in truly separate sets of progenitor cells.

Taken together, the examination of the endogenous localization of Pax6 and Olig2 in adult neural precursors revealed a striking difference along the rostro-caudal extension of the SEZ/RMS system that had previously not been noticed (**Fig. 25b-e; Fig. 27b,b'**). This analysis of the adult SEZ confirmed the correlation of Pax6 to PSA-NCAM-positive neurogenic precursors and Olig2 to PSA-NCAM-negative fast proliferating precursors, most likely type C cells. Moreover in contrast to Olig2 expression, Pax6 remains to be expressed in matured neurons in the OB and more specifically in the TH-positive dopaminergic neurons of the GL.

6.4.2.2.4 The role of Pax6 and Olig2 in adult neural precursors

Next, I examined the cell autonomous function of Pax6 and Olig2 by the use the replication-incompetent retroviral vectors. Given the pronounced gradient of Pax6 and Olig2 in the SEZ/RMS system I decided to compare the manipulation of these transcription factors at both positions. When, viral infections were stereotactically targeted to the SEZ (Belluzzi et al., 2003; Carleton et al., 2003; Petreanu and Alvarez-Buylla, 2002), $95\pm 2\%$ of all GFP-positive cells were still located close to the SEZ three days after injection and only $5\pm 2\%$ were detected at some distance within the RMS ($n = 45$, 1 animal; **Fig. 28a,b,c**). When the injection coordinates were modified to target the central RMS (see Materials and Methods), I reliably observed the vast majority of GFP-positive cells 3 days after injection migrating forward in the RMS ($72\pm 1\%$ in the RMS outside the OB, $21\pm 5\%$ in the RMS inside the OB) with only $6\pm 1\%$ of cells apparently migrating backwards to the SEZ ($n = 66$, 1 animal; **Fig. 28d**). Thus, the targeted injection of viral vectors allows manipulating gene expression locally at two distinct places of the SEZ/RMS system.

To manipulate the expression patterns of Pax6 and Olig2 in the SEZ and the RMS, I used vectors containing the wildtype forms of Pax6 or Olig2 coexpressing the green fluorescent protein (GFP) mediated by the IRES sequence (Hack et al., 2004), see above, **Fig. 3**). As dominant-negative construct I used Pax6-engrailed (Yamasaki et al.,

2001) that contained the Engrailed repressor domain instead of the normal transactivating domain of Pax6, whereas the repressor domain of Olig2 was removed (see Materials and Methods) or replaced with Olig2-VP16 (as described above, Mizuguchi et al., 2001) replacing its normal repressor domain (**Fig. 3**). Previous in vivo and in vitro studies showed that these constructs produce the opposite effect as the wildtype transcription factor, suggesting that they indeed antagonize the function of Olig2 and Pax6 respectively (Hack et al., 2004; Mizuguchi et al., 2001; Novitsch et al., 2001; Yamasaki et al., 2001).

I have performed further control experiments by comparison to loss of function conditions (**Fig. 30**). I used a dissociated cell culture system of embryonic E14 cortex or striatum (GE) for analysis of precursors infected at the day of plating and the progeny analyzed 7 days later (Heins et al., 2002). This is a well-established in vitro system for the analysis of telencephalic precursor fate, where the effect of Pax6 is particularly well characterized (Haubst et al., 2004; Heins et al., 2002). Previous work had shown that Pax6 overexpression promotes neurogenesis and reduces clone size, *i.e.* the number of descendants generated by a single precursor cell, while the loss of functional Pax6 in Small Eye mutant mice (Sey/Sey; Heins et al., 2002) results in decreased neurogenesis and an increase in clone size (Haubst et al., 2004; Heins et al., 2002). As expected, infection with the Pax6-engrailed containing virus resulted also in a decrease of neurogenesis that was almost identical to the effect in Sey/Sey mutant cells deficient of functional Pax6 protein compared to wildtype cells. Thus, the Pax6-engrailed is as sufficient as the loss of functional Pax6 protein. Next, I also examined the specificity of both, the Pax6-engrailed and the Olig2VP16 constructs by expression in cells that do not contain Pax6 or Olig2 respectively. For example, cells from the embryonic cortex do not express Olig2 and should therefore not be affected by Olig2-VP16 transduction, as is indeed the case. Thus, Olig2-VP16 does not superactivate target genes in cells where Olig2 plays no endogenous role. Similarly, Pax6-engrailed transduction of precursors from the ventral telencephalon that do not contain endogenous Pax6 protein exerted no effect, despite its pronounced effect in the cortical progenitor cells. Taken together these experiments showed that dominant-negative constructs are specific and exert no effects in cells that do not endogenously express the respective transcription factor.

When Pax6-containing was injected into the adult SEZ (**Fig. 29a,c**), a larger number of Pax6-transduced precursors had progressed to the neuronal lineage (DCX-immunopositive; $n = 281$, 3 hemispheres, 3 animals) compared to those infected with the control virus containing GFP only ($n = 183$, 4 hemispheres, 3 animals; $p < 0,05$) one week after injection (**Fig. 29c**). Conversely, a prominent reduction in the proportion of neuroblasts (to 42% of the control, $n = 100$, 3 hemispheres, 2 animals; $p < 0,05$) and a respective increase in other precursors was observed in the SEZ and initial RMS one week following transduction with Pax6-engrailed containing vectors (**Fig. 29b,c**). As depicted in **Figure 31a**, a comparable reduction of infected precursors assuming a neuronal precursor fate (DCX-positive, to $39 \pm 11\%$, $n = 83$, 3 hemispheres, 2 animals) of the control virus injections (control: $n = 70$, 2 hemispheres, 2 animals; $p = 0,013$) was observed by deleting Pax6 using Cre-virus injection into mice in which the N-terminal part including the paired domain of the Pax6 gene was flanked by loxP sites (Ashery-Padan et al., 2000). These effects are not due to selective death of precursor subtypes, since analysis of DAPI-labeled nuclei or tunel-staining performed 3 or 7 days after viral injection showed no differences in death of infected cells. These results rather imply Pax6 in the regulation of adult neurogenesis, supposedly via its coordinated effects on cell proliferation and cell fate as observed in cerebral cortex development (Haubst et al., 2004; Heins et al., 2002).

Intriguingly, Olig2 exerted the opposite effects to Pax6 on precursor cells in the adult SEZ. Olig2-overexpression resulted in a decrease of neuronal precursors immunoreactive for DCX (**Fig. 29f**; to $35 \pm 3\%$ of control; $n = 181$, 3 hemispheres, 3 animals, $p < 0,0001$) to comparable levels as achieved by Pax6-engrailed expression (compare **Fig. 29c and f**). Notably, however, the decrease of neuronal precursors resulted mostly from an increase in precursors negative for both GFAP and DCX, supposedly the transit-amplifying type C cells. Indeed, consistent with the expression of endogenous Olig2 exclusively in this precursor type, expression of the dominant-negative form, Olig2-VP16, virtually abolished this precursor cell type. Similar effects were obtained with a loss of function construct containing the Olig2 bHLH (**Fig. 3**), but no repressor domain (**Fig. 31b**). Thus, Olig2 is necessary and sufficient to specify transit-amplifying precursors in the SEZ. Taken together, these data support the functional role as deduced

from the protein localization: Olig2 is crucial to specify transit-amplifying and Pax6 neuronal precursors.

6.4.2.2.5 Olig2 promotes adult oligodendrogenesis

With Olig2 overexpression I also noted a prominent emigration from the SEZ/RMS system already apparent 3 days after viral injection (**Fig. 29e**), while no cells infected with the control virus were located outside the SEZ/RMS system, at this stage (<1%, $n = 45$, 1 animal, see also above). However, 7 days postinjection also in control virus injections some descendants of the infected cells had left the RMS and migrated to the corpus callosum (CC, **Fig. 32e**, $1 \pm 1\%$, $n = 201$, 4 hemispheres, 3 animals). These cells were identified as oligodendrocytes, or their precursors, by CC1 or Sox10-immunoreactivity, respectively. Since no infected cells could be detected within the CC shortly after injection, precursors of the adult SEZ also generate oligodendrocytes one week after Olig2-virus injection into the SEZ, however, $50 \pm 9\%$ of all infected cells ($n = 207$, 3 hemispheres, 3 animals, $p < 0,001$ compared to GFP-control injections) were detected within the CC (**Fig. 32b**) 1 week post-injection and had acquired oligodendrocyte identity (**Fig. 29e**). Notably, the increase in oligodendroglialogenesis was accompanied by a decrease in neuronal precursors as well as the proportion of neurons reaching the OB (**Fig. 29f**, **Fig. 32b**), suggesting that neurons and oligodendrocytes originate from the same progenitors in the SEZ rather than from direct transfection of oligodendrocyte precursors in the CC. Indeed, the maintenance of Olig2 expression interferes with neuronal differentiation as previously shown (Lee et al., 2005; Lu et al., 2002). Consistent with an endogenous role of Olig2 in the endogenous low degree of oligodendroglialogenesis, this was completely blocked after injection of Olig2-VP16 in the SEZ (**Fig. 32c**).

6.4.2.2.6 RMS precursors are further restricted towards the neuronal fate

Given the gradient of these transcription factors along the RMS, I next performed the same functional analysis by injection into the RMS (**Fig. 28c,d**). These experiments revealed intriguing differences in the cell type specification at this position. When the

Pax6-engrailed containing virus was injected into the RMS, the effect on neurogenesis was notably weaker (control $94\pm 1\%$ DCX-positive cells amongst GFP-positive cells, $n = 80$, 2 hemispheres, 1 animal, Pax6engrailed: $78\pm 4\%$, $n = 80$, 2 hemispheres, 1 animal, see also **Fig. 32e**). Thus, precursors are further committed to the neuronal lineage within the RMS and this commitment is hardly reversible by Pax6-engrailed transduction. Similarly, overexpression of Olig2 in the RMS could not elicit oligodendrocyte generation (**Fig. 32b**). Taken together, these data indicate that precursors in the RMS are further fate-restricted and instead of promoting the generation of non-neuronal cells, both Pax6-engrailed and Olig2 transduction still resulted in a large number of cells progressing towards the neuronal lineage.

6.4.2.2.7 The role of Pax6 for the specification of dopaminergic periglomerular neurons

Next, I examined neuronal subtypes generated by precursors manipulated within the SEZ or the RMS 2-3 weeks after injection. First, I compared the neuronal subtypes generated by cells infected with the GFP-control virus in the SEZ or the RMS. Consistent with previous data (Belluzzi et al., 2003; Carleton et al., 2003; Luskin, 1993; Petreanu and Alvarez-Buylla, 2002), most SEZ precursors gave rise to GFP-positive neurons (NeuN-immunopositive) in the GCL ($94\pm 2\%$, $n = 316$, 4 hemispheres, 3 animals) and only few neurons were detected in the GL ($2\pm 1\%$, **Fig. 33e**). Remarkably, control virus injection into the RMS resulted in a significantly larger proportion of periglomerular neurons (PGN) amongst all GFP-positive cells in the OB ($30\pm 3\%$, $n = 379$, 3 hemispheres, 2 animals, **Fig. 33f**, $p < 0,001$ compared to GFP injections into SEZ). These results suggest a new concept, namely that PGNs originate mostly at a rostral position of the SEZ/RMS system and few are derived from SEZ precursors. Notably, however, the majority of progenitor cells infected in the RMS ($70\%\pm 2$, $n = 379$, 3 hemispheres, 2 animals, **Fig. 33f**) were still granule neuron (GN) precursors. Since most neuronal precursors in the RMS contain Pax6 ($64\%\pm 2$, $n = 235$, 2 animals), these data further support that Pax6 is also contained in GN precursors.

Given that Pax6 persisted in postmitotic PGNs while it was down-regulated in postmitotic GNs, I next examined whether the retrovirally mediated persistence of Pax6 protein in OB neurons would be sufficient to instruct the differentiation towards the PGN fate. Indeed, Pax6 overexpression in RMS precursors is sufficient to convert the fate of $70\pm 2\%$ GN neurons in the control injections towards a PGN fate with almost all of the neurons overexpressing Pax6 located then in the GL ($85\pm 5\%$, $n = 90$, 3 hemispheres, 3 animals, $p < 0,0001$ compared to GFP-control injections into the RMS, **Fig. 33f**). These data imply Pax6 as a key determinant for PGN neuronal subtype specification. Indeed, injection of Pax6-engrailed virus into the RMS significantly reduces the proportion of PGN normally generated here to less than a third of the value obtained in control virus injections ($6\pm 2\%$, $n = 141$, 4 hemispheres, 3 animals, **Fig. 33f**, $p < 0,001$ compared to GFP injections into RMS), suggesting that the maintenance of endogenous Pax6 expression in RMS precursor cells is required to progress towards a PGN subtype. Pax6-virus injection into the SEZ was also sufficient to instruct PGN fate ($30\pm 5\%$, $p < 0,001$, compared to GFP control injection into SEZ, $n = 80$, 3 hemispheres, 3 animals, **Fig. 33e**), albeit to significantly lower levels as seen in the RMS injections ($p < 0,001$ comparison Pax6 injection into SEZ and RMS). These data may be explained by SEZ precursors being biased – either by intrinsic or extrinsic factors – towards a GN fate, suggesting a new concept of early subtype specification during adult neurogenesis.

Given the close correlation of Pax6- and TH-immunoreactivity I next examined whether Pax6 overexpression is also sufficient to induce differentiation of PGNs towards a dopaminergic transmitter phenotype. Indeed, already 2-3 weeks after viral injection, the number of TH-positive PGNs was significantly increased after Pax6 transduction compared to the control virus injections in both SEZ (**Fig. 34b**). Since it is well established that the final acquisition of TH-immunoreactivity for newborn neurons takes several weeks (Winner et al., 2002) and requires synaptic contacts (Brunjes, 1994), I also examined TH-immunoreactivity 3 months after viral injection. Now $33.2\pm 5.7\%$ of all GFP-positive PGNs resulting from control virus injections in the RMS had acquired TH-immunoreactivity ($n = 123$, 3 hemispheres, 2 animals; **Fig. 34a**). Strikingly, about half of all GFP-positive PGN had acquired TH-immunoreactivity 2-3 months after injection of Pax6-containing virus into the RMS ($48.1\pm 1.4\%$, $n = 116$ GFP-positive PGN from 4

hemispheres, 3 animals; $p < 0.05$ as compared to control vector injection to the RMS). These results strongly suggest that Pax6 overexpression significantly promotes the acquisition of a dopaminergic transmitter phenotype in adult neurogenesis.

In the RMS injections, Olig2 was able to interfere with the differentiation of PGNs (**Fig. 33f**; $n = 373$, 4 hemispheres, 2 animal, $p < 0,0001$ compared to GFP-control virus injection into the RMS). In contrast, Olig2-VP16 exerted no significant effects on neuronal subtype specification in the RMS (**Fig. 33f**), further supporting that it does not exert unspecific effects on precursors devoid of endogenous Olig2. Since Olig2 is not expressed in RMS precursors I wondered whether the ectopic expression by Olig2-containing virus may exert its effects by downregulation of Pax6. Indeed, few Olig2-infected precursor cells in the RMS expressed Pax6 7 days after infection (Olig2IRESGFP: $19 \pm 1\%$, $n = 99$, 1 hemisphere, 1 animal) compared to a majority of Pax6-positive cells ($80 \pm 3\%$, $n = 163$, 1 hemisphere, 1 animal) after control virus injection. However, injections of Olig2 or Olig2-VP16 constructs into the SEZ were not able to elicit any change in neuronal subtype specification (**Fig. 33e**; Olig2: $p < 0,05$ compared to GFP control in the SEZ, $n = 176$, 3 hemispheres, 3 animals; Olig2-VP16: $p = 0,21$ compared to GFP control in the SEZ, $n = 406$, 4 hemispheres, 3 animals) Taken together, these data suggest that olig2 exerts no direct effect on neuronal subtypes and endogenous Olig2 expression in the immature type C precursors is not required for granule cell specification. These data, taken together with the results for Pax6, would imply that neuronal subtypes are specified at later stages in the lineage progression.

6.4.2.3 Overexpression of Pax6 in non neurogenic astrocytes in vivo

The results presented above revealed a potent role of Pax6 as neurogenic fate determinant in endogenous adult neurogenesis originating from astrocytes. Therefore one could suggest that Pax6 may be sufficient to convert non-neurogenic astrocytes towards neurogenesis in endogenous adult neurogenesis

However, most other astrocytes in the adult brain are not neurogenic under normal conditions. Indeed it was recently shown that astrocytes isolated from non neurogenic regions of the postnatal (P11) brain could still differentiate into neurons by

overexpression of the transcription factor Pax6 (Heins et al., 2002). However since these experiments were carried out *in vitro* it was not possible to distinguish if it was the intrinsic change of the astrocytes by Pax6 alone or if other alterations of the astrocytes or their environment helped these cells to differentiate into neurons. Towards this end, I decided to carry out these overexpression experiments *in vivo* at comparably early postnatal stages (P8) when many GFAP-positive cells in the cortex are still dividing. Retroviral vectors (control and Pax6) described above were injected into the cerebral cortex of p8 pups (see Materials and Methods) and the animals were sacrificed after two different survival times, namely after 7 and 14 days.

After transduction with the control virus almost all GFP-positive cells were GFAP-positive astrocytes ($91\% \pm 9\%$, $n = 119$, 3 animals, **Fig. 36f**) 7 days after injection. No neurons or cells expressing early neuronal markers (PSANCAM or DCX) were observed amongst the GFP-positive cells after control virus injection. To study the amount of endogenous neurogenesis ongoing in the postnatal cortex, I examined the phenotype of the control infected cells also 14 days post injection. Again I found no neurons and no cells expressing early neuronal markers (PSANCAM or DCX) in these experiments. Notably, however, some cells seem to lose GFAP-expression, but the vast majority of all GFP-infected cells were still GFAP positive astrocytes ($75\% \pm 19\%$, $n = 109$, 4 animals, **Fig. 36b,f**). These data indicate that GFAP positive astrocytes were the main cell type affected by the injection of the retroviral particles and therefore validated the experimental system as useful for studying the effect of Pax6 on astrocytes in their *in vivo* environment.

In contrast to these control injections, the number of GFAP-positive, GFP-positive cells was reduced ($62\% \pm 11\%$, $n = 25$, 3 animals, **Fig. 36d,f**) compared to control injections 7 days after transduction with the Pax6 containing virus. Furthermore, a larger number of Pax6 transduced cells expressed of early neuronal markers (DCX: $8\% \pm 1\%$, $n = 33$, 3 animals; PSANCAM $6\% \pm 6\%$, $n = 31$, 3 animals, **Fig. 36f**). However no NeuN positive neurons could be detected (0% , $n = 18$, 3 animals, **Fig. 36f**), suggesting that the neuroblasts/ neurons induced by Pax6 are still immature. To determine whether the number of newly born neurons would increase and differentiate in the adult cortex, I examined the phenotype of the Pax6 transduced cells 14 days post injection. Indeed a

further increase in the number of cells with neuronal characteristics was observed (DCX: $20\% \pm 6\%$, $n = 29$, 3 animals; PSANCAM $10\% \pm 9\%$, $n = 32$, 3 animals, **Fig. 36c,e,f**) and also the number of GFAP positive cells were further decreased ($20\% \pm 6\%$, $n = 23$, 3 animals, **Fig. 36d,f**). Taken together these results indicate that non neurogenic endogenous astrocytes of the cerebral cortex can be induced to differentiate into cells with early neuronal characteristics in situ by overexpression of the transcription factor Pax6.

7 Discussion

The molecular signals specifying neuronal, glial or multipotent precursors in the developing and adult CNS are largely unknown. Radial glial cells have recently been discovered as major precursor population generating neurons or glial cells in separate lineages in the developing CNS.

Here I present a novel method to selectively enrich neurogenic or non-neurogenic radial glia. Towards the aim to identify fate determinants I compared their gene expression to multipotent precursors *in vitro* and *in vivo*. Olig2 was expressed to higher levels in multipotent compared to neuronal or glial precursors, while Pax6 showed the converse expression profile.

Therefore I focused further on the functional analysis of Pax6 and Olig2 in neural stem cell *in vitro* and *in vivo*. Pax6 expression is enriched in neurogenic radial glia and adult SEZ precursors, while Olig2 expression levels are higher in neural stem cells *in vitro* and transit-amplifying precursors of the SEZ. Interference with Olig2 in neural stem cells *in vitro* revealed its role in self-renewal.

In adult neural stem cells of the SEZ overexpression of Olig2 promoted oligodendrocyte formation. Pax6, in contrast, proved to be a very potent neurogenic determinant since neurogenesis is not only Pax6-dependent in neural stem cells *in vitro*, but also in adult neural stem cell *in vitro*.

Taken together, these results demonstrate a pathway combining transcription factors of dorsal and ventral regions that is activated in a specific lineage progression of adult neural stem cells *in vitro* and *in vivo*. Most importantly also in regard to therapeutic approaches, this work revealed the molecular mechanisms to direct adult neural stem cells towards a specific cell fate, neuronal or oligodendroglial.

7.1 Regional heterogeneity of radial glial cells

Radial glial cells have recently been discovered as an important CNS precursor population comprising neurogenic and non-neurogenic lineages in the cortex (Malatesta et al., 2003; Malatesta et al., 2000; Miyata et al., 2001; Noctor et al., 2001; Tamamaki et

al., 2001). My experiments show that the fate of radial glia progeny differs if radial glia are isolated from different brain regions. Cortical radial glia mostly generated neurons, whereas GE radial glia generated mostly glial cells (**Fig.7**). Importantly, this did not change, when these radial glia were cultured in the GE or the cortex environment, respectively. Cortical radial glia (cultured in a GE environment) still generated mostly neurons and GE radial glia still generated mostly glia in a cortex environment in vitro (**Fig.7**). Therefore, I conclude that these subpopulations of radial glia are intrinsically different. Since the transcription factor Pax6 is expressed only in cortical but not GE radial glia (Götz et al., 1998) and the neurogenic radial glia is severely reduced in the Pax6 mutant cortex (Ericson et al., 1997; Heins et al., 2002), Pax6 seems to act as cell-autonomous determinant of neurogenic radial glial fate in the developing telencephalon. Interestingly, Pax6 is also expressed in a subset of radial glia in the spinal cord (Ericson et al., 1997) and might also contribute to the neuronal lineage of the radial glia in this region.

Since radial glia in the ventral telencephalon contribute little to the generation of neurons in the basal ganglia, different precursors must be responsible for their generation. Indeed, the GE contains a particularly prominent subventricular zone (SVZ) during embryogenesis, a region populated by precursors that undergo mitosis at some distance from the ventricular surface (Smart, 1976). In contrast to the cortex where the SVZ is very small, almost half of the progenitor pool of the GE is located in the SVZ (Smart, 1976). I confirmed this hypothesis, that SVZ cells generate the neurons in the GE by subdissection of the GE VZ and SVZ (**Fig. 8**). Selective enrichment of VZ or SVZ precursors confirms that few of the VZ precursors in the GE generate neurons, while precursors located above the VZ generate neurons more frequently. My in vitro data are further supported by previous genetic evidence implying the embryonic SVZ as the source of striatal neurons. The embryonic SVZ precursors express the transcription factors Dlx1, Dlx2, Mash1, and Ebf1 (Eisenstat et al., 1999; Garel et al., 1999; Porteus et al., 1994) that have been implicated with neurogenesis in the GE (Xu et al., 2003). Importantly, mouse mutants for these transcription factors expressed mostly in the embryonic SVZ of the GE have defects in neurons of the striatum (Anderson et al., 1999; Casarosa et al., 1999; Eisenstat et al., 1999), supporting the role of Mash1 and Dlx genes

in neurogenesis from SVZ precursors. Lineage tracing in the GE revealed clones containing neurons and radial glial cells (Reid and Walsh, 2002) that derive either from a radial glia cell generating a neuron and a radial glia (as observed in the cortex by Noctor et al., (Noctor et al., 2001) or from an earlier neuroepithelial precursor giving rise to a radial glia and neurogenic precursors, e.g., located in the SVZ (Haubensak et al., 2004; Miyata et al., 2001; Noctor et al., 2004). Indeed, neuroepithelial cells generating both SVZ cells and radial glia with mostly the former continuing to produce neurons is a scenario that would unify all presently available data. Surprisingly few clones containing neurons and radial glia have been described in the cortex, where radial glia are the main source of neurons. This is explained by the observations of Miyata et al. and Noctor et al. (Miyata et al., 2001; Noctor et al., 2001; Noctor et al., 2004; see also **Fig. 1**) that radial glial cells transform into postmitotic neurons (Malatesta et al., 2003). Thus, these data suggest that there are two different ways to generate neurons. One from radial glial cells that seems the predominant mode in the developing CNS, and a second way to generate neurons from SVZ precursors as observed in the developing basal ganglia.

Interestingly, when GFP positive radial glial cells are isolated from transgenic mice expressing GFP driven by the brain lipid binding protein (BLBP) promoter and examined at E10 or mid-neurogenesis stages, only the former, but not the later generate neurons (Anthony et al., 2004) Thus, my analysis and Anthony et al. agree in the observation that radial glial cells in the ventral telencephalon are mostly not neurogenic except at very early stages. However, it should be noted, that in the developing mouse brain, VZ cells generate SVZ cells already around E11 (Hashimoto and Mikoshiba, 2004). Thus, the early onset of GFP expression under the control of the BLBP promoter in the basal telencephalon can label not only early precursors/radial glia themselves but of course also their descendant SVZ precursors. Since SVZ cells are neurogenic, the neurons that are supposed to be generated from radial glia may be generated indirectly via SVZ cells

Additionally, Anthony et al (Anthony et al., 2004) also showed that the majority of BLBP-positive cortical radial glia at E14 generated mixed clones while the majority of clones were composed only of neurons and were not committed to the neuronal fate. There are two important differences between my data and the ones from Anthony et al

(Anthony et al., 2004). First I isolated GLAST-positive radial glia (see also page 37, Malatesta et al., 2000), but Anthony et al. isolated BLBP-positive radial glia. It was shown that there are different subsets of radial glia and the composition of these subsets changes during development (Hartfuss et al., 2001). Most radial glia express GLAST throughout embryonic development, whereas BLBP is up-regulated in the radial glia during development becoming the major population of all radial glial cells at late developmental stages (E18). (Hartfuss et al., 2001) These facts suggest that BLBP-positive radial glia are precursor restricted to the glial lineage, but can not be taken into account for the higher proportion of mixed clones observed by Anthony et al.

However, the second important difference can be found the cell culture system used. Anthony et al. cultured isolated radial glia on feeder cells, but added high concentration of FGF2 to the medium. Even though it was shown by many labs that the culturing of primary cells in chemically defined medium can very well mimic the in vivo environment (Hack et al., 2004; Hajihosseini and Dickson, 1999; Lillien, 1997; Qian et al., 1998), I have found FGF2 or EGF elicit prominent changes in transcription factor expression in this cell culture system. For example, Olig2 was strongly upregulated also in neurosphere cultures, a culture system to specifically enrich multipotent neural stem cells. Therefore these changes could well impose such changes in cell fate and could therefore explain the high proportion of mixed clones generated by cortical radial glia at E14. Taken together, these different lines of evidences suggest that the mode of neurogenesis is different between dorsal and ventral telencephalon, the former generates neurons mostly from radial glial cells while in the latter region most neurons are generated from SVZ precursors.

7.2 Radial glial cells from the cortex are heterogeneous

Given that radial glial cells even within the cortex gave rise to distinct lineages (multipotent, glial-restricted, and neuronal-restricted), I aimed to separate these to determine their intrinsic fate differences. The isolation of the strongly green fluorescent fraction of cells from the cortex of hGFAP-eGFP mice lead to an enrichment in non-neurogenic precursors while the neurogenic precursors were depleted to a fifth of the

content in the weakly green fluorescent fraction. This enrichment allowed me to detect significant differences in expression levels of several candidate genes (**Fig. 11**), for example a five-fold increase in the expression levels of Olig2 and Emx2 in the fraction enriched in non-neurogenic precursors. Notably, the non-neurogenic progeny is heterogeneous with only some precursors generating differentiated glial progeny (most GFAP-positive astrocytes and very few O4-positive oligodendrocytes), while many cells remain undifferentiated and contain only nestin (Malatesta et al., 2003; Malatesta et al., 2000). Since these less differentiated cells do not generate neurons and hardly any oligodendrocytes in dissociated cell cultures, even after growth factor addition (Götz et al., 2002), I interpret these as immature astroglial cells and refer to this fraction of precursors as ‘gliogenic’ with a predominant astroglial fate (**Fig. 2**). However, at least some of these astroglial precursors can still react to the neurosphere culture conditions, since the strongly green fluorescent cells generated more neurospheres than the weakly green fluorescent fraction see Results page 41). Thus, the increased level of Olig2 expression in this fraction also correlates to an increased neurosphere-forming capacity, consistent with the upregulation of Olig2 in neurosphere cultures and its role in undifferentiated multipotent precursors. Similarly, the increased level of Emx2-expression might be linked to a more immature precursor state of this fraction, since our previous functional analysis implied Emx2 as a positive signal for immature and bi-/multipotent precursors in dissociated cell cultures without growth factor addition (Heins et al., 2001).

In the fraction of radial glia enriched in neurogenic cells, I detected a five-fold higher expression level of Pax6, consistent with the previous evidence for a role of Pax6 in neurogenesis from cortical radial glia (Heins et al., 2002). Ngn2 is a direct target of Pax6 (Scardigli et al., 2003), and hence would be expected to be up-regulated as well in neurogenic precursors. However, the mRNA level of Ngn2 proved to be sensitive to the FACS procedure and was reduced in all the cells sorted from cortex even below the levels normally seen in the GE. No conclusions can therefore be drawn about Ngn2. Notably all the other transcription factors examined here were not affected in their expression level by the FACS procedure in comparison to un-dissociated cortical tissue from the same embryonic stage. The sorted cells also maintained region-specific

differences in expression levels (high levels of Emx1, 2 and Pax6 and low levels of Dlx1, 2, Mash1, Gsh2 and Olig2). Taken together, the five-fold enrichment of neurogenic versus gliogenic/immature precursors by FACS is a useful procedure to identify relevant differences in gene expression levels.

7.3 Changes of gene expression patterns upon EGF and FGF2 in neurosphere cultures

In comparison to the sorted precursors I examined gene expression patterns in the widely used culture model of neurospheres that takes advantage of the dedifferentiating function of EGF and FGF2. When I analyzed the influence of these growth factors on gene expression, I observed prominent changes even after short-term exposure to these growth factors in adherent dissociated cell cultures. While the regional specification is well conserved in these cultures without growth factor addition, the number of Olig2- and Mash1-immunoreactive precursors is increased already two days after EGF or FGF2 addition until almost all precursors from the cortex or GE become Olig2-immunopositive after 1 week in FGF or EGF (**Fig. 14,15**). Conversely, Pax6 and Emx1 were down regulated, while Dlx- and Gsh2-immunoreactivity was not affected (**Fig. 14,15**). Thus, at least some of the gene expression changes observed in neurosphere cultures seem to be due to the growth factor exposure.

Indeed, EGF infusion in vivo elicits similar changes in the adult subependymal zone (SEZ; Doetsch et al., 2002) with a decrease in PSA-NCAM-positive type A and a corresponding increase in the fast proliferating type C cells. These data are well consistent with my data on a downregulation of Pax6 upon EGF exposure in vitro and the localization of Pax6 in the PSA-NCAM-positive type A cells in vivo (**Fig. 25**). Furthermore, I observed an upregulation of Olig2 upon EGF in vitro and found Olig2 in the fast proliferating precursors labeled by a short BrdU-pulse in the adult SEZ in vivo.

These data obtained with telencephalic cells are well consistent with recent data obtained with precursors from the spinal cord that also up-regulate Olig2 and down-regulate the dorsal spinal cord transcription factors Pax3 and Pax7 upon FGF2 exposure

(Gabay et al., 2003). Interestingly, FGF4 was recently also identified as signal from presomitic mesoderm restraining neuronal differentiation by interfering with e.g. the onset of Pax6 expression (Bertrand et al., 2000; Diez del Corral et al., 2003; Novitch et al., 2003), suggesting a common dedifferentiating function of FGF2 and FGF4 signaling. Taken together, these data suggest that the ventralizing function of FGF2 is rather context- and stage-dependent, while the inhibitory effect on cell differentiation seems rather widespread during nervous system development.

Indeed, the neurosphere culture model may be best viewed as an environment repressing regional or cell type specific differentiation accompanied by high rates of proliferation. Notably, telencephalic cells cultured for 4 passages as neurospheres seemingly had lost any patterning information, and undergone more severe changes in gene expression than observed after short-term exposure to growth factors when cells still maintained some region-specific patterns (Dlx and Gsh2 in GE cells). No or negligible differences were detectable in the expression levels of 14 transcription factors that normally differ between cortex or GE cells after exposure to neurosphere culture conditions for 5 weeks. Consistent with a general dedifferentiation, the expression levels of most transcription factors were reduced in the neurosphere cultures, regardless of their normal expression in the dorsal (Pax6, Ngn2, Emx1, 2) or ventral telencephalon (Dlx, Gsh2, Vax1, islet-1; Nkx2.2), with the exception of Olig1 and 2 that were up-regulated to even higher levels than normally in the GE. These gene expression changes therefore abolished almost all region-specific differences between the precursors from which the neurosphere cultures were originally started. This dedifferentiation to a pan-neurosphere expression level might explain the surprising similarity in the transcriptom analysis of neurosphere and embryonic stem cells (Ramalho-Santos et al., 2002). Thus, this profile of gene expression may reflect the undifferentiated state of an early, not yet regionally specified neural precursor, similar to the type of precursor that is maintained by FGF signaling during development in the neural tube in vivo until retinoid signaling initiates neurogenesis accompanied by dorso-ventral patterning (Diez del Corral et al., 2003; Novitch et al., 2001; Sockanathan et al., 2003).

However, how can these data that suggest dedifferentiation and/or loss of regionalization of neural cells in neurosphere cultures (Gabay et al., 2003; Santa-Olalla et

al., 2003), be reconciled with previous work claiming a maintenance of region-specific differences in neurosphere cultures (Hitoshi et al., 2002b; Ostenfeld et al., 2002; Parmar et al., 2002). One interesting explanation could be the effect of cell density that would also explain some of the differences seen with adherent cell cultures and neurosphere cultures. As long as cells still interact with their normal neighbors they might still receive positional information that is only partially overridden by the potent growth factor signaling. This effect is known as ‘community effect’ and may account for the maintenance of some regional differences in the high density neurosphere cultures (Ostenfeld et al., 2002; Parmar et al., 2002) where cells were grown at 25-40x higher concentrations than in my clonal culture conditions (Morshead et al., 2003). Interestingly, loss of regionalization has been reported by Santa-Olalla et al. (Santa-Olalla et al., 2003) that also use relatively high density cultures, but also use 5-10x higher growth factor concentrations. There is, however, also a technical concern with studies that only rely on semi-quantitative RT-PCR data (Hitoshi et al., 2002b; Santa-Olalla et al., 2003). Here I have used real-time RT-PCR that is certainly a technical improvement in accuracy, since it allows data analysis in the phase of constant amplification efficiency and normalized relative quantification is not dependant anymore from estimating DNA band densities on agarose gels that is subject to contamination and lack of sensitivity. Moreover, I have confirmed my data at the protein level, especially for those genes where there are discrepancies to other studies (*Emx1*, *Pax6*, and *Dlx*). However, it is also important to realize that some region-specific differences between neurosphere cells might not be completely lost, since there are still small differences in the number of neuronal subtypes generated from neurosphere cells of different origin. For example, I also observed that *Dlx2* (one of the 4 genes that were maintained in a region-specific manner in the analysis of Hitoshi et al., (Hitoshi et al., 2002b)) is up-regulated during differentiation of neurosphere cells only in those originating from the GE, but not in those of the cortex (**Fig. 16**). Indeed, these subtle differences upon differentiation may also explain the distinct cell migration behavior after transplantation on slices (Hitoshi et al., 2002b). However, it is important to realize that even though some subtle regional differences may still exist they are minor compared to the in vivo situation. For example, the ‘region-specific’ *Dlx2*-expression levels in GE neurospheres were 1000x lower than the normal

Dlx2 expression level in the ventral telencephalon. Indeed, the loss of regionalization is also obvious at the functional level, e.g. in regard to neuronal differentiation. Notably, neurosphere cells from different regions mostly generate GABAergic neurons (own observations; (Ciccolini et al., 2003; Hitoshi et al., 2002b; Parmar et al., 2002), a widespread neuronal subtype, while those subtypes that occur only in specific regions, such as dopaminergic neurons, are notoriously difficult to produce from neurospheres even if they originate from the region that generates dopaminergic neurons in vivo (Yan et al., 2001). Taken together, these results underline the concept that regionalisation and neurogenesis are inseparably linked during normal development (Bertrand et al., 2002; Götz et al., 1998) and the loss of regionalisation in neurosphere cultures impairs neurogenesis.

7.4 Transcriptom analysis

The characterization of the global gene expression profiles described in this Ph.D. work gives me and others a database to explore the basic biology of functionally distinct precursor populations. In the current study, I performed an oligonucleotide microarray analysis on the neurogenic precursors (GFP+) and the more non-neurogenic population (GFP++) from E14 hGFAP-eGFP mice and the neurosphere cells isolated from the E14 cortex undifferentiated and differentiated for 1 days. The undifferentiated neurospheres are a population enriched for multipotent precursors. The neurosphere cultures differentiated for 1 day are a population of mostly gliogenic precursors, and would therefore be most similar to the non-neurogenic population (GFP++) from E14 hGFAP-eGFP mice (**Fig. 3**).

The comparison of gene expression in the model of multipotent cells, the neurosphere cultures, to previous analysis revealed several similarities (Geschwind et al., 2001; Ivanova et al., 2002; Ramalho-Santos et al., 2002). Recent descriptions of gene expression patterns within stem-cell populations are starting to define their molecular profiles (Geschwind et al., 2001; Ivanova et al., 2002; Ramalho-Santos et al., 2002). Ivanova et al. generated neurospheres from the embryonic ganglionic eminence, while Ramolho-Santos derived their neurospheres from the adult mouse SEZ. As discussed

previously, there are at least for some important candidate genes no significant differences in gene expression between both regions. These authors then compared the gene expression in neurosphere cells to embryonic or hematopoietic stem cells to identify common genes determining “stemness” multipotent fate.

Notably I also observed upregulation of a number of genes in the undifferentiated neurosphere cultures that were identified as stem-cell specific in common by those groups (Ivanova et al., 2002; Ramalho-Santos et al., 2002). These genes include Fyn, Slit2, tenascin C, and insulin-like growth factor binding protein 2 or cyclin D.

Furthermore I looked for genes specifically associated with neural development. It is of interest that only few of the Wnt genes are expressed within the neurospheres (Wnt 5a, 7a, 7b). Wnt has recently been shown to antagonize neural development in mouse ES cells (Aubert et al., 2002). In some cases, these findings may be very relevant to future studies looking at differentiation or proliferation of these cells. For example, the FGF receptors FGFR1 and FGFR3 were expressed but not FGFR2. The expression of FGF-2 and its receptor FGFR1 may imply paracrine or autocrine effects of this mitogen on the growth of these neurosphere cells. Similarly, platelet-derived growth factor receptor (PDGFR) alpha, but not beta, was expressed. However, a number of genes that I expected to be expressed at high levels were not expressed. For example, *musashi1* has been associated with neural stem cell populations (Kaneko et al., 2000; Keyoung et al., 2001), but was absent in the mRNA of undifferentiated neurospheres. As Keyoung et al. examined *musashi1* in short-term cultures only, it is possible that this RNA-binding protein is down-regulated after the longer growth periods used in this study.

Since I was able to isolate and to enrich three to four functionally distinct precursor populations (**Fig. 3**), I wanted to assess which genes might be linked to different fate decisions. Several known genes were expressed in only one or two related populations of the four different precursor populations. Some of these genes have not yet been implicated with neural development. Some genes are specifically highly expressed in undifferentiated neurosphere cultures and would therefore be expected to play a role in multipotent cell fate. One of these was *tweety* is a novel maxi-Cl(-) channel (Suzuki and Mizuno, 2004) and FABP7 is the brain specific fatty acid binding protein (Hartfuss et al., 2003; Hartfuss et al., 2001; Veerkamp and Zimmerman, 2001). While the function of

tweety in multipotent precursors remains to be determined, FABP7 (BLBP) was shown to label a population of cells in the embryonic telencephalon enriched for multipotent precursors (Anthony et al., 2004). The expression levels of sirtuin2, a NAD-dependent deacetylase that regulates muscle gene expression and differentiation by possibly functioning as a redox sensor (Fulco et al., 2003), were also increased in undifferentiated neurosphere cultures.

The expression of Sox9 peaked in the populations enriched for gliogenic precursors (GFP⁺⁺, dd1) and indeed when Sox9 is ablated in neural stem cells the specification of astrocytes and oligodendrocytes is strongly affected (Stolt et al., 2003). Finally Sox4 and LMO-1 (Lim domain only-1) were strongest expressed in the neurogenic precursors. Both of them are known to be expressed in the developing and adult CNS in specific precursor populations, but their specific function in cell fate specification still remains to be determined (Cheung et al., 2000; Hinks et al., 1997).

Clearly, the limitations of detection of the microarray system preclude the complete description of gene expression in neural stem cells and restricted precursors. However, given this caveat, this database displays highly reliable gene expression data and may be considered as at least a representative part of distinct telencephalic precursors.

Taken together this gene expression analysis revealed the differential gene expression of several interesting candidates that could be grouped to functionally distinct precursor subsets. Most importantly, the expression of Pax6 could be linked to neuronal-restricted precursors, whereas the expression of Olig2 could be restricted to multipotent neural stem cells. A further analysis of the microarray data may allow us to understand the transcriptional context in which these two fate determinants act.

7.5 The role of Pax6 in neurogenic precursors

7.5.1 Role of Pax6 in vitro in neurosphere cultures

Since I detected this strong upregulation of Pax6 in neurogenic precursors of the developing cortex in the gene expression analysis, I decided to analyze Pax6 functionally

in vitro. Previously, Pax6 transduction has been shown to have a potent neurogenic effect in precursors from the embryonic cortex (Heins et al., 2002), but no effect could be detected upon transduction of cells from the GE. In contrast, neurosphere cultures, however, all cells, independent of their region of origin reacted strongly to Pax6 expression and turned to more than 80% into neurons. Importantly, this was not only true for neurospheres generated of the embryonic brain, but also for neurospheres generated from the adult SEZ.

Moreover, neurogenesis from all neurosphere cells even became dependent on Pax6, indicated by the almost complete loss of neurogenesis from neurospheres independent from their region of origin of homozygous Pax6 mutant mice. In contrast, in vivo, neurogenesis in the cortex depends only partially on Pax6 (neurons are reduced by half) and Pax6 plays no role in neurogenesis in the GE (Heins et al., 2002; Schmahl et al., 1993). Notably, the Pax6-dependent neurogenic pathway was activated not only along the dorso-ventral axes, but also along the anterior-posterior axes since even cells from midbrain became Pax6-dependent for neurogenesis after neurosphere expansion. Thus, Pax6-mediated neurogenesis is the neurogenesis pathway activated in neurosphere cultures.

It will be important to determine the signaling mechanisms inducing this pathway in vitro as a lead into the mechanisms instructing this mode of fate specification in vivo. One explanation for the activation of this pathway, however, might be our previous suggestion that neurosphere cells assume a radial glia like phenotype (Hartfuss et al., 2001) and that Pax6 is the major neurogenic determinant for radial glial cells (Heins et al., 2002). Moreover, when mouse embryonic stem (ES) cells are treated with retinoic acid they generate an essentially pure population of glutamatergic projection neurons (Bibel et al., 2004; Plachta et al., 2004). Surprisingly this neuronal differentiation happens via a Pax6-positive radial glial-like cell like it is present in the dorsal telencephalon, but also in the spinal cord (Bibel et al., 2004), highlighting again Pax6 as a strong neurogenic fate determinant in different precursor cells.

By itself, however, the potent neurogenic role of Pax6 in neurosphere cultures is highly relevant for the attempts to reconstitute neurons in the adult mammalian brain that have so far suffered from the low degree of neuronal differentiation from neurosphere

cells *in vitro* (Song et al., 2002) and upon transplantation *in vivo* (Fricker et al., 1999; Herrera et al., 1999; Lim et al., 2000; Winkler et al., 1998). Indeed, I know that the neurons generated by Pax6-overexpression are functionally, even receiving synaptic inputs (Berninger, Hack, Grothe and Götz, unpublished observations). These data provide a promising avenue to improve functional reconstitution *in vivo*.

7.5.2 Role of Pax6 in vivo

7.5.2.1 Pax6 in adult neurogenesis

In fact, adult neural stem cells might depend on the same fate determinants as radial glial cells since I also detected Pax6 in neuroblasts migrating along the RMS. Indeed, adult neural stem cells have been identified as astrocytes and share not only many cell biological characteristics with radial glia but even have a common lineage origin (Merkle et al., 2004). This is in line with the observation that similar molecular pathways are involved in their specification.

Therefore the neurogenesis supplying the adult olfactory bulb (OB) is an excellent system to address the role of Pax6 *in vivo*. During adult neurogenesis distinct types of interneurons are continuously generated throughout adulthood (Altman, 1969; Lois and Alvarez-Buylla, 1994; Luskin, 1993). These are the GABAergic interneurons located in the granule cell layer (GCL) and glomerular layer (GL) as well as dopaminergic interneurons in the GL (Carleton et al., 2003; Kosaka et al., 1998; Kosaka et al., 1985). Important progress has been made in the identification of factors regulating stem or transit-amplifying cell fate as well as asymmetric cell division (Doetsch et al., 2002; Molofsky et al., 2003; Shi et al., 2004), but still nothing is known about the mechanisms directing cell progenitors towards specific neuronal or glial subtypes in the adult brain. Since Pax6 is contained only in adult neuroblasts (**Fig. 25**), I suggested that it may play an important role in this fate decision.

However, in the absence of functional Pax6 protein in the Small Eye mice, the OB fails to form altogether (Dellovade et al., 1998; Stoykova et al., 2003). Remnants of the OB lie as ectopic vesicles in the ventral telencephalon, and consist mostly of reelin-positive cells, potentially remnants of the mitral cells (Jimenez et al., 2000). Therefore, it

is impossible to conclude whether other neuronal subtypes fail to be generated, are misspecified or alternatively fail to migrate to this mislocalized vesicle.

My results imply Pax6 acts in the adult neurogenesis as a key factor in regulating this progression towards the neuronal lineage. Pax6 overexpression increases the proportion of neuroblasts amongst the infected cells, while interference with its normal function of transactivating specific target genes reduces the proportion of neuroblasts amongst the infected cells. This reduction seems not to be due to selective cell death upon viral infection, but rather to the effect of Pax6 to direct precursors towards a neurogenic fate. Notably, neurogenesis eventually leads to the generation of postmitotic daughter cells, a function combined by the target genes regulated via the paired domain of Pax6 that acts neurogenic and anti-proliferative in cortical precursors (Haubst et al., 2004; Heins et al., 2002). Indeed, the endogenous gradient of Pax6-positive precursors increasing rostrally within the RMS correlates to a reduced cell proliferation with increasing distance from the SEZ (Smith and Luskin, 1998).

These data prompt two important conclusions. First, Pax6 is involved in neurogenesis throughout the SEZ/RMS system, and second, SEZ and RMS precursors differ in their fate restriction mediated by Pax6. In regard to the first conclusion, it is important to bear in mind that GN precursors are the most frequent cell type throughout the SEZ/RMS (more than 90% in SEZ and still 70% in the center of the RMS). Thus, Pax6 is expressed in 50% of the GN precursors in the caudal RMS and all of them in the center of the RMS. Thus the effect of Pax6 deletion or dominant-negative constructs in the SEZ obviously blocks further Pax6 upregulation necessary for progression of the neuronal lineage. When Pax6 function is blocked in the SEZ, almost all infected precursors are deviated from the neuronal lineage – only 30% DCX-positive precursors are detectable 1 week after Pax6-engrailed virus infection, but none of these ever makes it to the OB and differentiates into a proper neuron. Since similar results were obtained by deletion of Pax6 in the SEZ, I conclude that neuronal specification is still reversible in almost all transduced SEZ precursors. This scenario fits well with the idea that upregulation of Pax6 mediates an irreversible commitment to the neuronal lineage. Most neuronal precursors in the SEZ have still very low levels of Pax6 not yet detectable by immunocytochemistry but soon become Pax6-immunoreactive within the RMS already

adjacent to the SEZ and most neuronal precursors migrating along the RMS express high levels of Pax6 and have obviously up-regulated its crucial target genes for neurogenesis. At this stage, the fate of most neuronal precursors (70% GN precursors in the RMS) can not be reversed anymore with the exception of the PGN precursors (30% GN precursors in the RMS) that seem to be specified much closer to the OB than the GN precursors.

The neurogenic role of Pax6 in adult neurogenesis is of interest also with regard to the origin of adult OB precursors. There is evidence suggesting that some adult SEZ precursors are derived from the ventral telencephalon (Merkle et al., 2004; Tramontin et al., 2003) as well as for extensive mixing between precursors from the dorsal and ventral telencephalon at early postnatal stages in this region (Marshall et al., 2003). Notably, Pax6 plays no role for neurogenesis in the ventral telencephalon (Heins et al., 2002) where neurons are generated by a very different precursor population during most of neurogenesis (Anthony et al., 2004; Malatesta et al., 2003). However, the OB originates from a unique domain in the dorso-lateral telencephalic neuroepithelium characterized by the expression of several ventral telencephalic transcription factors, such as Gsh2 and Dlx, together with Er81 and Pax6 (Stenman et al., 2003). Thus, adult OB precursors may maintain these characteristics from an earlier developmental stage and henceforth exhibit the unique combination of these transcription factors into adulthood. However, further lineage analysis is required to clearly define the fate of dorsal telencephalic progenitors melting into this region at postnatal stages (Marshall et al., 2003).

7.5.2.2 Neural subtype specification by Pax6

During development the local environment specifies fate by regulating intrinsic determinants. My results imply Pax6 in such a role, since GNs down-regulate Pax6 during neuronal differentiation within the OB, while Pax6 is maintained in the TH- and calbindin-positive subset of PGNs. The importance of the late expression of Pax6 in a specific neuronal sublineage was confirmed at the functional level, since retroviral transduction of Pax6 allows maintaining Pax6-expression and this resulted in the almost complete conversion of all precursors in the RMS towards a PGN fate. Thus, while GN precursors in the RMS are firmly restricted to the neuronal lineage and can no longer be

converted to a glial lineage – at least by the cues assessed here –their neuronal subtype is not yet fixed and maintenance of Pax6 is sufficient to direct them to a PGN fate. These data show that Pax6 is sufficient to instruct a PGN fate in adult neurogenesis, even though SEZ precursors seem to be less amenable to this fate conversion. My results also suggest that endogenous Pax6 levels are important for PGN specification while Pax6-engrailed transduction was not conclusive in this regard, because neurogenesis of PGN precursors was abolished altogether. Olig2-containing virus injected into the RMS still allowed neuronal differentiation of most infected precursors (90%), but none acquired a PGN identity. These data suggest that the delayed downregulation of Pax6 in Olig2-infected precursors still allowed neuronal differentiation but not anymore the acquisition of a PGN fate for which a late phase of Pax6 expression seems to be crucial. These data are particularly exciting since Pax6 imposed not only a lamina bias in the differentiation of OB neurons, but also promoted the acquisition of a dopaminergic transmitter phenotype. Thus, this study discovered the first fate determinant for the generation of dopaminergic neurons in the adult mammalian forebrain. This finding may have profound implications for human patients, where adult neurogenesis also continues in the OB (Bedard and Parent, 2004), despite a first failure to localize an RMS at more caudal positions (Sanai et al., 2004).

Taken together, the identification of a key fate regulator of adult dopaminergic neurogenesis combined with methods to allow RMS precursors to spread into the adjacent striatum (Saghatelian et al., 2004) may hence provide a powerful tool to improve the dopaminergic supply to diseased basal ganglia.

7.5.2.3 Pax6 in non neurogenic astrocytes

Besides rerouting the endogenous precursors present in the adult, an alternative approach may be to evoke neurogenic potential in astrocytes of other brain regions. Since my experiments showed that Pax6 has a potent neurogenic role in radial glia astrocytes could be an ideal system to utilize the neurogenic role of Pax6 for therapeutic purposes. This question was addressed in preparations of astrocytes from the postnatal cortex that generate functional neurons upon Pax6 transduction (Heins et al., 2002). Importantly this

is therapeutically very interesting since these experiments instruct the most frequent cell type in the adult brain, the astrocytes, towards the reconstitution of neurons. Moreover, astrocyte cultures in contrast to neurosphere cultures can be expanded in vitro without losing their region-specific properties (as outlined above), and also instruct specific neuronal phenotypes depending on their region of origin (Barbin et al., 1988; Denis-Donini et al., 1984; Wagner et al., 1999). These region-specific differences might be highly relevant for the attempts to reconstitute specific types of degenerating neurons.

The astrocyte cultures might serve as source for cell transplantation into lesioned brains, but the even better approach is for sure to activate endogenous astrocytes towards neurogenesis in vivo. Towards this end I examined whether astroglial cells in the mouse postnatal cortex, a non-neurogenic brain region, can be instructed towards neurogenesis by Pax6 transduction. Indeed, almost 20% of all infected cells expressed immature neuronal markers 2 weeks after infection with the Pax6-containing virus while no such cells could be observed after control virus injection. These experiments need to be continued for longer survival times to examine the neuronal survival and subtype identity. However, retrovirally mediated sustained expression of Pax6 in neurons of the cortex, that normally lose Pax6 during the maturation process, might be detrimental for the survival of the newly generated neurons. Inducible retroviral constructs allowing the initiation but also the termination of transcription of retrovirally transduced Pax6 might help to circumvent this problem.

The observation that there might be endogenous precursors with the ability to act as stem cells, but which are missing the right cues is also supported by other publications (Belachew et al., 2003; Chen et al., 2004; Magavi et al., 2000). In the specific lesion paradigm of phototoxic lesions in the cortex, neurogenesis was observed and it was reported that the new neurons differentiated from two different precursor populations, the SEZ precursors and precursors residing in the parenchyma (Chen et al., 2004; Magavi et al., 2000). Interestingly, in these photolytic injured brains, Leavitt et al. described that mature astrocytes dedifferentiated into RC2 + radial glia (Leavitt et al., 1999). As mentioned above, Pax6 is expressed in radial glial cells during neurogenesis (Götz et al., 1998) and is then down-regulated at the end of neurogenesis when radial glial cells differentiate in astrocytes and lose RC2 expression. It was further shown that cells

expressing NG2, a marker used for oligodendrocyte precursors, are neurogenic and can form neurospheres in vitro (Belachew et al., 2003). Taken together, these data imply that subpopulations of glial cells reside in the parenchyma outside of the neurogenic niches can act as neurogenic precursors. Therefore it might be necessary that mature astrocytes dedifferentiate in an earlier radial glia like state that enables them again to divide and to give rise to new neurons. The dedifferentiation seemingly can be induced by lesion (Leavitt et al., 1999) or overexpression of Pax6.

This leads us to the issue why some astrocytes in the adult CNS are neurogenic and others are not. These astrocytes could differ intrinsically or the local environment outside of the neurogenic niches may not be permissive. Shh and BMPs, which form opposing gradients of diffusible signaling molecules along the dorso-ventral axis (Tekki-Kessaris et al., 2001), respectively promote oligodendroglialogenesis during embryogenesis at the ventral telencephalon in vivo (Tekki-Kessaris et al., 2001) and astrocytogenesis (Mabie et al., 1997; Mehler et al., 2000; Nakashima et al., 2001). In dorsal regions BMPs not only promote astrocyte fate, but also inhibit neurogenesis and oligodendrocytogenesis, both of which developments can be inhibited by the antagonist, Noggin. Many, if not all, of these molecules are expressed within the SEZ. For example, BMP4 is expressed in SVZ/SEZ cells from the embryonic period through adulthood, along with type I and II BMP receptors, suggestive of an autocrine loop (Gross et al., 1996). In the adult telencephalon, BMPs are expressed by SEZ cells while the antagonist Noggin is expressed by ependymal cells adjacent to the SEZ (Lim et al., 2000). Indeed Lim et al. further showed that overexpression of BMPs in ependymal cells inhibits neuronal differentiation in vivo, and ectopic overexpression of noggin in the striatum creates a neurogenic environment for transplanted neurosphere cells (Lim et al., 2000). Therefore, the blocking of BMPs might be one way to convert a non-neurogenic into a neurogenic environment. Also Shh has also been localized only so far within the SEZ in the developing brain (Murray et al., 2002).

7.6 The role of Olig2 in multipotent precursors

7.6.1 Olig2 in vitro in neurosphere cells

Since Olig2 expression levels correlated to a multipotent fate, I examined this at the functional level first in neurosphere cells. The two main characteristics of a stem cells are the multipotency and the ability to self renew. Therefore, I performed experiments to assess if Olig2 has a role in one of these stem cell characteristics or even in both. Indeed, interference with Olig2 function in differentiating neurosphere cells impaired both the generation of neurons as well as oligodendrocytes, consistent with a role of Olig2 in neurogenesis and oligodendrocyte specification (Lu et al., 2002; Mizuguchi et al., 2001; Novitch et al., 2001; Park and Appel, 2003; Tekki-Kessararis et al., 2001; Zhou and Anderson, 2002). The competition of the repressor Olig2 and the activator Olig2VP16 in neurosphere cells exposed to differentiation conditions results in a 70% reduction in neuronal and oligodendrocyte differentiation. The remaining neurogenesis and oligodendrogenesis seen in Olig2VP16-expressing cells may be due to effects of Olig1 that is also increased in neurosphere cultures, or to the high endogenous Olig2 expression levels. Indeed it was observed that Olig1 can compensate for functions of Olig2 in studies that compared Olig2(-/-) mutants to Olig1/2(-/-) in the spinal cord (Lu et al., 2002; Zhou and Anderson, 2002). Due to the high degree of protein conservation, Olig1 could partially compensate the loss of Olig2, so that several markers of the pMN domain were maintained (Lu et al., 2002). While Olig2 is required in most cells to generate neurons and/or oligodendrocytes, it is not sufficient to instruct neurons or oligodendrocytes in neurosphere cells, in contrast to Pax6. Notably, at the time of Olig2 infection most neurosphere cells still expressed Olig2 and higher levels do not further promote the generation of neurons or oligodendrocytes. Thus, other crucial fate determinants are lacking, such as Pax6 and Ngn2 for neurogenesis and Nkx2.2 for oligodendroglialogenesis (Mizuguchi et al., 2001; Novitch et al., 2001). Conversely, however, the downregulation of Olig2 in neurosphere cells exposed to differentiation conditions seems to be required for the differentiation into GFAP-positive astrocytes, since overexpression of Olig2 potently repressed the acquisition of astroglial fate, consistent with previous data (Gabay et al., 2003; Zhou and Anderson, 2002; Zhou et al., 2001). Thus, Olig2 as a repressor

inhibits astroglial differentiation and this may be one reason why the few neuronal and oligodendrocyte precursors differentiating in this system require Olig2 function for their differentiation.

However, under expansion conditions with high levels of EGF and FGF2, Olig2 obviously does not promote the generation of neurons and oligodendrocytes, but rather is required for the proliferation and self-renewal of neurosphere cells, since interference with Olig2 under these growth conditions severely reduced the generation of new neurospheres.

Similar to the effect of Bmi-1 deletion (Molofsky et al., 2003), interference with Olig2 under these growth conditions severely reduced the number and size of neurospheres, implying Olig2 also in self-renewal and proliferation of neurosphere stem cells. However, how similar is a neurosphere stem cell *in vitro* to a neural stem cell *in vivo*? The SEZ can be temporarily depleted of fast proliferating cells using the anti-mitotic agent cytosine- β -D-arabinofuranoside (Ara-C) thereby deleting neurogenesis. These studies revealed that cells positive GFAP were the slow dividing neural stem cells since they were able to reconstitute all other types of precursors (Doetsch et al., 1999; Kirschenbaum et al., 1999). And indeed, neurosphere stem cells differ from neural stem cells *in vivo* by their fast proliferation. Indeed, Olig2 may also mediate proliferation upon exposure to EGF or FGF2, as its expression was also increased in adherent cells treated with these growth factors that may be less multipotent.

7.6.2 Olig2 in vivo in adult neurogenesis

Consistent with these *in vitro* data, I observed Olig2 in fast proliferating cells in the adult SEZ *in vivo* where Olig2 mostly co-localized with Lewis X, but not with PSA-NCAM or GFAP, suggesting a role of Olig2 in transit-amplifying type C cells. Interestingly, *in vivo* infusion of EGF enhanced the proliferation of these transit amplifying that express high levels of the EGF receptor (Doetsch et al., 2002). These *in vivo* results together with my *in vitro* data indicate Olig2 is expressed in EGF-responsive type C cells. My data were further confirmed by a study from Aguirre et al. (Aguirre et al., 2004), in which NG2 expressing fast proliferating precursors in the adult SEZ were

identified coexpressing Olig2 and Lewis X. Taken together, these data suggest that Olig2 may act in transit-amplifying precursors in vivo and mediate their proliferation.

Consistent with this scenario of progressive neuronal fate specification observed with Pax6 (discussed above), high levels of Olig2 were only able to convert neurogenesis to oligodendroglialogenesis in the SEZ, but not RMS. Olig2 is almost exclusively expressed by the transit-amplifying cells in the SEZ, but not in the RMS. While cells with the antigenic characteristics of transit-amplifying precursors are detectable in the RMS, they are not Olig2-immunopositive, suggesting that this lineage differs intrinsically from the lineage in the SEZ. One interpretation is that these cells are also not bi-potent as there is no oligodendroglialogenesis from RMS cells (**Fig. 3**), consistent with a role of Olig2 in bi- or tri-potent cells (Gabay et al., 2003; Hack et al., 2004; Lu et al., 2002; Zhou and Anderson, 2002). However, further analysis is required to characterize the nature of precursor subtypes within the RMS, since it is not yet clear to which extent the supposed type C cells in the RMS really have transit-amplifying identity (Doetsch et al., 2002; Garcia et al., 2004; Gritti et al., 2002). Importantly, however, precursors in the RMS (even the PGN precursors) can not be converted to the oligodendroglial lineage by transduction with Olig2, in contrast to half of the SEZ precursors diverted to the oligodendroglial fate by Olig2 overexpression. Notably, a small but significant lineage of oligodendrocytes was also apparent in control virus injections into the SEZ, and was completely blocked by the loss of function and dominant-negative construct of Olig2. Thus, my study demonstrates that adult SEZ cells commit to both neuronal and glial lineages that take respectively, a rostral migratory route toward the bulb, where they give rise to interneurons (Lois and Alvarez-Buylla, 1994; Luskin, 1993) or migrate radially to the white matter where they give rise to oligodendrocytes (Zerlin et al., 1995). The difference between these two lineages seems to be determined by factors regulating Olig2. If Olig2 is down-regulated progression to the neuronal lineage occurs (see also Lu et al., 2001; Zhou and Anderson, 2002), while its maintenance promotes an oligodendroglial fate (see also Results for downregulation of Olig2 in neurons derived from retrovirally infected precursors). Importantly, this regulation may change after certain brain lesions with an obvious increase in the recruitment of endogenous oligodendrocyte precursors from the SEZ (Picard-Riera et al., 2002).

As during embryogenesis, I observe a role of Olig2 in the specification of oligodendrocytes, revealing quite a strong increase in oligodendrocytes migrating to the CC upon overexpression. In the developing brain, some SVZ cells become specified as oligodendroblasts or astroblasts (Levison and Goldman, 1993; Parnavelas, 1999) while others remain uncommitted as glioblasts until they migrate into the overlying parenchyma, where they diverge into lineages of astrocytes or oligodendrocytes (Levison and Goldman, 1993). This study demonstrates that postnatal SVZ cells commit to both neuronal and glial lineages that take respectively, a rostral migratory route toward the bulb, where they give rise to interneurons (Lois and Alvarez-Buylla, 1994; Luskin, 1993) or radial migration to the white matter where they give rise to oligodendrocytes. It is important to realize, however, that the endogenous degree of oligodendroglialogenesis is very low, suggesting that most Olig2-positive precursors are in type C cells in the SEZ and are therefore involved in the generation of GABAergic GN, the majority of neurons generated from the adult SEZ (Ciccolini et al., 2003; Parmar et al., 2002). Notably, this specification occurs at an early stage within the lineage, since Olig2 was hardly detected in neuroblasts and neither in postmitotic neurons (see also Material and Methods), but is mostly contained in precursors at earlier stages in the lineage progression (Hack et al., 2004).

While Olig2 is downregulated in neurons, it is maintained, however, in oligodendrocyte precursors, and hence maintenance of high levels of Olig2 expression as mediated by retroviral vector transduction directs most progenitors towards an oligodendroglial fate (**Fig. 32**). During development of the spinal cord, Olig2 functions in context with other transcriptional fate determinants, Olig2 together with neurogenin 2 (Ngn2) result in motoneuron generation while Olig2 and Nkx2.2 result in oligodendroglialogenesis (Novitsch et al., 2001; Zhou et al., 2001). In the adult SEZ/RMS Ngn1 or 2 are not expressed at detectable levels, but Mash1 is contained also in a subset of PSA-NCAM-negative and GFAP-negative precursors, similar to its colocalization with Olig2 in the developing central telencephalon. However, since also Mash1 is involved in the specification of both, neurons and oligodendrocytes, during adult neurogenesis (Parras et al., 2004), probably other mechanisms must be involved in the choice between these two fates. The bHLH transcriptional code, described above, may not be sufficient to

account for the choice between neuronal and glial fates, since precursors for GABAergic interneurons and oligodendrocytes share the same protein profile.

Therefore, I suggest that other signals could be implicated in this fate specification. As noted previously, Olig2 is expressed in immature precursors of the developing brain and spinal cord in regions that give rise both to oligodendrocytes and neurons (Lu et al., 2002; Zhou and Anderson, 2002). Olig2 is expressed in the VZ where Notch activity maintains a population of Olig2-positive cells in the proliferative state (Park and Appel, 2003). Notch signaling promotes neurosphere formation (Chojnacki et al., 2003; Grandbarbe et al., 2003; Hitoshi et al., 2002a; Nakamura et al., 2000) and promotes astrocytogenesis (Tanigaki et al., 2001), while inhibiting oligodendrocytogenesis (Wang et al., 1998a) and neurogenesis (Morrison et al., 2000), through binding their ligands Jagged and Delta and activating the signaling pathway towards their downstream effectors, the Hes genes (Furukawa et al., 2000; Hojo et al., 2000). Therefore, I would suggest that high levels of Olig2 in the presence of active Notch signaling maintain a neural stem cell fate. Consistent with this scenario, the role of Olig2 in neuronal fate specification requires downregulation of Notch signaling (Mizuguchi et al., 2001; Zhou et al., 2001). Along these lines, radial glia, infected at E14, remain undifferentiated in the presence of high Notch levels and differentiate into neurons in the presence of low Notch levels. Nonetheless, sustained overexpression of Olig2 under control of a retroviral promoter causes postnatal cell death of neurons generated from cortical precursors in vivo and in vitro (**Fig. 22**). The undifferentiated radial glia infected with Olig2-containing retrovirus at E14 then differentiated into astrocytes at later developmental stages when neurogenesis has ceased. Interestingly, it was found that cortical radial glia expressed Olig2 robustly during the perinatal period (P0-P10; C. Marshall, personal communication). Therefore, Notch signaling can promote astroglial specification together with high levels of Olig2 such as in the differentiating conditions of neurosphere cells or cortical radial glia at late developmental stages. Interestingly, the expression of Notch1 and its ligands, as well as Hes5, was shown in the SEZ including the RMS of adult brains (Stump et al., 2002), indicating that similar mechanisms could act during development and adult neurogenesis.

The postnatal cell death of neurons upon Olig2 overexpression raised the idea of a relationship between Olig2 gene dose and Down syndrome comes up. A universal feature of the Down syndrome phenotype is mental retardation resulting, in part, from age-related neuronal degeneration (Holtzman et al., 1996). Olig2 maps to a region of chromosome 21 associated with severe mental retardation in Down patients (Korenberg, 1991). There are less than 50 known or predicted genes within this region, and Olig1 and 2 are the only bHLH genes within this domain (Hattori et al., 2000). The present data suggest that sustained overexpression of Olig2 through trisomy 21 could contribute, at least in part, to the neuronal degeneration observed in Down syndrome patients.

7.6.3 Are Olig2-positive precursors in the adult SEZ neuron-oligodendrocyte precursors (NOPs) or glial restricted precursors (GRPs)?

One of the striking features of studies on the development of oligodendrocytes is that different experimental approaches have led to strikingly different theoretical views regarding the ancestry of these cells. One hypothesis is that the steps leading to the generation of oligodendrocytes begin with the generation of a glial-restricted precursor (GRP) cell from neuroepithelial stem cells. GRP cells are thought to be capable of giving rise to all glial cells (including oligodendrocytes and multiple astrocyte populations, Rao and Mayer-Proschel, 1997), but not to neurons. The latter are generated by neuron-restricted precursor (NRP) cells, and were shown to give rise to multiple different kinds of neurons, but not to glia (Mayer-Proschel et al., 1997). The other hypothesis is that oligodendrocytes are derived from a bipotent precursor cell that generates only motor neurons and oligodendrocytes (NOP), with astrocytes being generated through a separate lineage. This so called NOP hypothesis was based initially on data from the Jack Price lab (Williams et al., 1991) and on observations in the spinal cord that both motor neurons and oligodendrocytes arise in a similar (and possibly identical) discrete zone of the ventral spinal cord (Richardson et al., 1997; Richardson et al., 2000).

The idea that motor neurons and oligodendrocytes might be developmentally related was given a further boost by the findings, from three separate laboratories, that

compromising the function of members of the Olig gene family can prevent the generation of both motor neurons and oligodendrocytes (Lu et al., 2002; Takebayashi et al., 2000; Zhou and Anderson, 2002). However, since these studies provide no evidence that has been presented of the derivation of both motor neurons and oligodendrocytes from a single lineage-restricted founder cell, the only conclusion that can be drawn from these experiments is that Olig1 and Olig2 genes are expressed in a population of ancestral cells of unknown heterogeneity and that this population may well consist of separate Olig1-positive/Olig2-positive precursors for neurons and for oligodendrocytes (Rowitch et al., 2002).

Unfortunately, from my data it is also not possible to discriminate whether there are two subsets of Olig2-positive precursors in the adult SEZ, or whether indeed the same precursor generates mostly neurons and occasionally oligodendrocytes. Notably however, the decrease in neurogenesis accompanying the increase in oligodendroglialogenesis and the absence of astroglialogenesis seen upon Olig2 overexpression (**Fig. 24**) suggests a bipotent lineage. This would be the first proof of NOPs in the adult SEZ.

One should keep in mind, however, that high endogenous Olig2-protein levels can be detected *in vivo* in both, astrocytes and oligodendrocytes of the white matter, the cortex and the striatum (**Fig. 23**). Indeed when Olig2 was injected into the embryonic cortex, it mostly lead to the generation of astrocytes (after a period of neuronal death discussed above) as has been recently demonstrated for Olig1 (Lu et al., 2001). This points to the fact that Olig2 permits, and perhaps even promotes, additionally the formation and survival of astrocytes (Cai et al., 2000; Gangemi et al., 2001).

7.7 Patterning of the SEZ/RMS system

From the *in vivo* results of Pax6 and Olig2 in adult neurogenesis discussed above, two observations pointed to a regionalization of lineage and fate along the SEZ/RMS system. First, transit-amplifying precursors in the SEZ and RMS differ by their expression of Olig2, suggesting that these lineages diverge at an early stage of commitment. Second, most PGN precursors become fate-restricted at a much more rostral position than GN precursors (see above). These data imply that the majority of GNs and PGNs,

respectively are specified at distinct locations along the SEZ/RMS system. Indeed, the spatially distinct specification and birth of PGN precursors was also apparent from two further independent sets of experiments (Hack et al., 2005). BrdU-birthdating analysis revealed that a significant proportion of PGNs arrives in the OB only few days after BrdU-injection, while this takes about 2 weeks for GNs (Hack et al., 2005). These data could either be explained by different speeds of cell migration in which case the PGNs should migrate with 5-10 higher speed of migration (about 170-340 μ m/hour). While this seems unlikely (Davenne et al., 2004; Wichterle et al., 1997), the BrdU-birthdating results would still be consistent with a single lineage of GN and PGNs, both originating in the SEZ, but the latter becoming postmitotic at latter stages of cell migration. When the control retrovirus was injected into the SEZ, the vast majority of labeled cells became GNs consistent with previous data (Belluzzi et al., 2003; Carleton et al., 2003). In contrast, when control virus was injected into the central RMS a higher proportion of labeled newborn neurons became PGNs. These results indicate that there are laminar differences between the fate of cells originating in the central RMS compared to those originating in the SEZ.

Possibly, the RMS and SEZ precursors may differ already since early developmental stages and the spatial differences seen in the adult may result from early patterning along the rostral-caudal axis. This issue could be addressed by Cre-based fate-mapping analysis (Merkle et al., 2004), at earlier developmental stages. Notably, during development the OB originates from the most rostral portion of the telencephalon, where Pax6 levels are highest and specific extrinsic factors, such as FGF8 act as important fate determinants (Meyers et al., 1998). Taken together, my data challenge the concept of a single lineage of adult precursors originating from the SEZ, and rather support a concept with diversity of progenitor cells along the rostral-caudal axis – despite the migration of one cell lineage, namely the GN precursors, from caudal to rostral positions.

Interestingly, similar differences in fate of precursors have been suggested along the rostral-caudal axis of the lateral ventricle with precursors at more caudal positions biased more towards gliogenesis (Luskin, 1993). This does not exclude that neuronal precursors originate also in the most caudal areas of the wall of the lateral ventricle, as demonstrated beautifully in the whole-mounts of the lateral ventricle wall (Doetsch et al.,

1999), but it rather implies that in addition to neurogenesis there may be a larger number of glial precursors at caudal positions respectively. While I did not examine this gradient specifically, I noted that the number of Pax6-positive precursors was much lower in the posterior parts of the SEZ, consistent with its developmental gradient rostral high and caudal low (Mallamaci et al., 2000; Muzio et al., 2002), while Olig2-immunoreactive cells were more frequent in posterior parts of the SEZ. Moreover, my results also suggest a greater degree of plasticity within the SEZ (i.e. more caudally), compared to further rostral levels of the RMS where precursors seem firmly restricted towards neurogenesis. Taken together, patterning cues seem to persist into adulthood and position may be as important for cell fate as it is during development.

7.8 Cell therapy for human neurodegenerative disorders

In this study I discovered important fate determinants for the generation of dopaminergic neurons and oligodendrocytes in the adult mammalian forebrain. Besides instructing the PGN fate, Pax6 further promotes the acquisition of a dopaminergic transmitter phenotype and is the first fate determinant for dopaminergic neurons in the adult mammalian brain. This finding may have profound implications for reconstitutive therapies that can be applied to human patients. Strikingly, patients with Pax6 mutations suffer from hypo- or anosmia (Martha et al., 1995) consistent with a similar role of Pax6 in the adult human OB, where adult neurogenesis continues also in humans (Bedard and Parent, 2004), despite a first failure to localize a RMS at more caudal positions as reported in (Sanai et al., 2004). Furthermore, an upregulation of TH-positive PGN has been detected in Parkinson's patients, reflecting the apparent attempt to increase this neuronal phenotype (Huisman et al., 2004). As mentioned above, Pax6 as a key fate regulator of adult dopaminergic neurogenesis combined with methods to allow RMS precursors to spread into the adjacent striatum (Saghatelian et al., 2004) may hence provide a powerful tool to improve the dopaminergic supply to diseased basal ganglia. Similarly, the results with Olig2-overexpression promoting the generation of oligodendrocytes may be beneficial for cell therapy aiming to restore brain function in demyelinating disorders.

8 FIGURES

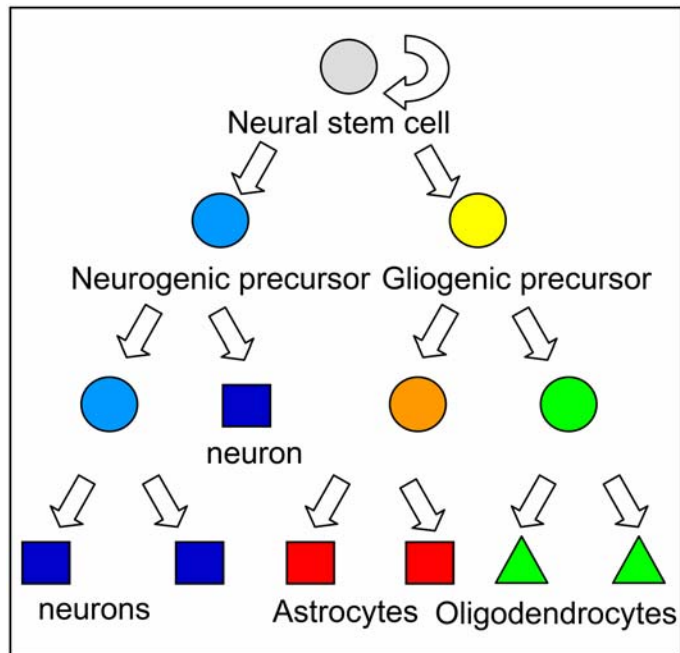


Figure 1. Schematic lineage diagram during embryonic neurogenesis. This lineage diagram depicts the progression from multipotent precursors to the differentiated progeny via lineage-restricted precursors

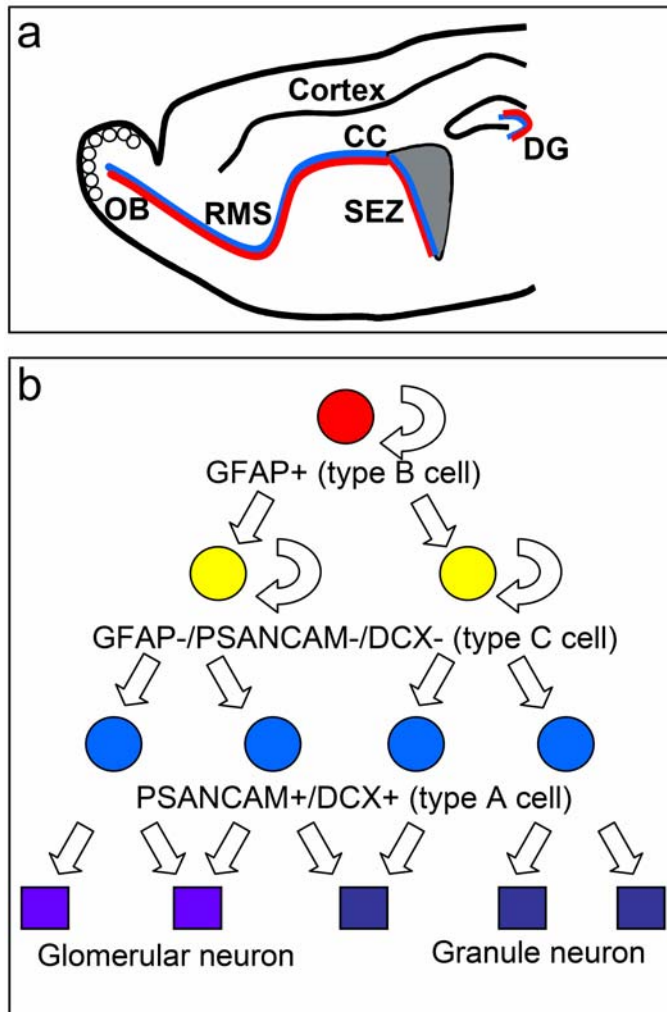


Figure 2. Location of adult neurogenesis and lineage diagram. (a) Scheme of a sagittal section of an adult mouse brain, indicating the locations of adult neurogenesis (SEZ and DG) with GFAP-positive type B cells (red) and migrating neuroblasts (blue). (b) Schematic drawing illustrating the lineage and cell type markers of adult neural precursors. Multipotent precursors are located in the adult SEZ and consist of astrocytes, the type B cells (red), that give rise to the transit-amplifying type C cells (yellow) and the PSA-NCAM (polysialylated form of the neural cell adhesion molecule)-positive neuronal precursors (blue). The type A cells then migrate along the RMS in the OB where they differentiate into different types of GABAergic interneurons (Glomerular neurons or granule neurons). *CC*: corpus callosum; *SEZ*: subependymal zone, *RMS*: rostral migratory stream, *OB*: olfactory bulb.

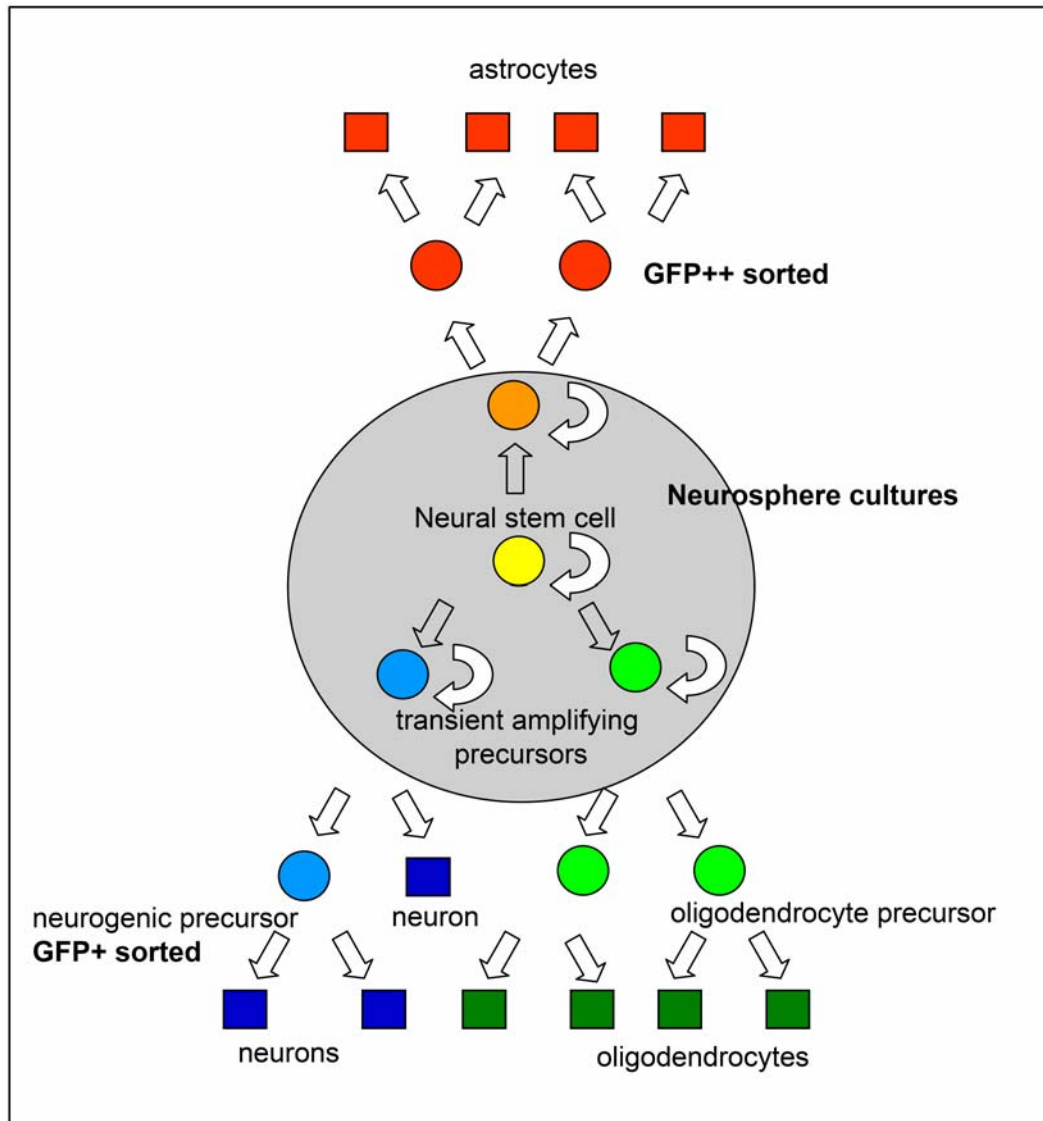


Figure 3. Revised lineage diagram. This lineage diagram depicts the progression from multipotent precursors to the differentiated progeny via lineage-restricted precursors (see text for details). I also incorporated the potential heterogeneity of precursors able to contribute to the formation of neurospheres (see text for details), as indicated by the grey shading. Note that the neurosphere culture system combined with the separation of strongly fluorescent hGFAPeGFP-positive radial glia (GFP++) and weakly green fluorescent radial glia (GFP+) covers three major precursor fates – a bi/multipotent fate (neurosphere model), mostly neuron-restricted precursors (GFP+ radial glia) and mostly astroglia-restricted precursors (GFP++ radial glia) as indicated in the drawing.

a	LTR	Pax6	IRES	GFP	LTR
b	LTR	Pax6eng	IRES	GFP	LTR
c	LTR	Olig2	IRES	GFP	LTR
d	LTR	Olig2VP16	IRES	GFP	LTR
e	LTR	Olig2 bHLH	IRES	GFP	LTR
f	LTR	Pax6	IRES	lacZ	LTR
g	LTR	lacZ	SV40	neo	LTR
h	LTR	GFP			LTR

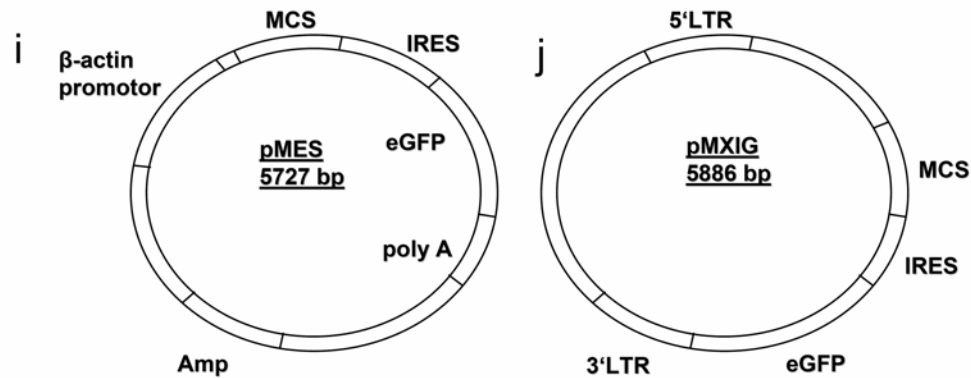


Figure 4. Schematic drawing of the retroviral constructs used

Schemes depicting the retroviral vectors used in during my studies (see Materials and Methods). The Pax6-containing vectors co-express either lacZ (**f**) or GFP (**a**) and Pax6 cDNA. Pax6eng mediated the co-expression of GFP and Pax6 cDNA fused to the repressor domain of engrailed (Pax6eng, **b**). The control retroviral vector contained only GFP (**g**) and or lacZ (**h**) and the neomycin resistance gene (Neo). The Olig2-containing vectors co-express GFP and Olig2 cDNA (**c**). Olig2VP16 mediated the co-expression of GFP and Olig2 cDNA fused to the herpes simplex virion protein VP16 (Olig2VP16, **d**). Olig2 bHLH-only construct (see Materials and Methods for details) coexpressed the bHLH domain of Olig2 together with GFP. (**i**) pMES (Swartz et al., 2001a; Swartz et al., 2001b) (**j**) pMXIG (Nosaka et al., 1999. *MCS*: Multiple cloning site, *bHLH* basic Helix-Loop-Helix, *LTR*: Long terminal repeat, *IRES*: Internal ribosomal entry site.

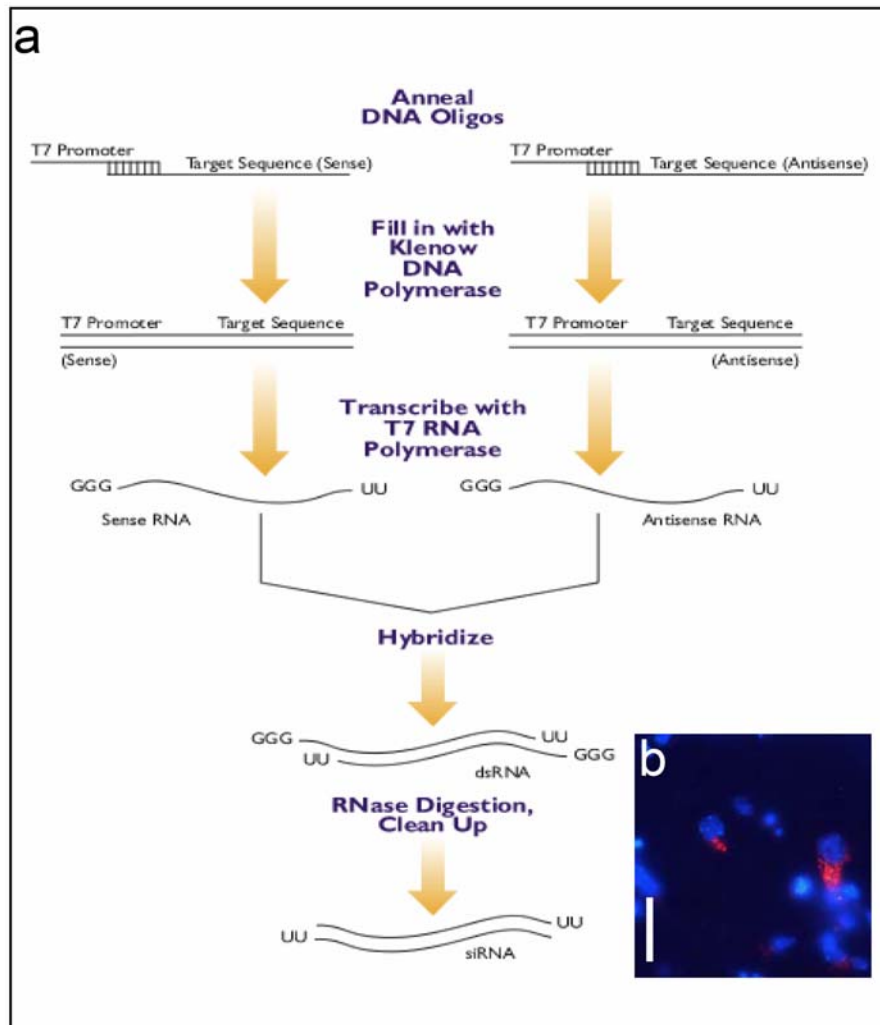


Figure 5. Silencer siRNA construction Kit procedure overview. (a) 29-mer-DNA-oligonucleotides (siRNA oligonucleotide templates) with 21 nucleotides encoding the siRNA and 8 nucleotides complementary to the T7 promoter sequence were designed and ordered at TibMolBiol (Berlin). The siRNA templates were hybridized to a T7 Promotor primer and the 3' ends of the hybridized oligonucleotides are extended by the Klenow fragment. The sense and the antisense siRNA templates were then transcribed by T7 RNA polymerase and the resulting RNA transcripts are hybridized to create dsRNA. The dsRNA consists of 5' terminal single-stranded leader sequences, a 19 nucleotide target specific dsRNA, and 3' terminal UU. The leader sequence is removed by digesting the dsRNA with a single-strand specific ribonuclease. Overhanging UU dinucleotide will remain because the RNase does not cleave U residues. The DNA template is removed at the same time by a deoxyribonuclease. The resulting siRNA is purified by glass fiber binding and elution which removes excess nucleotides, short oligomers, proteins, and salts in the reaction. (b) shows a cortical precursor (nuclei are labeled with DAPI in blue) transfected with Cy3-labeled RNAi (red dots). This confirmed that primary embryonic precursor cells could be successfully transfected with self synthesized and self purified siRNAs. Scale bar: 3µm.

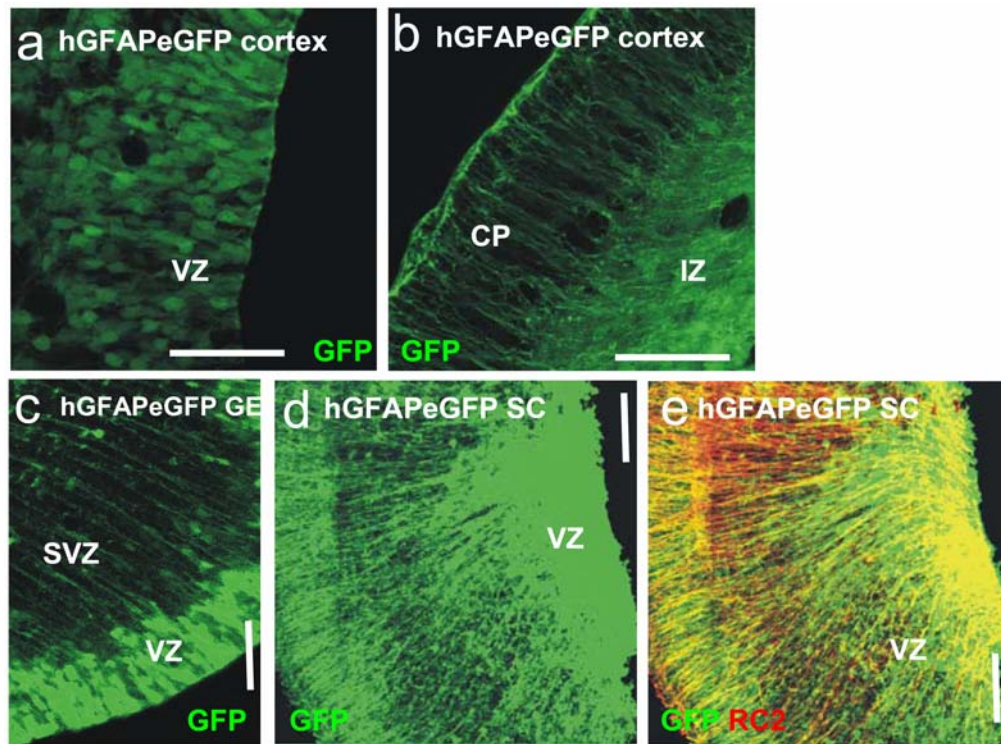


Figure 6. Characterization of radial glial cells in the hGFAPeGFP transgenic mouse. Green fluorescent cells were analyzed in the transgenic mouse line hGFAPeGFP expressing eGFP under the control of the human GFAP promoter (Nolte et al., 2001). **(a,b)** depict micrographs of a maximum intensity projection confocal image of the different regions in a frontal section of the cortex from an E14 hGFAPeGFP embryo, stained with GFP antibody (green): in the CP **(b)** and the VZ **(a)**. **(c-e)** Confocal images **(c)**, single optical section, **(d,e)**, maximum intensity projection) of frontal sections of the ganglionic eminence **(c)** or spinal cord **(d,e)** of an E14 hGFAP-eGFP mouse embryo, stained with GFP antibody (green) and RC2 (red, **e**). Scale Bars: **(a)**: 40 μ m, **(b)**: 80 μ m, **(c)**: 40 μ m, **(d,e)**: 80 μ m. VZ: ventricular zone, SVZ: subventricular zone, IZ: intermediate zone, CP: cortical plate,

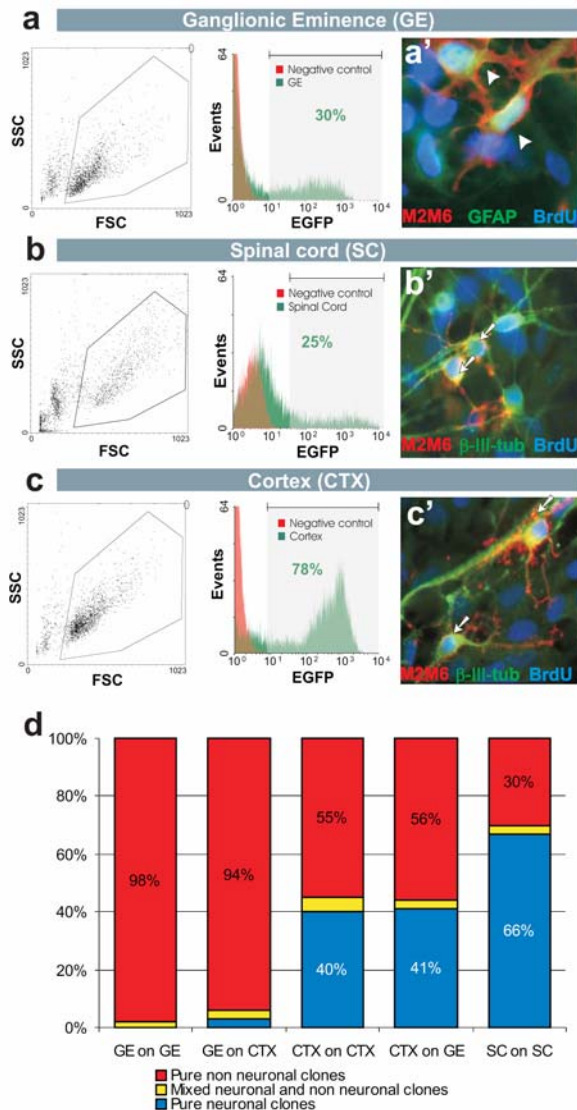


Figure 7. Clonal analysis of radial glia progeny from the cortex, the GE and the SC in vitro. (a-c) depict examples of fluorescent-activated cell sort (FACS) profiles of cells from the respective region of hGFAP-EGFP mice at E14 (a,c) and E12 (b). The left columns show the dot plots of cells in forward scatter (FSC) and side scatter (SSC) with a polygon indicating the gate selecting healthy cells. The histograms in the middle columns show the number of cells ('events', y-axes) with a fluorescent intensity indicated on the x-axis of wild-type controls (red) and hGFAP-EGFP transgenic littermates (green). The percentage of fluorescent cells in the sort gate (grey shading: light green) is indicated. (a'-c') depict examples of clones derived from single sorted radial glial cells of the respective brain region. Sorted cells are plated at clonal density on a rat feeder layer and their progeny is detected after 7 days in vitro as distinct cell clusters labeled by the mouse neural-specific monoclonal antibody mix M2M6 (in red), the neuron-specific β -tubulin-III (green in b',c') or the astrocyte-specific GFAP (green in a'). The incorporation of the DNA-base analog BrdU (blue) indicates that cells divided in vitro. a' depicts a pure non-neuronal clone, b' and b' show each a pure neuronal clone composed of two neurons. (d) Histogram represents the composition of the progeny of radial glial cells isolated by FACS after 5-7 days in vitro plated on different feeder layers. The progeny of a single sorted cell is a clone, classified as pure neuronal when all cells were β -tubulin-III immunoreactive, as pure non-neuronal when no cell of a clone was β -tubulin-III immunoreactive, and as mixed neuronal and non-neuronal when clones contained β -tubulin-III-positive and -negative cells. Scale Bar: a': 10 μ m, b',c': 15 μ m.

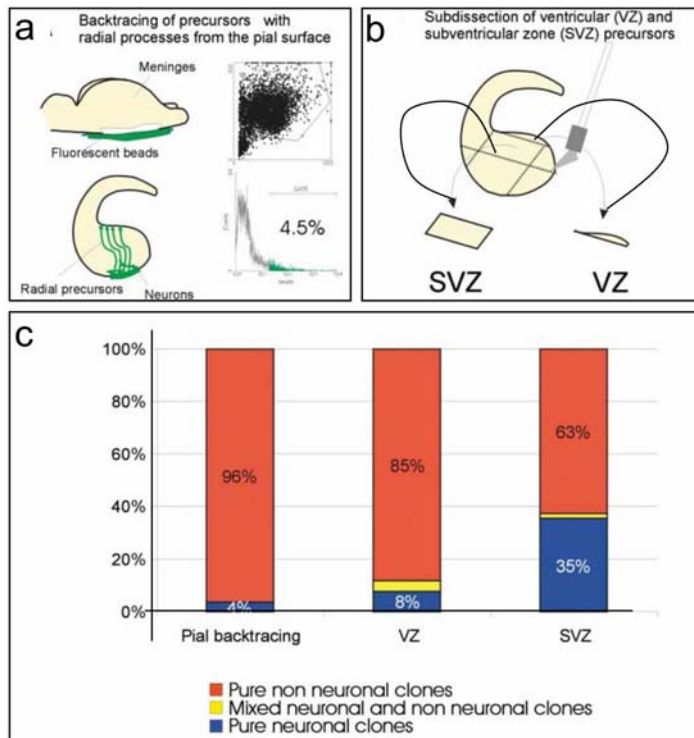


Figure 8. Clonal Analysis of Precursors from the Ventricular and Subventricular Zone In Vitro (a) and (b) depict two ways to isolate ventricular zone (VZ) precursors independent of the hGFAP promoter activity. (a) Precursors with long radial processes were back labeled by green fluorescent beads applied to the surface of the GE after removal of the meninges. Cells that incorporated the green fluorescent beads were then isolated by FACS (profiles in right panels of (a)), and their clonal progeny was analyzed in vitro as described in Figure 6. (b) Schematic drawing illustrating the surgical separation of the VZ and SVZ regions in the GE in slices cut frontally with a tissue chopper. Cells were then dissociated and plated at clonal density on a rat feeder layer from GE as described in Figure 6. (c) The histogram depicts the composition of BrdU-positive clones generated by the precursors isolated as depicted in (a) and (b). Note that VZ precursors from the E14 GE enriched either by dissection or tracing from the pial surface generate few neurons, while precursors residing above the VZ mostly in the SVZ are more neurogenic. Number of clones analyzed: 27 (pial tracing), 138 (VZ), 72 (SVZ). VZ ventricular zone, SVZ subventricular zone.

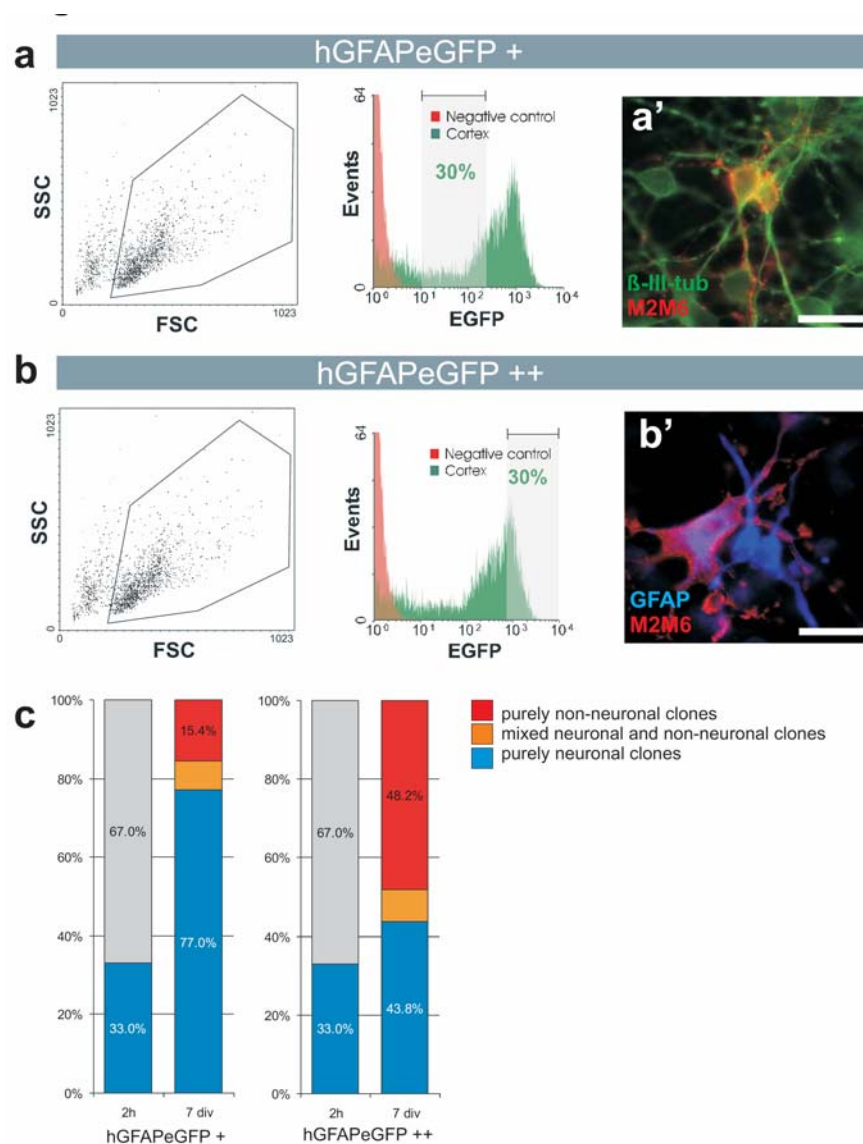


Figure 9. Characterization of subsets of hGFAPeGFP sorted cortical radial glia and their progeny isolated from the cortex of hGFAPeGFP transgenic mice and their progeny. (a,b) depict examples of sort profiles of cells from E14 cortex. The left columns show the dot plots of cells in forward scatter (FSC) and side scatter (SSC) with a polygon indicating the gate selecting the healthy cells. The histograms in the right columns show the number of cells ('events', y-axes) with the fluorescent intensity indicated on the x-axis. The percentage of fluorescent cells in the sort gate (gray shading, a,b) is indicated. (a',b') depict examples of clones derived from single sorted radial glial cells of the respective sort gate. Sorted cells are plated at clonal density on a rat feeder layer and their progeny is detected after 7 days *in vitro* as distinct cell clusters defined as clones labeled by the mouse neural-specific monoclonal antibody mix M2M6 (in red), the neuron-specific anti β -III-tubulin (green in a') or the astrocyte-specific anti-GFAP (blue in b'). (c) depicts the composition of cells 2 hours (2h) or 5-7 days after the sort (days *in vitro*, div). Neurons are depicted in blue, precursor cells in gray. Note the enrichment in the number of pure neuronal clones generated by the weakly green fluorescent radial glia. Scale bar: a',b' 30 μ m.

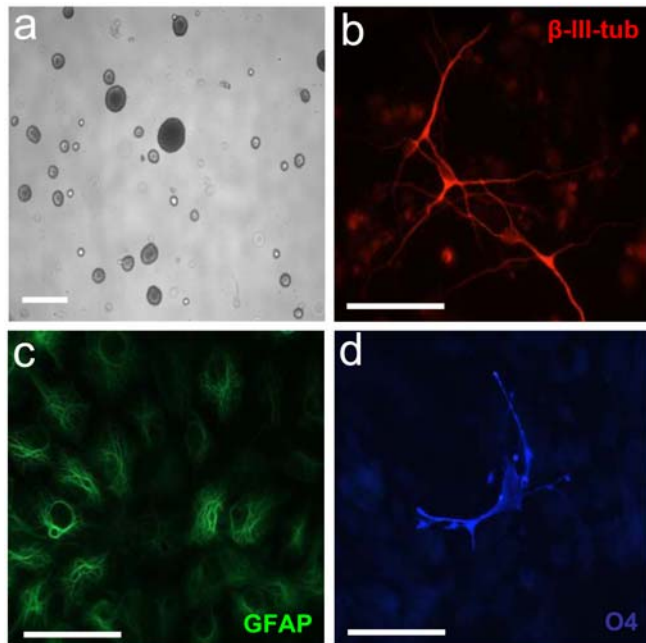


Figure 10. Neurosphere cultures. (a) Shows a phase contrast micrograph of neurosphere cultures. (b) Micrographs of neurons (anti β -III-tubulin-positive), (c) astrocytes (anti-GFAP-positive) and (d) oligodendrocytes (anti-O4-positive) derived from neurosphere cells. Precursors in neurospheres cultured after the fourth passage followed by 7 days in differentiating conditions. a 100 μ m, b, c 70 μ m, d 30 μ m

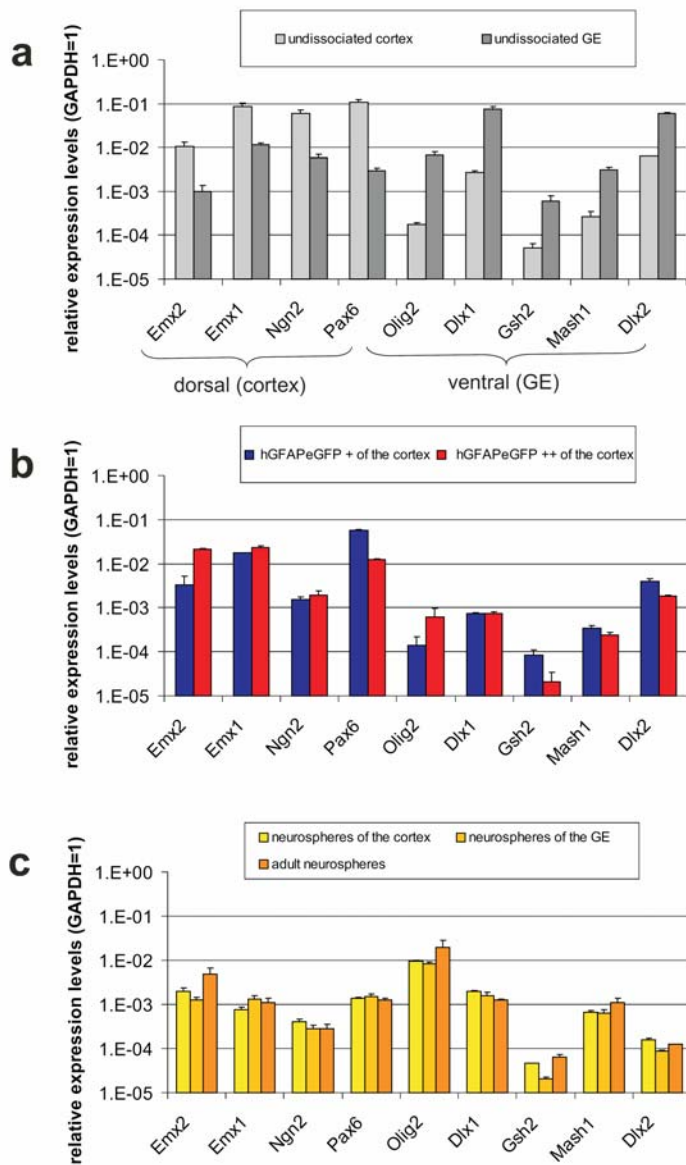


Figure 11. Quantitative RNA analysis of transcription factors in different subsets of telencephalic precursors. Gene expression levels of the transcription factors (Emx1/2, Ngn2, Pax6, Olig2, Dlx1/2, Gsh2, Mash1) are depicted relative to the expression levels of GAPDH (for quantification, see also Material and Methods). **(a)** Primary tissue isolates from the E14 cortex or GE. Note that all of the tested genes showed differential expression between the dorsal (cortex) and ventral (GE) telencephalic regions **(b)**. Quantitative mRNA analysis of precursors sorted on the basis of their GFP content from the cortex of E14 hGFAPeGFP mice. Note that the neurogenic populations (GFP+) expressed 4.6 fold higher levels of Pax6 compared to the non-neurogenic population (GFP++). **(c)** Quantitative mRNA analysis of neurosphere cultures from E14 cortex, GE, or the adult SEZ. Note, that neurosphere cells exhibit little difference in their gene expression patterns independent from their region of expression.

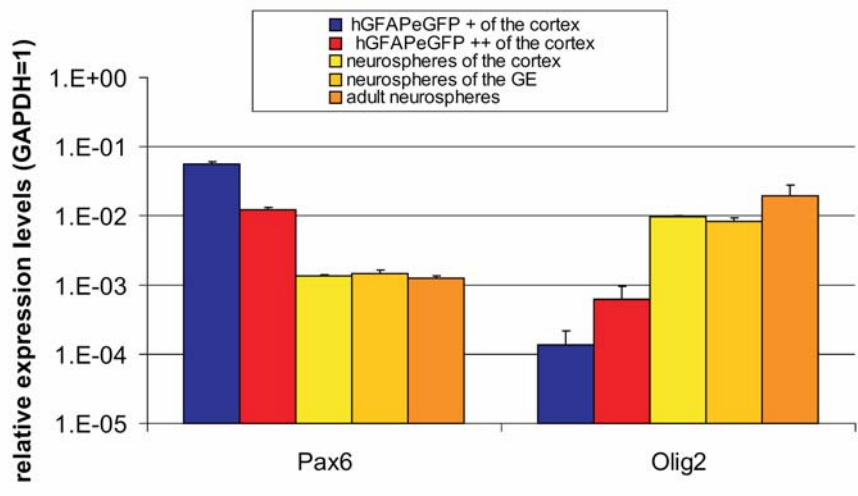


Figure 12. Summary of the expression levels of Olig2 and Pax6 in the functionally distinct precursor subtypes for direct comparison. Note the high expression levels of Pax6 in the neurogenic precursors and the high expression levels of Olig2 in the multipotent precursors.

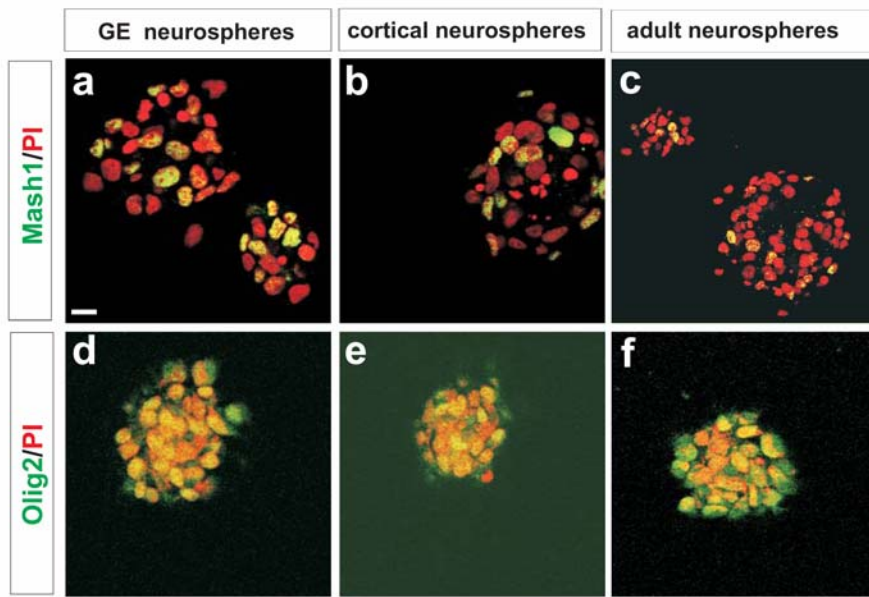


Figure 13. Immunohistochemical analysis of Mash1 and Olig2 in neurospheres Single optical sections of confocal images of single neurospheres stained for Mash1 (**a,b,c**) and Olig2 (**d,e,f**) in green, and propidium iodide in red. Note that almost all cells in neurospheres are Olig2-immunoreactive, independent of their region of origin as indicated in the panel. Scale bar, (**a,b,d,e,f**) 10 μ m, (**c**) 20 μ m

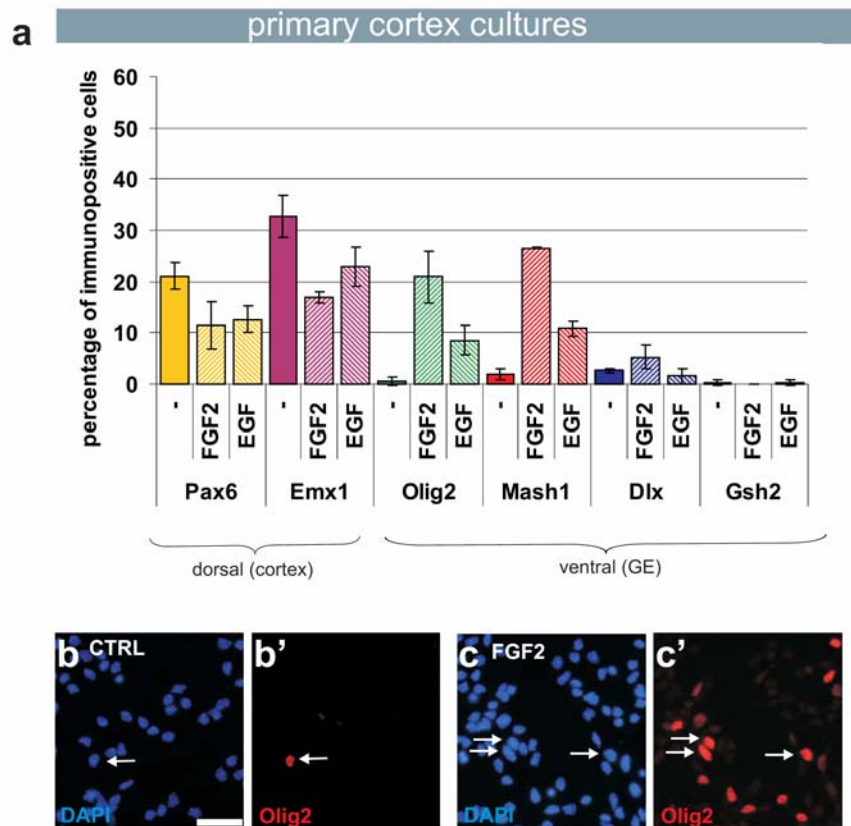


Figure 14. Immunohistochemical analysis of transcription factors in cortical precursors after exposure to the growth factors FGF2 or EGF. Histogram in **a** depicts the percentage of immunopositive cells from E14 cortex (**a**) cultured for 48 hours on poly-D-lysine –coated coverslips in the absence (-) or presence of 20ng/ml EGF or FGF2. Note that the number of Olig2 and Mash1 immunoreactive cells increases, while the number of cells immunoreactive for Emx1 and Pax6 decreases in cortical cultures exposed to EGF or FGF2. In contrast, Dlx- or Gsh2-immunopositive cells were not affected upon addition of EGF or FGF2. (**b–c'**) depict micrographs of cortical cells cultured for 48 hours in the absence (**b**, CTRL) or presence of 20ng/ml FGF2 (**c**, FGF2) stained with anti-Olig2 (red, **b,c**) and DAPI (blue **b',c'**). Arrows indicate the double positive cells. Scale bars, **b,b',c,c'** 60µm.

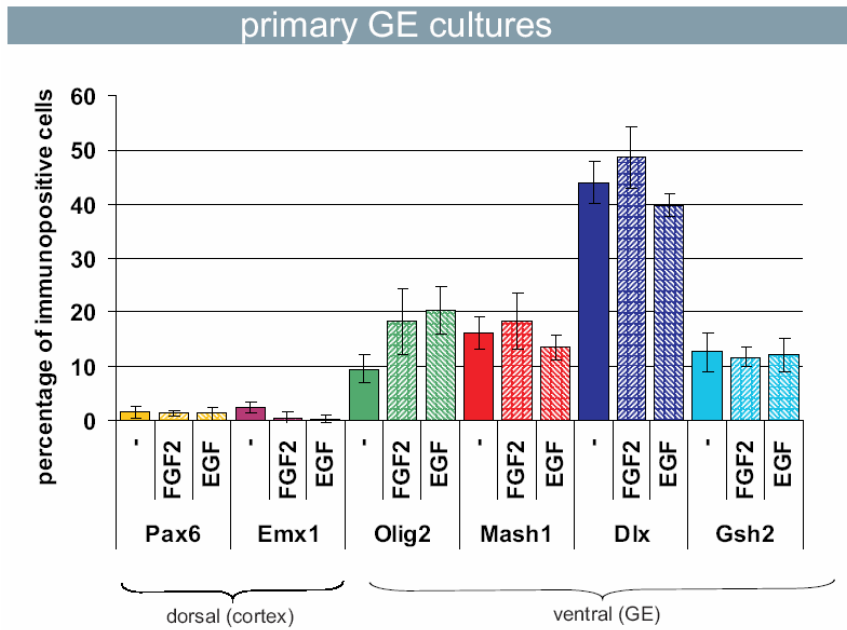


Figure 15. Immunohistochemical analysis of transcription factors in precursors of the GE after exposure to the growth factors FGF2 or EGF. Histogram depicts the percentage of immunopositive cells from E14 GE (a) cultured for 48 hours on poly-D-lysine –coated coverslips in the absence (-) or presence of 20ng/ml EGF or FGF2. Note, that the number of Olig2-positive cells was doubled after 2 days.

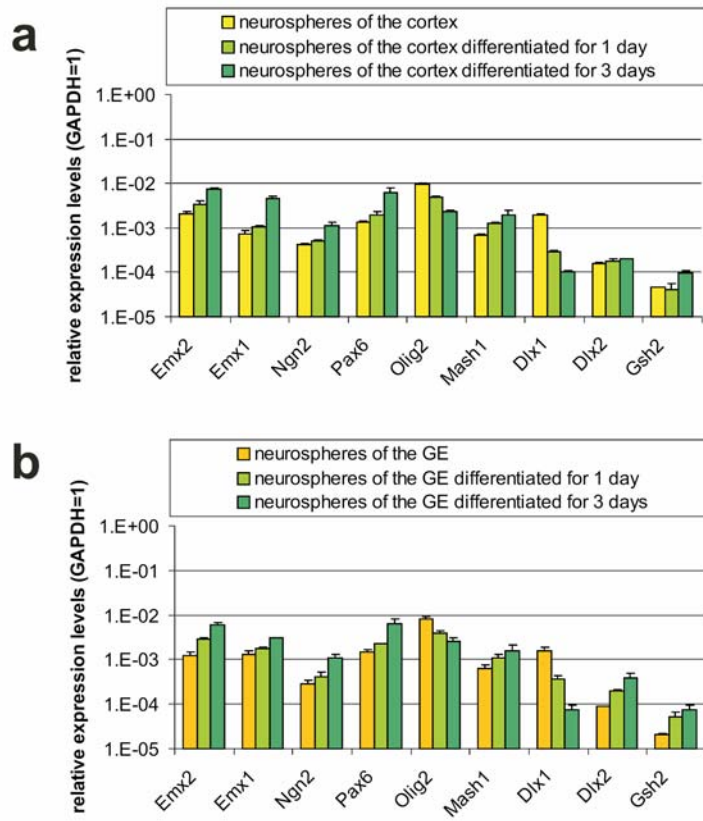


Figure 16. Quantitative RNA analysis of transcription factors in different subsets of telencephalic precursors. Gene expression levels of the transcription factors (Emx1/2, Ngn2, Pax6, Olig2, Dlx1/2, Gsh2, Mash1) are depicted relative to the expression levels of GAPDH (for quantification, see also Material and Methods). Quantitative mRNA analysis of neurosphere cultures from E14 cortex (**a**) or GE (**b**) exposed for 1 and 3 days to differentiating conditions (plating on adherent substrate and growth factor withdrawal). Note, that the highest expression levels of Olig2 are present during expansion conditions of neurosphere cells, while Pax6 was most prominently up-regulated in differentiation conditions

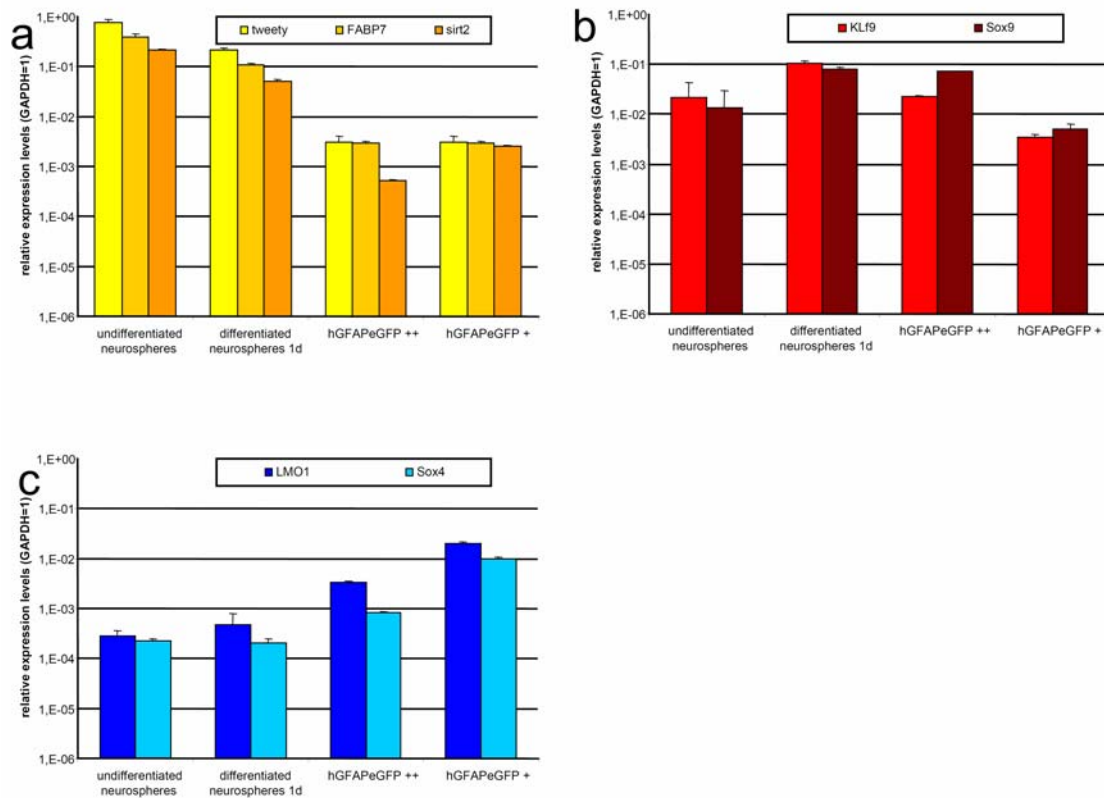


Figure 17. Verification of the gene expression levels detected on the microarray by quantitative RNA analysis in different subsets of telencephalic precursors. Gene expression levels of tweety, FABP7 and sirtuin (sirt2, **a**), and Klf9 and Sox9 (**b**), and Sox4 and Lmo1 (**c**) are depicted relative to the expression levels of GAPDH (for quantification, see also Material and Methods). Quantitative mRNA analysis of these genes was performed on the precursors sorted on the basis of their GFP content from the cortex of E14 hGFAPeGFP mice (+ and ++), on undifferentiated neurosphere cultures from E14 cortex and on undifferentiated neurosphere cultures from E14 cortex exposed for 1 to differentiating conditions. Note, that selected genes can be grouped in 3 different categories: 1) Genes expressed in multipotent stem cells (yellow and orange bars, **a**); 2) Genes expressed in neurogenic precursors (blue bars, **c**); 3) Genes expressed in gliogenic precursors (red and brown bars, **b**).

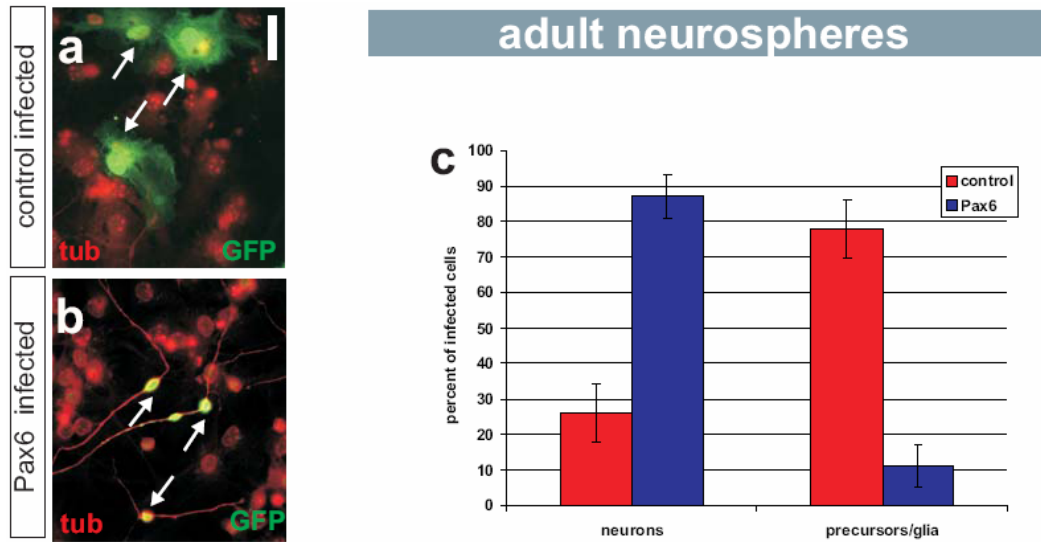
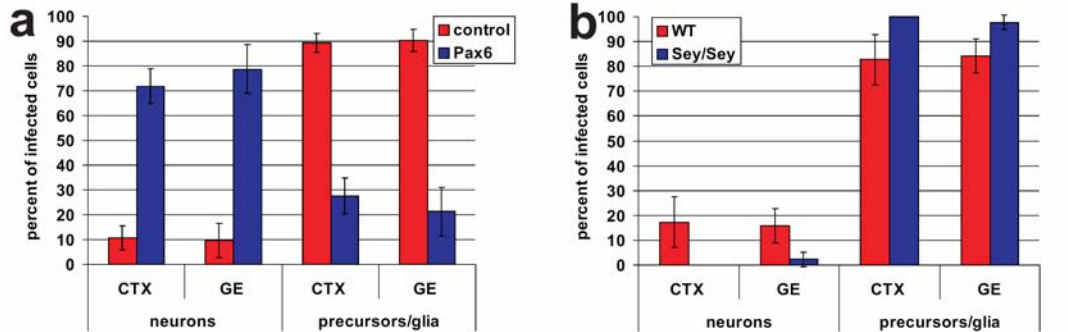


Figure 18. Functional analysis of Pax6 in adult neurosphere cells. (a) Micrograph of examples of control infected adult neurosphere cells generated from E14 cortex (green, arrows) Note that none of the infected cells colocalizes with β -III-tubulin (b) Micrograph of examples of cells from neurospheres infected with the GFP-containing control virus (green in a) or the Pax6IRESGFP virus (green in b) fixed 7 days after infection and culturing in differentiation conditions and immunostained for the neuron-specific antigen anti- β -III-tubulin (red). Note the prominent increase in β -III-tubulin-immunoreactive neurons amongst Pax6-transduced cells (Arrows indicate the double positive cells in (b) compared to cells infected with the control virus (arrowheads indicate the cells that are only GFP-positive (a)). (c) Histogram of cell type analysis of cells from adult neurosphere cultures dissociated after the fourth passage and infected with control (red bars) or Pax6-containing virus (blue bars) analyzed after 7 d in differentiation conditions. Note the high number of neurons (cells immunopositive for β -III-tubulin) after Pax6 transduction. Scale bar 50 μ m.

embryonic neurospheres



primary cortex and GE cultures

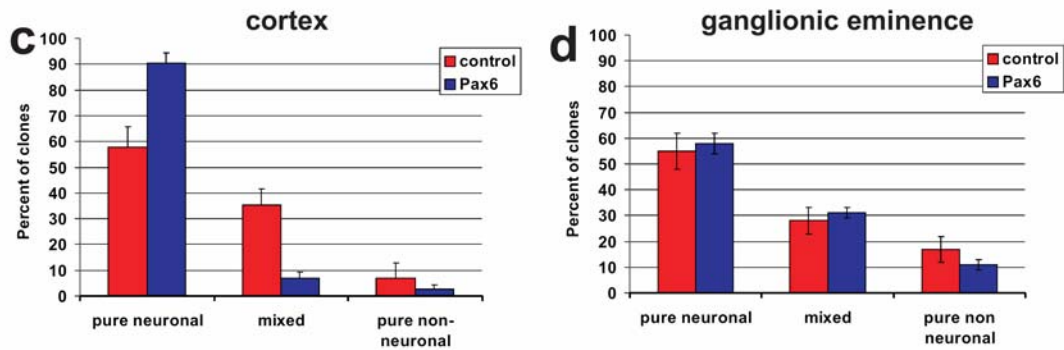


Figure 19. Functional analysis of Pax6 in embryonic neurosphere cells. (a) Histogram of cell type analysis of cells from neurospheres derived from E14 GE or cortex upon viral infection. Note the high number of neurons after Pax6 transduction. (b) Histogram of cell type analysis of neurosphere cells from Pax6 mutant (Sey/Sey; blue bars) and wildtype (WT) littermate (red bars) cortex or GE infected with control virus and analyzed after 7 days in differentiating conditions. Note, that neurogenesis depends on functional Pax6 independent of the region of origin. (c,d) Histograms of clonal analysis in dissociated cells cultures from E14 cortex (c) or GE (d) infected with the control (red bars) or Pax6 containing virus (blue bars) after 7 days in vitro. Note that the number pure neuronal clones (containing only β -III-tubulin- or NeuN-immunoreactive cells) increases significantly after Pax6 transduction in cortical, but not in GE cells.

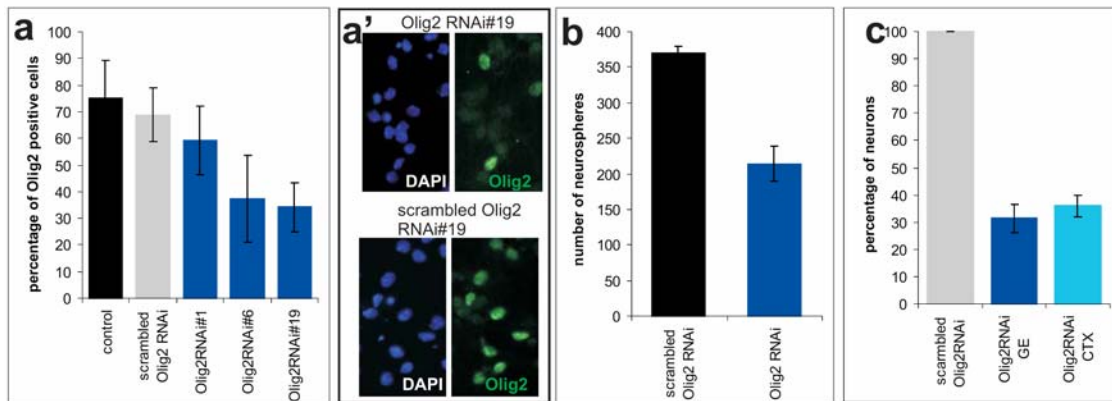


Figure 20. Functional analysis of Olig2 in neurosphere cells. (a) Reduction of Olig2 by means of the siRNA technology. Neurosphere cultures were plated after 4 passages, not transfected (black bar) or transfected with different siRNAs targeting the Olig2mRNA (blue bars) or the respective control construct (gray bar) and immunostained for Olig2 48 hours later. (a') depicts cells from neurosphere cultures 2 days after transfection with Olig2 RNA#19 and its control construct stained with anti-Olig2 (green) and DAPI (blue). Note, that RNAi#19 was most effective in the reduction of Olig2 protein. (b) Effect of Olig2 reduction on self-renewal of neurosphere cells. After transfection of cells from neurosphere cultures as described above the number of neurospheres was quantified 7 days after the fourth passage. Note that only about half the number of neurospheres was generated by cells transfected with Olig2 RNAi compared to the cultures transfected with the scrambled control. (c) Influence of Olig2 on cell fate. Neurosphere cultures derived from the GE (blue bar) or cortex (light blue bar) were plated after 4 passages, transfected with Olig2 RNAi and the control construct (gray bar) and immunostained for the neuron-specific antigen β -III-tubulin. Note, that the number of neurons was decreased to a third of the number of neurons present in control cultures.

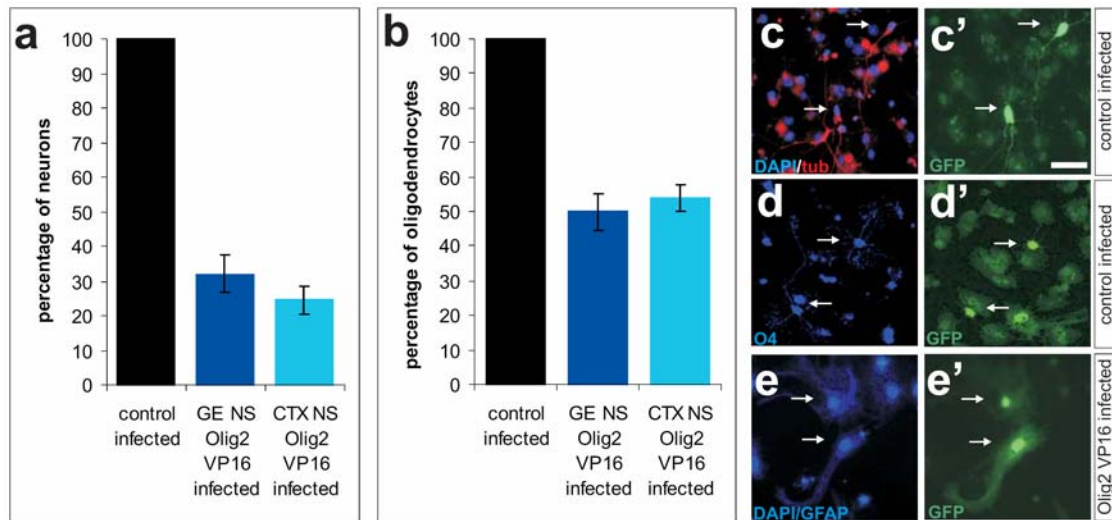


Figure 21. Functional analysis of Olig2 in neurosphere cells

(a,b) Histogram of cell types generated from neurosphere cells derived from the GE (blue bars) or the cortex (light blue bars) infected with the control (black bars) or Olig2VP16 virus 7 d after culturing in differentiation conditions. Cells were stained for either the neuron-specific antigen β -III-tubulin (a) or the oligodendrocyte-specific O4 (b). Note that the number neurons, as well as the number of oligodendrocytes decreases after Olig2VP16 transduction. (c-e'). Pairs of corresponding micrographs (c,c',d,d',e,e') showing examples of virally infected cells labeled with GFP (c',d',e') cultured for 7 days in differentiating conditions and stained for the neuron-specific antigen anti- β -III-tubulin (red in c, DAPI in blue), the astrocyte-specific GFAP (blue in f, DAPI also in blue) and the oligodendrocyte-specific O4 (blue in I, DAPI also in blue). Arrows indicate the double positive cells. Scale bars: (c,c'): 30 μ m, (d,d'): 45 μ m, (e,e'): 20 μ m.

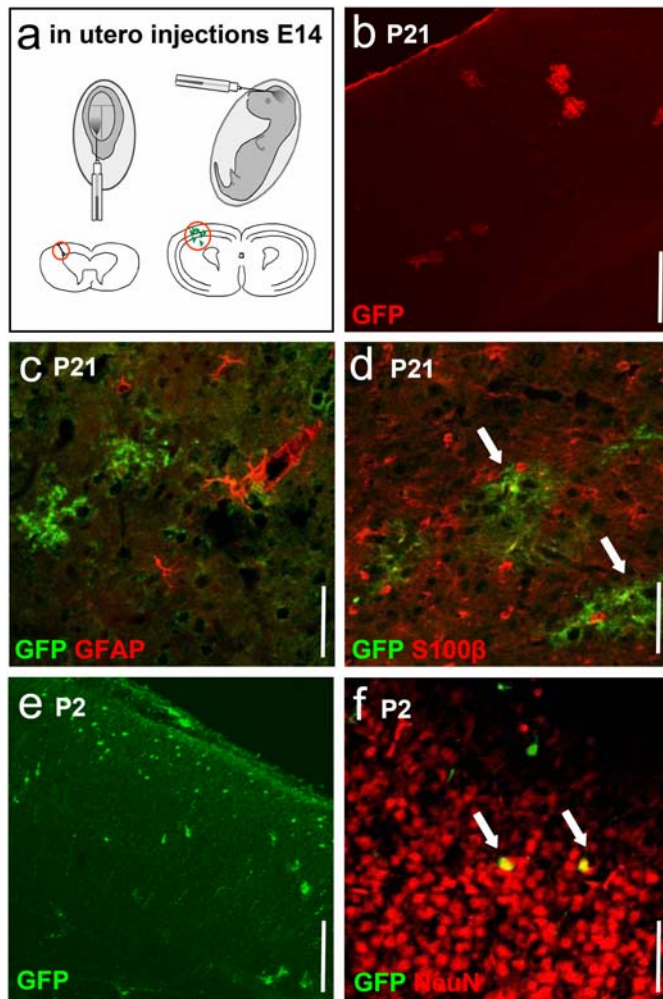


Figure 22. Ectopic expression of Olig2 gene induces age-related neuronal degeneration and astrocyte development. (a) Schematic overview of an in utero injection. The virus containing solution is injected in the ventricles of the embryo (see Material and Methods for details). Schematic brain sections (below) show the distribution of the infected cells shortly after injection (left) and 21 days after injection (right). (b-d) Brain tissue was harvested at P21 and immunostained for GFP activity after retroviral infection of embryos at E14. Ectopic expression of Olig2 in mouse brain resulted in a large population of astrocytes visible in gray matter of the cerebral cortex (b). Morphology-based identification of astrocytes (b) was validated by immunostaining with astrocyte marker antibodies GFAP (c) and S100β (d, arrows indicate the doublepositive cells). Note that Olig2 overexpressing astroglial-like cells do not express GFAP (c). (e,f) Representative examples of neurons infected with the Olig2 containing retroviral construct at E14 and harvested at P2. (e) At P2, most Olig2 -infected (green) cells show neuronal morphology. Note the axons projecting in the corpus callosum (f) A GFP+ cell (green) with neuronal morphology is immunostained with NeuN (red). Arrows indicate the doublepositive cells. Scale bars: 50 μm (b,e); 10 μm (c,d,f).

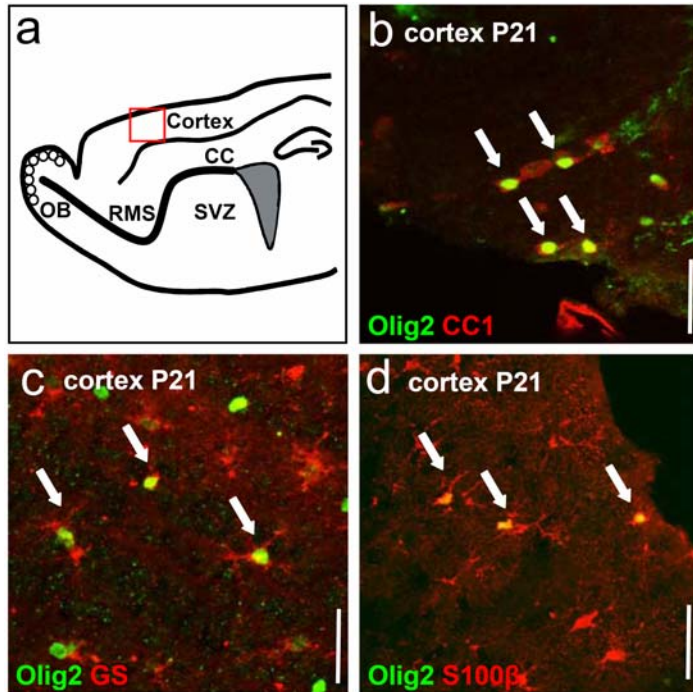


Figure 23. Olig2 expression pattern in the adult cortex. (a) scheme of a sagittal section of a postnatal mouse brain at postnatal day 21 (P21) depicting the localization of the micrographs (b,c,d; red insets). (b-e) show micrographs of Olig2-immunoreactivity (green) combined with CC1 (red, b), GS (red,c) and S100 β (red, d). Arrows indicate the doublepositive cells. Note, that many astrocytes in the postnatal and adult brain express Olig2, but also all the oligodendrocytes. *SEZ*: subependymal zone, *RMS*: rostral migratory stream, *OB*: olfactory bulb, *CC* Corpus Callosum. Scale bars, 7 μ m (b,c,d).

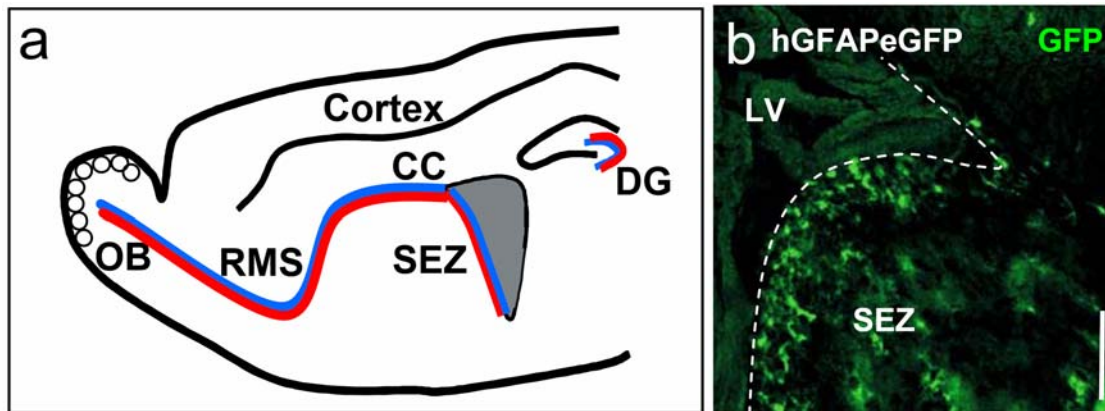


Figure 24. Regions of ongoing neurogenesis in the adult forebrain. (a) Schematic drawing of the adult forebrain highlighting in color the regions with ongoing neurogenesis, the dentate gyrus of the hippocampus and the adult subependymal zone (SEZ) with the rostral migratory stream (RMS). Regions containing astrocytes (the SEZ of the basal ganglia, the RMS or the subgranular layer of the dentate gyrus) at the source of adult neurogenesis are indicated in red, neuron-restricted precursors ('neuroblasts') are indicated in blue (Doetsch et al., 1999; Seri et al., 2001). (b) Micrograph of a sagittal section of the telencephalon of an hGFAPeGFP adult mouse forebrain stained for GFP. Note the high number of GFP-positive cells in the SEZ. *LV*: lateral ventricle, *SEZ*: subependymal zone, *RMS*: rostral migratory stream, *OB*: olfactory bulb, *CC* Corpus Callosum. Scale bars, (b) 15 μ m, (d) 400 μ m

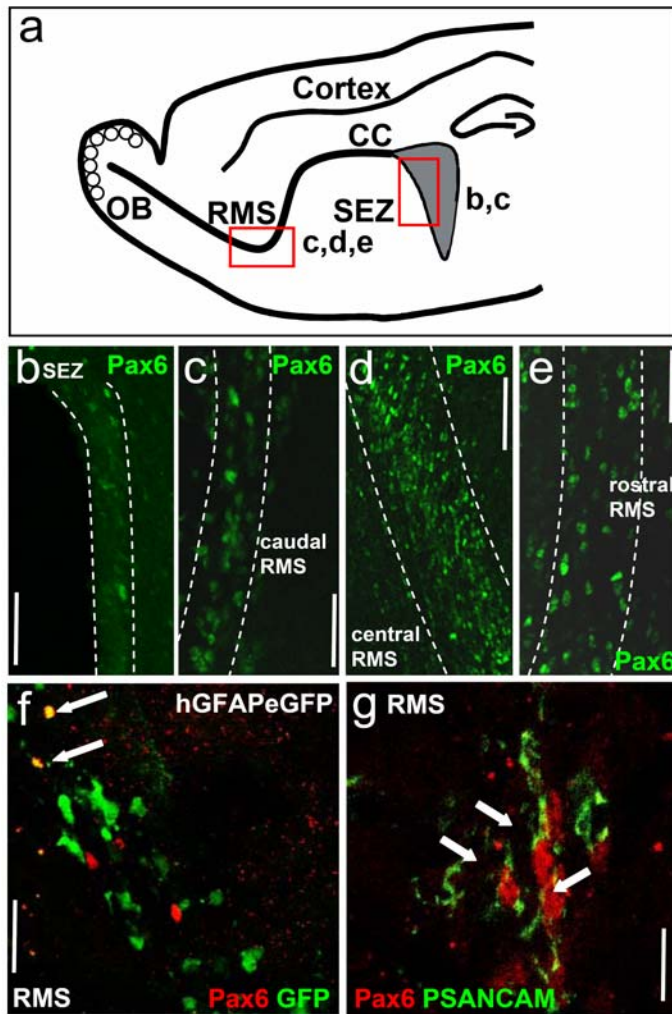


Figure 25. Expression pattern of the transcription factors Pax6 in the SEZ and RMS. (a) scheme of a sagittal section of an adult mouse brain depicting the localization of the micrographs (b,c,d,e; red insets). (c-g) show micrographs of Pax6-immunoreactivity (green or red) combined with PSANCAM (green, g), or GFP-immunoreactivity (green, f) Note the higher frequency of Pax6-positive cells in the caudal, central and rostral RMS (c,d,e) compared to the SEZ (b). Note that Pax6-immunoreactivity is contained within PSANCAM-positive neuroblasts (examples indicated by arrows, g). (f) depicts Pax6-immunoreactivity (red) in a subset of GFP-positive cells in the RMS of adult hGFAPeGFP mice (double-labeled cells are indicated by arrows). Arrows in (f,g) depict double positive cells. Scale bars (b,c,e) 60µm, (d) 150µm, (f) 60µm, (g) 15µm, SEZ: subependymal zone, RMS: rostral migratory stream, OB: olfactory bulb, CC: Corpus Callosum, GL: glomerular layer; GCL: granule cell layer.

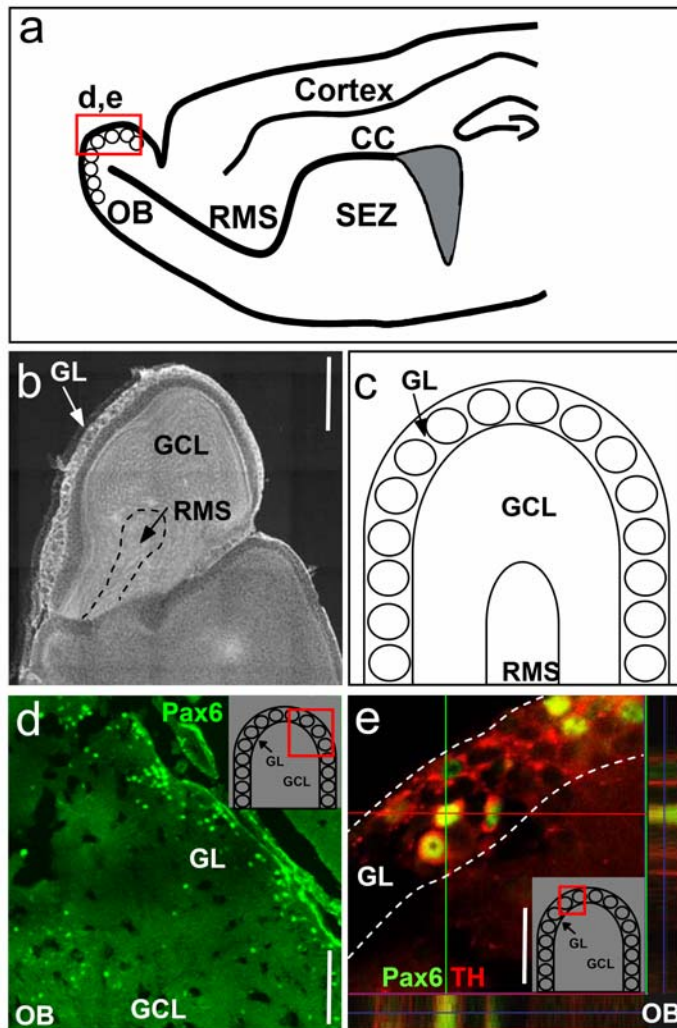


Figure 26. Expression pattern of the transcription factors Pax6 in the OB. (a) scheme of a sagittal section of an adult mouse brain depicting the localization of the micrographs (d,e; red inset). (b) micrograph of a section of the OB, indicating the different regions of the OB. (c) scheme of a section of the OB. Precursors migrate into the OB and then leave the RMS to migrate radially in the neuronal layers (GL and GCL). (d,e) show micrographs of Pax6-immunoreactivity (green) combined with TH-immunostaining (red, e), (inset in d and e: scheme of the OB). Z axes in (i) confirm that GFP and TH are colocalized in one cell body. Scale bars (b) 400 μ m, (d) 150 μ m, (e) 20 μ m. SEZ: subependymal zone, RMS: rostral migratory stream, OB: olfactory bulb, CC: Corpus Callosum, GL: glomerular layer; GCL: granule cell layer.

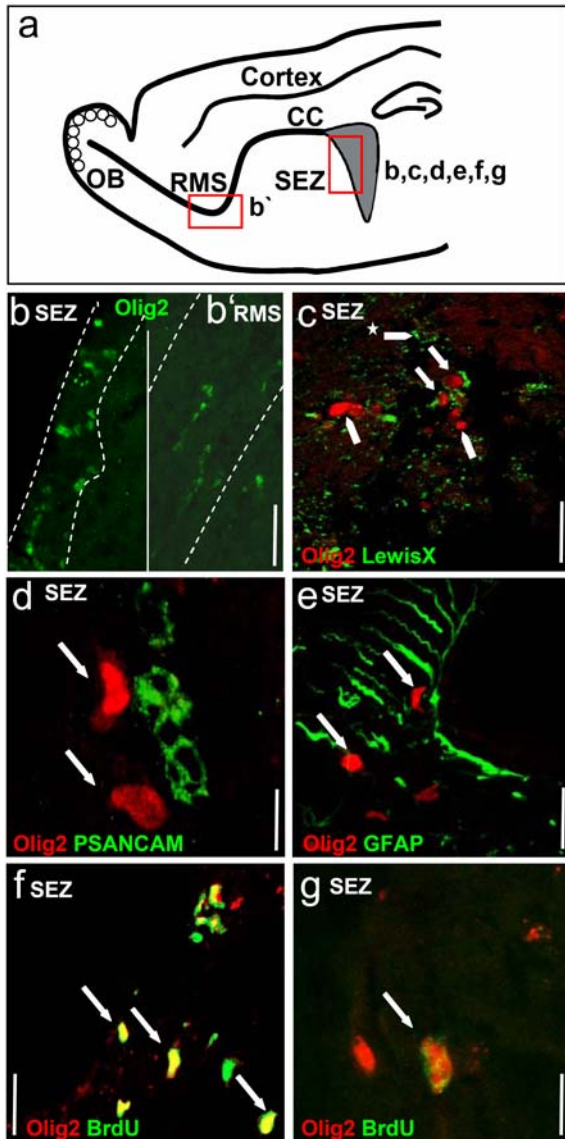


Figure 27. Expression pattern of the transcription factors Olig2 in the SEZ-OB pathway. (a) scheme of a sagittal section of an adult mouse brain depicting the localization of the micrographs (b,b',c,d,e,f,g; red insets). (c-g) show micrographs of Olig2-immunoreactivity (red) combined with LewisX-immunostaining (green, c), PSANCAM (green, d), GFAP (green, e), or BrdU-immunoreactivity (green, f,g). Note the lower frequency of Olig2-positive cells in the RMS (b') compared to the SEZ (b). (c) depicts Olig2- (red) and LewisX- (green) immunoreactive cells in the SEZ. Arrows indicate the Olig2/LewisX double-positive cells, arrowheads indicate the cells that are only Olig2-positive, and the arrowhead with asterisk indicates a single LewisX-positive cell. (d) Note the lack of colocalization of Olig2 and PSANCAM as indicated by arrows. Note that Olig2 is not contained in GFAP-positive cells as indicated by arrows depicting cells that are only Olig2-positive (e). (f,g) Micrographs depicting Olig2- (red) and BrdU- (green) immunoreactive cells in the SEZ (f), BrdU was provided for 14 days in the drinking water, labeling all proliferating cells; (g), BrdU was infused twice a day for three days 14 days before sacrifice, and mostly slowly dividing precursors should maintain the label in this paradigm). Arrows in (e,f,g) depict double positive cells. Arrows in (c,d) indicate single positive cells. Scale bar, b, b' 60 μ m, c 20 μ m, d 7 μ m, e 45 μ m, f 20 μ m, g 45 μ m. SEZ: subependymal zone, RMS: rostral migratory stream, OB: olfactory bulb, CC Corpus Callosum.

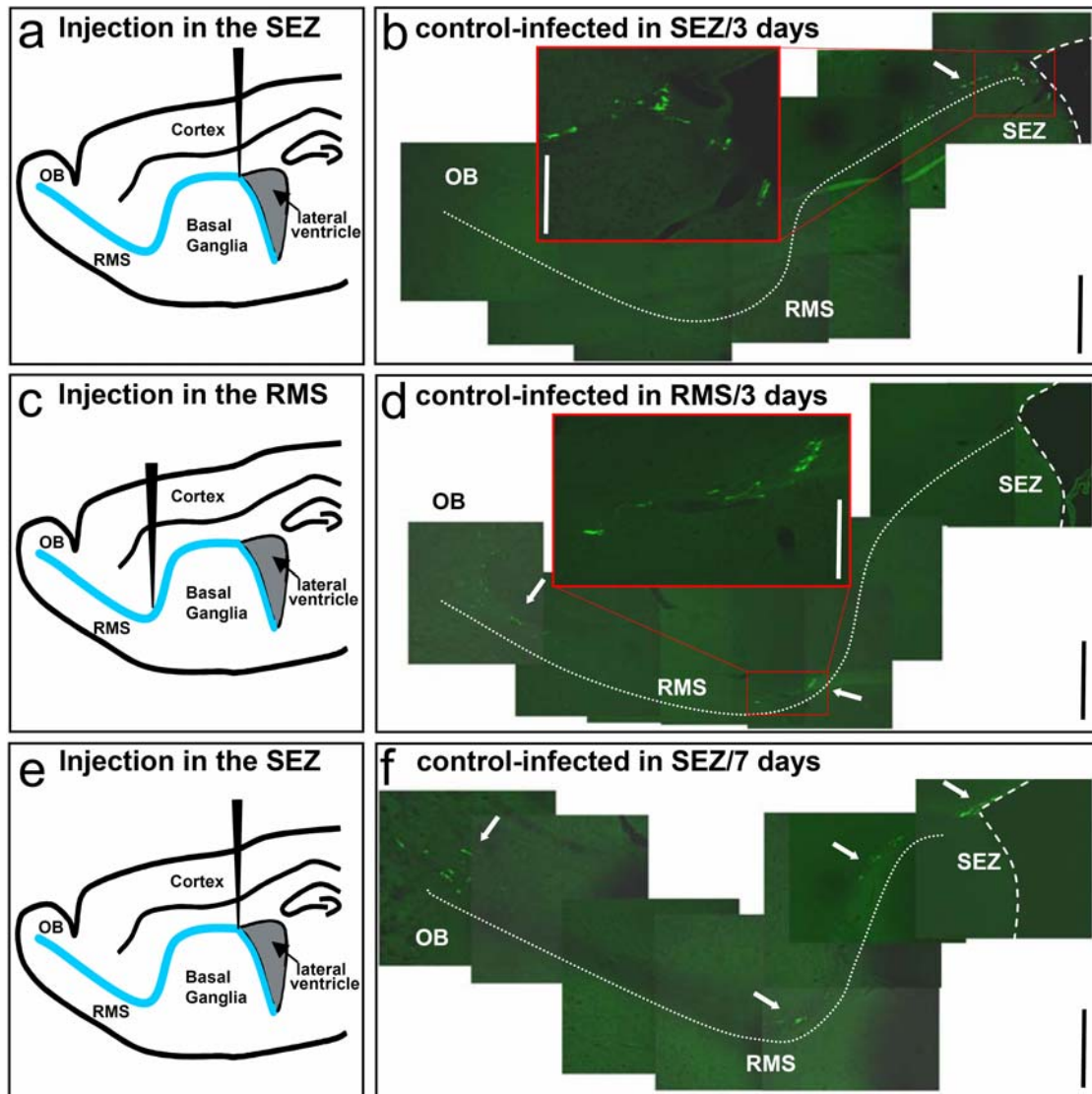


Figure 28. Viral infections can be specifically targeted to the SEZ/RMS by stereotaxic injections. **a,c,e** Schematic drawings illustrating the injection sites (RMS, SEZ) of the virus. **(b,d,f)** micrographs of stainings in sagittal sections of the adult mouse subependymal zone (SEZ), rostral migratory stream (RMS) and olfactory bulb (OB), 3 **(b,d)** and 7 **(f)** days after vector injection. Insets (red) in **(b)** and **(d)** show infected cells in higher magnification. Scale bars in **(b,d,f)**: 500 μm (for insets: 200 μm); *SEZ*: subependymal zone, *RMS*: rostral migratory stream, *OB*: olfactory bulb.

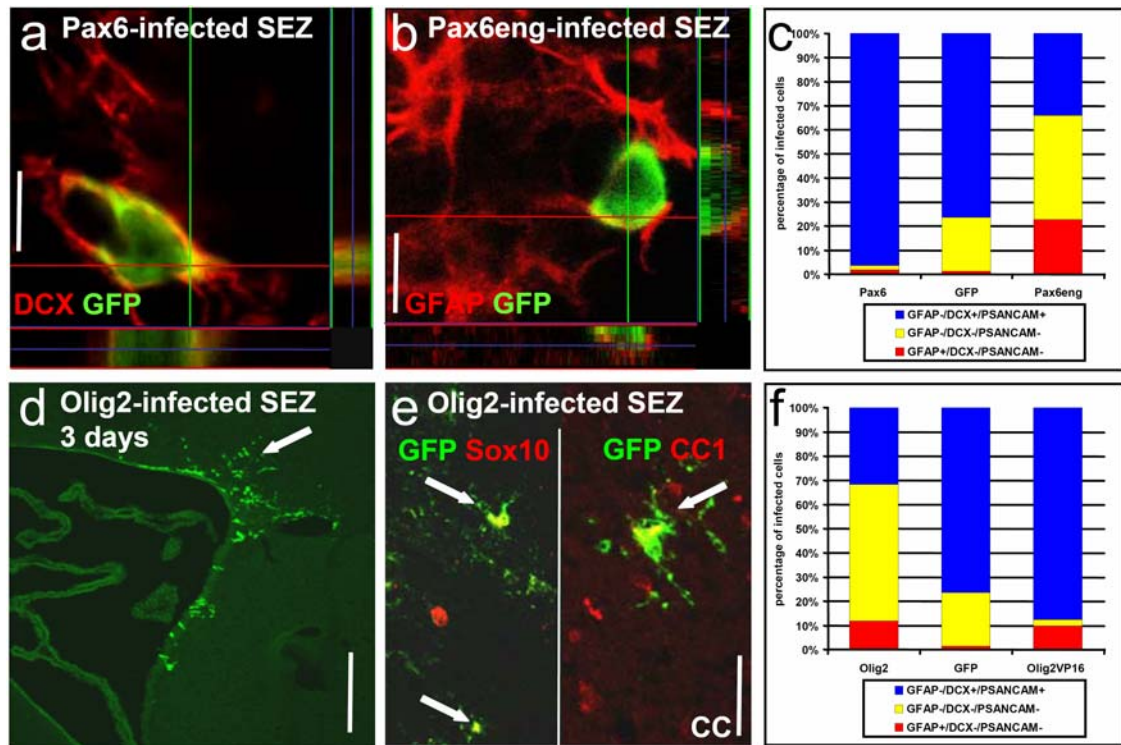


Figure 29. Functional analysis of the transcription factors Pax6 and Olig2 in adult neurogenesis. (a,b,d,e) micrographs of stainings in sagittal sections of the adult mouse subependymal zone (SEZ), rostral migratory stream (RMS) and corpus callosum (CC), 3 (d) and 7 (a,b,e) days after vector injection. Histograms in (c,f) summarize the quantification of SEZ cells 7 days after injection of the viral vectors indicated on the x-axis. Note, that Pax6 plays a role in neurogenesis, while Olig2 promotes the generation of oligodendrocytes and undifferentiated precursors. Z axes in (a) and (b) confirm that GFP and DCX (a) or GFAP (b) are colocalized in one cell body. Scale bars in (a) and (b): 8 μ m; (d): 180 μ m and (k): 40 μ m. CC: corpus callosum; SEZ: subependymal zone, RMS: rostral migratory stream.

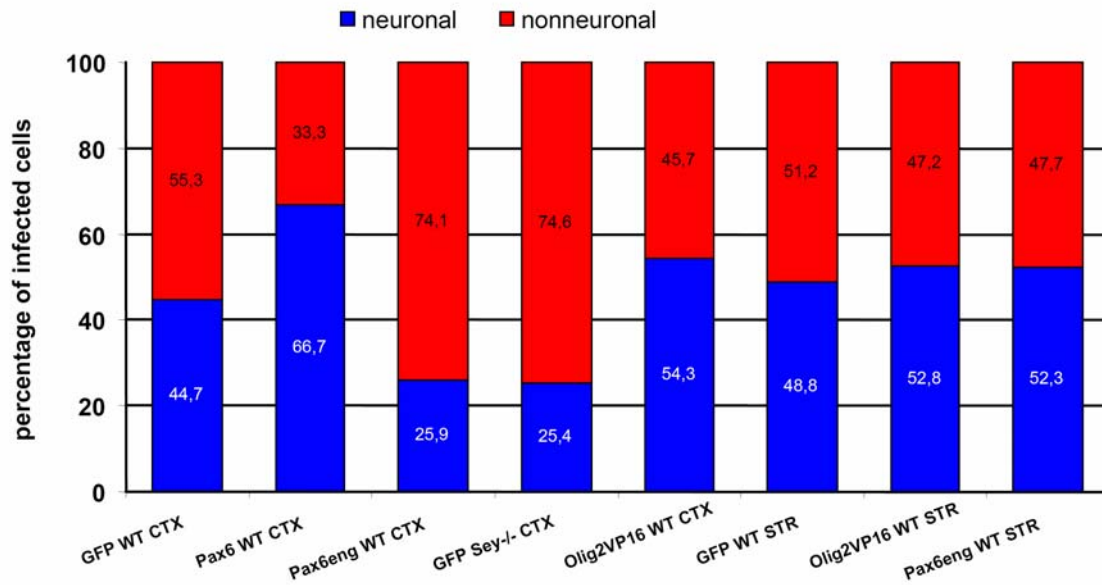


Figure 30. In vitro analysis of the retroviral vectors. Here I used a well-established in vitro system for the analysis of telencephalic precursors, where the effect of Pax6 is particularly well characterized (Haubst et al., 2004; Heins et al., 2002). Previous work had shown that Pax6 overexpression promotes neurogenesis and reduces clone size, *i.e.* the number of descendants generated by a single precursor cell, while the loss of functional Pax6 in Small Eye mutant mice (Sey/Sey) results in decreased neurogenesis and an increase in clone size (Haubst et al., 2004; Heins et al., 2002). As expected, infection with the Pax6-engrailed containing virus resulted also in a decrease of neurogenesis that was almost identical to the effect in Sey/Sey mutant cells deficient of functional Pax6 protein compared to wildtype cells. Thus, the Pax6-engrailed is as sufficient as the loss of functional Pax6 protein. Next, I also examined the specificity of both, the Pax6-engrailed and the Olig2VP16 constructs by expression in cells that do not contain Pax6 or Olig2 respectively. For example, cells from the embryonic cortex do not express Olig2 and should therefore not be affected by Olig2-VP16 transduction, as is indeed the case. Thus, Olig2-VP16 does not superactivate target genes in cells where Olig2 plays no endogenous role. Similarly, Pax6-engrailed transduction of precursors from the ventral telencephalon that do not contain endogenous Pax6 protein exerted no effect, despite its pronounced effect in the cortical progenitor cells.

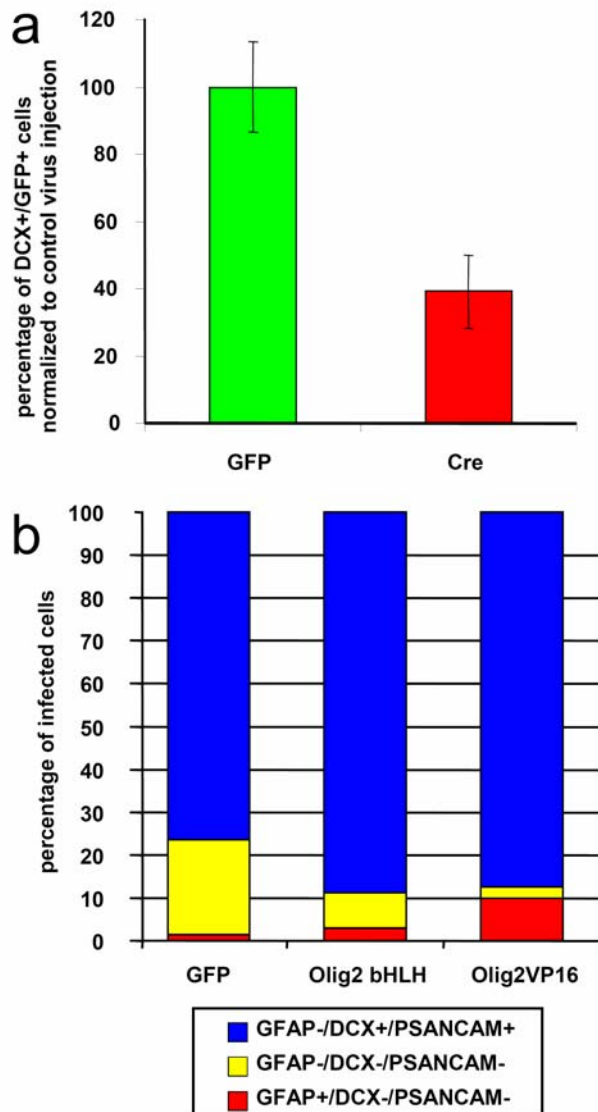


Figure 31. Functional analysis of the transcription factors Pax6 and Olig2 in adult neurogenesis by other means. (a) To address the neurogenic role of the transcription factors Pax6 in adult neurogenesis by other means I used the Cre-based deletion of Pax6 in *Pax6^{lox/lox}* mice (Ashery-Padan et al., 2004). Histogram shows the number of DCX+ cells among the GFP-positive cells after infection with the virus containing GFP (control) or Cre (see Materials and Methods). Virus was injected in the subependymal zone (SEZ) and animals were sacrificed 7 days after infection. The infected cells were analyzed in the SEZ. Note, that the percentage of DCX-positive cells is significantly reduced. The lentiviral vectors (LV-GFP and LV-Cre) used are based on a recently described vector system (Follenzi et al., 2000) and carry the enhanced green fluorescent protein (eGFP) reporter transgene or the Cre recombinase. Recombinant lentivirus was produced as previously described (Pfeifer et al., 2002). Histogram in (b) summarizes the quantification of SEZ cells 7 days after injection of the viral vectors indicated on the x-axis. Note, that the injection of the bHLH-only construct displays a similar effect as the Olig2VP16 construct, indicating that the reduction in type C cells is due to competition of these two constructs with the endogenous wildtype Olig2 for downstream targets.

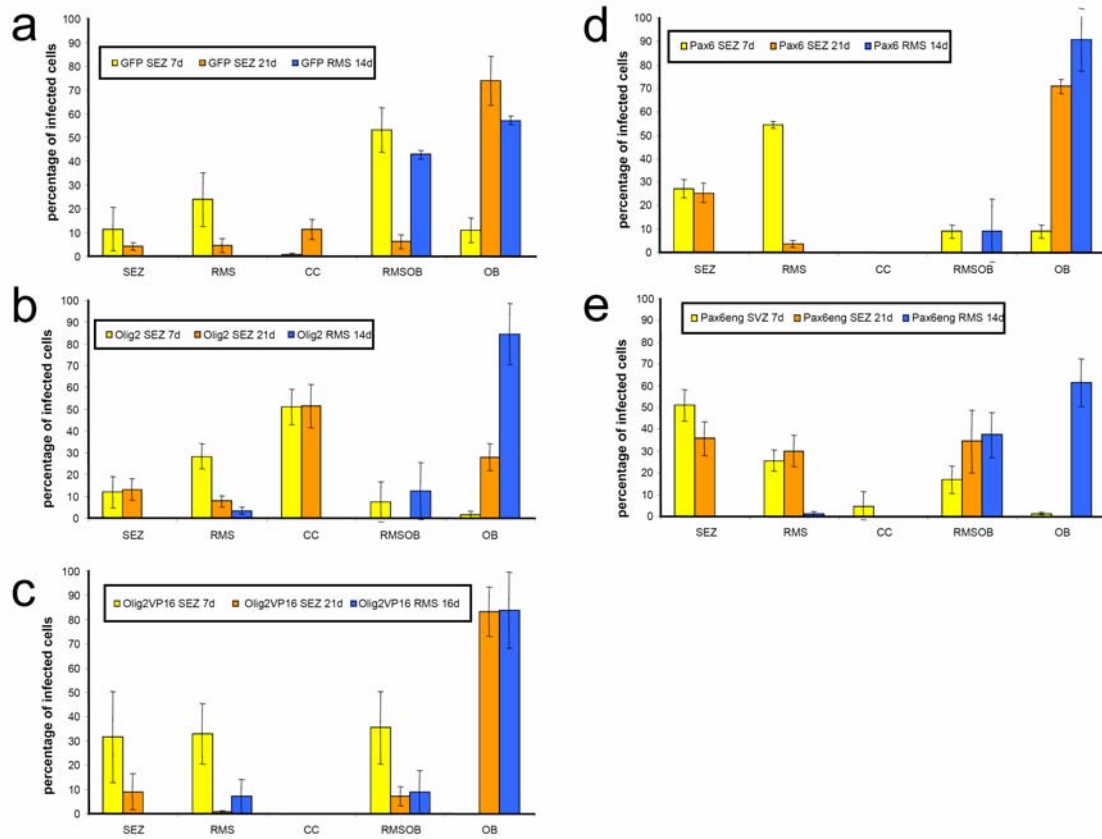


Figure 32. Quantitative localization analysis of infected cells after virus injection into the SEZ or the RMS of the adult forebrain. **a-d**, Histograms showing the localization of GFP-positive cells after infection with the control-virus containing GFP only (**a**), with the Olig2-IRES-GFP-containing virus (**b**), with the Olig2VP16-IRES-GFP viral vector, (**c**) with the Pax6-IRES-GFP-containing virus (**d**), or the Pax6-engrailed-IRES-GFP-containing viral vector (**e**). Virus was injected either in the subependymal zone (SEZ) or the rostral migratory stream (RMS) and animals were sacrificed at different times after infection [7 days (yellow bars), 21 days (orange bars) for SEZ infection and 14-18 days (blue bars) for RMS infection]. Note that only precursor cells infected in the SEZ, but not those in the RMS were able to generate oligodendrocytes and that Olig2-infected cells migrate faster into the CC and differentiate into many more oligodendrocytes than control infected cells. On the contrary, Pax6 increases the number of neuroblasts in the RMS 7 days after injection compared to the control virus injection (compare **a** and **d**, yellow bars), while after 21 days most cells have reached the OB in both conditions. Notably, a larger proportion of infected cells have reached the OB 14 days after injection of both the Pax6- or Olig2-containing viral vectors compared to the control injections (compare blue bars in **a,b,d**), while Pax6-engrailed containing virus reduces the proportion of neurons in the OB. Similarly, cells infected with the Pax6-engrailed containing virus in the SEZ remained to a larger extent in the SEZ and few of them had reached the OB (RMS/OB and OB) compared to control virus injection (compare yellow bars in **a** and **e**).

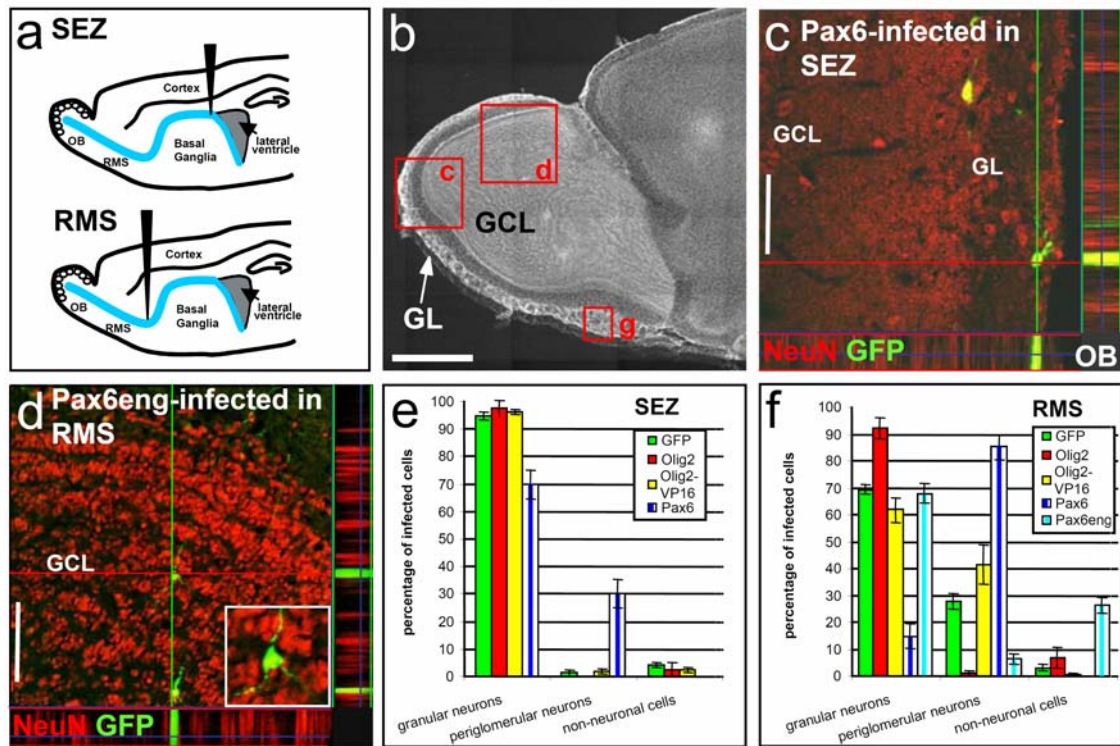


Figure 33. Functional analysis of Pax6 and Olig2 in the specification of neuronal subtypes in adult neurogenesis. Panel (a) depicts the injection sites as described in Fig.25. (b) depicts a micrograph of the OB with the red inserts indicating the position of the micrographs (c,d). (c,d) depict representative micrograph examples with z-stacks of the confocal pictures taken at the position of the red and green lines and higher magnification (inset in d). Histograms in (e,f) depict the quantification of GFP-positive cell types in the OB 21 (e) or 14-16 days (f) after viral infection as indicated in the panels in (c,d,g). c, depicts a double-stained (NeuN-immunopositive and GFP) periglomerular neuron in the GL. (d) shows double-stained neurons in the GCL. Note that Pax6 is involved in the specification of the periglomerular neurons located in the GL. SEZ: subependymal zone, RMS: rostral migratory stream, OB: olfactory bulb. GL: glomerular layer; GCL: granule cell layer. Scale bars: b: 400µm, c: 50 µm, d: 150 µm (inset 30 µm).

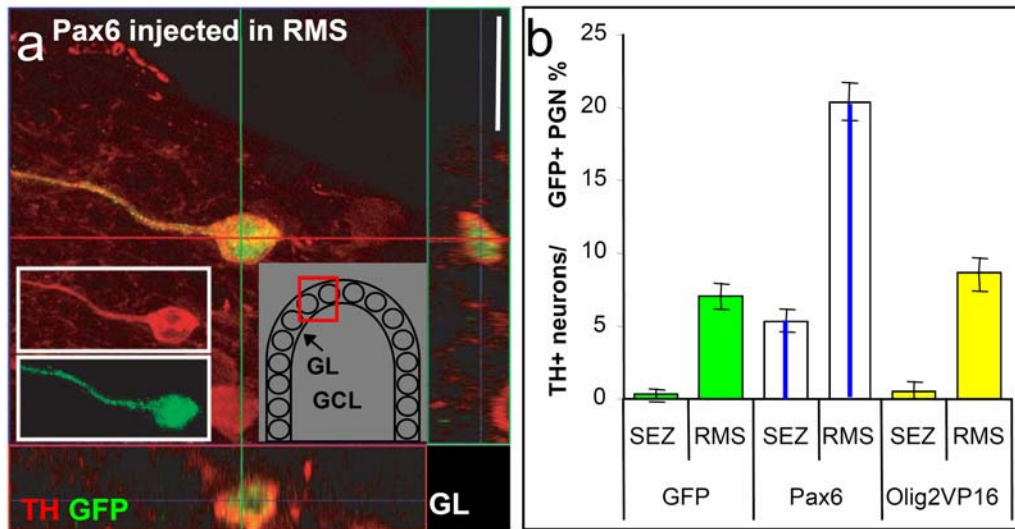


Figure 34. TH-positive periglomerular fate is strongly promoted by Pax6-overexpression. (a) depicts a representative micrograph examples of a GFP and TH double-immunoreactive cell with z-stacks of the confocal pictures taken at the position of the red and green lines and higher magnification **b**, Histogram of TH-positive periglomerular neurons (PGN, y-axis) after viral vector injection (x-axis) into the SEZ (3 weeks survival) or RMS (2 weeks). Note that only RMS, but not SEZ precursors, generate TH-positive PGN and that this fate is strongly promoted by Pax6, while blocking of Olig2 function (Olig2VP16) has no effect. *SEZ*: subependymal zone, *RMS*: rostral migratory stream, *OB*: olfactory bulb. *GL*: glomerular layer; Scale bars: **a**: 30 μ m.

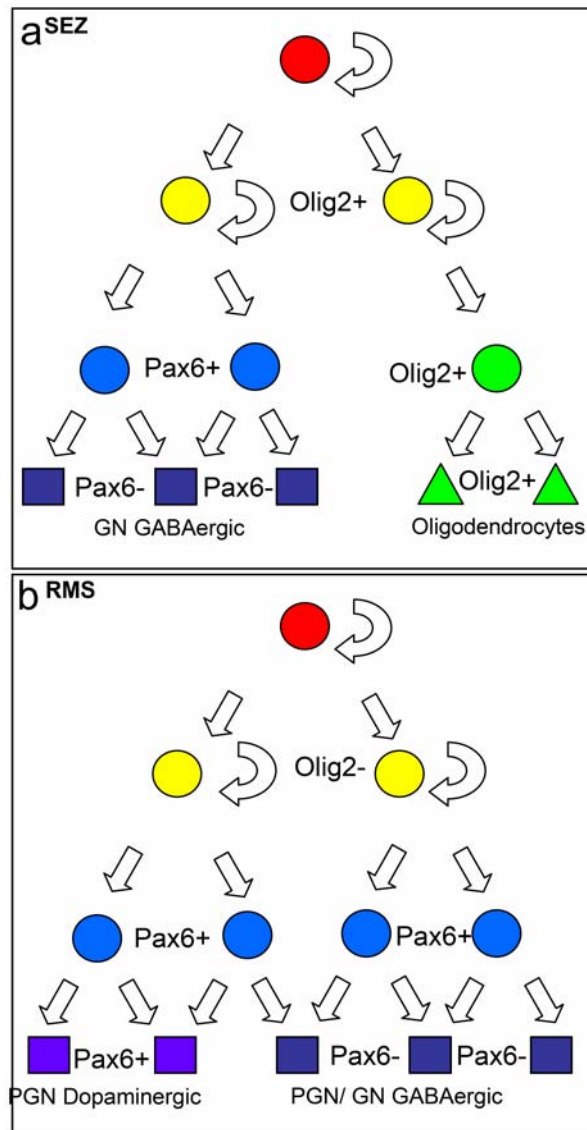


Figure 35. Separate lineages in SEZ and RMS. (a) and (b), summarize the content and function of Pax6 and Olig2 in the two lineages of adult neural precursors depicted as in **Fig.2b**. *SEZ*: subependymal zone, *RMS*: rostral migratory stream,

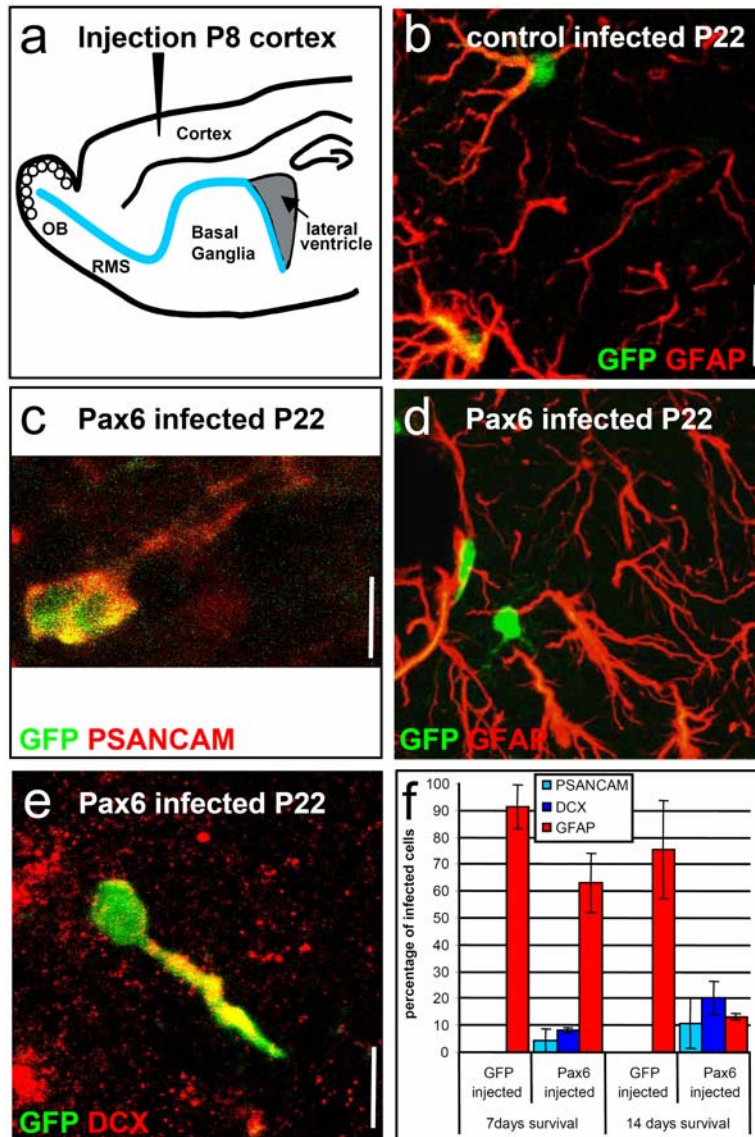


Figure 36. Generation of young neurons in the postnatal cerebral cortex by Pax6 transduction in vivo. (a) Schematic drawing of a sagittal sections of the adult mouse illustrating the injection sites (cortex) of the viruses. (b-e) show micrographs of the postnatal cortex 14 days after viral infection as indicated in the panels. GFP-immunostaining (green) is combined with cell type specific markers GFAP (red, b,d), PSANCAM (red, c) and DCX (red, e). Histogram in (f) depicts the quantification of GFP-positive cell types in the cortex 14 days after viral injection indicated on the x-axis. Note that the control GFP-virus infected cells are exclusively GFAP-positive and do not generate neurons 2 weeks after viral transduction. In contrast, almost 30% of GFP-positive cells have differentiated into young neurons 2 weeks after transduction with Pax6. RMS: rostral migratory stream, OB: olfactory bulb. Scale bars in (b,d) 3 μ m, (c) 1 μ m, (e) 2 μ m.

<i>Primer name</i>	<i>Forward sequence</i>	<i>Reverse sequence</i>
Pax6	CGGAGGGAGTAAGCCAAGAG	TCTGTCTCGGATTCCCAAG
Emx1	GAGCCTTTGAGAAGAATCAC	CTAGTCATTGGAGGTGACAT
Emx2	TCAGAACCGGAGAACGAAAT	TCTCCACCGGTTAATGTGGT
Ngn2	ACCGCATGCACAACCTAAAC	AGCGCCCAGATGTAATTGTG
Olig1	CCAAAGAGGAACAGCAGCAG	GTGGCAATCTTGGAGAGCTT
Olig2	CACAGGAGGGACTGTGTCCT	GGTGCTGGAGGAAGATGACT
Mash1	AGATGAGCAAGGTGGAGACG	TGGAGTAGTTGGGGGAGATG
Dlx1	TGGAATCCGAACTCCTCATC	TCACATCAGTTGAGGCTGCT
Dlx2	TTTGACAGTCTGGTGGCTGA	CTGTTGCTGCTGCTGCTGTT
Gsh2	CCTTTGCTCAAAAAGCCAGTT	GGTGATGGTGATGATGATGC
Vax1	ATTACTGTGCGCCGATCCTA	GTATTGGCAACGCTGGAACT
Prox1	AGGAAGGGCTATCACCCAAT	ACGCGCATACTTCTCCATCT
Nkx2.2	GCTGACCAACACAAAAGACG	CTCTCCTCCTCTGGCCCTTC
islet-1	GCAACCCAACGACAAAACCTA	GGCTGGTAACTTTGCACCTC
Sox4	CTGCCGCAAGAAAGTGAAG	TTCGTACAACCCCAAGTGGAT
tweety	CCgCAGACAGGAGAGAAAAG	CAATGGAAGGGCAGCATAAC
Klf9	CAATGGAAGGGCAGCATAAC	CTTACGACCTCCAAGGACCA
Sirt2	CCCTGACTGGGCATCTATGT	GTGGCATGGATTTTACTCC
Sox9	ATCAAGACGGAGCAGCTGAG	TCTGATGGTCAGCGTAGTCG
FABP7	ATCCAACCGAACCACAGACT	GAAGGTGGCAAAGTGGTGAT
LMO1	TCAAAGGTGCCATTGAGATG	AAGCTGATCCCAGCTTTTA
GAPDH	ATTCAACGGCACAGTCAAGG	TGGATGCAGGGATGATGTTT
HPRT	GTTGGATACAGGCCAGACTTTGT	CCACAGGACTAGAACACCTGCTA

Table 1. List of primers for quantitative RT-PCR

a

<i>Relative expression levels (GAPDH=1)</i>	<i>E14 CTX</i>	<i>E14 GE</i>	<i>CTX neuro-spheres</i>	<i>GE neuro-spheres</i>	<i>adult neuro-spheres</i>
cortex					
Pax6	1.1E-01	3.0E-03	1.3E-03	1.5E-03	1.3E-03
Emx1	8.4E-02	1.2E-02	7.5E-04	1.3E-03	1.1E-03
Emx2	1.0E-02	1.0E-03	2.0E-03	1.3E-03	5.0E-03
Ngn2	6.0E-02	6.0E-03	4.1E-04	2.9E-04	2.8E-04
GE					
Olig1	3.6E-03	1.8E-02	8.9E-02	6.2E-02	3.4E-02
Olig2	1.8E-04	6.8E-03	9.5E-03	8.2E-03	2.0E-02
Mash1	2.7E-04	3.1E-03	6.7E-04	6.3E-04	1.1E-03
Dlx1	2.7E-03	7.6E-02	2.0E-03	1.6E-03	1.3E-03
Dlx2	6.5E-03	5.9E-02	1.6E-04	8.7E-05	1.3E-04
Gsh2	5.2E-05	6.0E-04	4.6E-05	2.1E-05	6.2E-05
Vax1	2.7E-05	6.9E-03	1.1E-05	9.6E-06	7.8E-06
Prox1	8.6E-05	2.3E-02	5.4E-03	6.3E-03	3.8E-03
Nkx2.2	1.7E-04	6.1E-02	4.7E-04	6.7E-04	2.0E-04
islet-1	3.2E-04	5.2E-02	2.1E-05	3.4E-05	2.1E-04

b

<i>Relative expression levels (GAPDH=1)</i>	<i>hGFAP eGFP+</i>	<i>hGFAP eGFP++</i>	<i>CTX neurospheres differentiated for 1 day</i>	<i>neurospheres of the cortex differentiated for 3 days</i>	<i>neurospheres of the GE differentiated for 1 day</i>	<i>neurospheres of the GE differentiated for 3 days</i>
cortex						
Pax6	5.7E-02	1.2E-02	1.9E-03	6.1E-03	2.2E-03	6.3E-03
Emx1	1.8E-02	2.3E-02	1.1E-03	4.5E-03	1.8E-03	3.1E-03
Emx2	3.3E-03	2.1E-02	3.3E-03	7.6E-03	2.9E-03	6.2E-03
Ngn2	1.5E-03	1.9E-03	5.1E-04	1.1E-03	4.0E-04	1.1E-03
GE						
Olig1			3.1E-02	2.7E-03	2.7E-02	2.9E-03
Olig2	1.4E-04	6.2E-04	4.9E-03	2.4E-03	4.0E-03	2.5E-03
Mash1	3.5E-04	2.4E-04	1.3E-03	1.9E-03	1.1E-03	1.6E-03
Dlx1	7.3E-04	7.3E-04	2.9E-04	1.0E-04	3.6E-04	7.7E-05
Dlx2	3.9E-03	1.8E-03	1.7E-04	2.0E-04	2.0E-04	3.8E-04
Gsh2	8.2E-05	2.1E-05	4.2E-05	9.4E-05	5.1E-05	7.7E-05
Vax1			5.6E-06	5.0E-06	9.4E-06	1.1E-05
Prox1			2.1E-03	5.5E-04	2.4E-03	9.6E-04
Nkx2.2			9.0E-04	1.7E-03	8.1E-04	1.9E-03
islet-1			3.7E-05	4.3E-05	4.3E-05	4.2E-05

Table 2. Quantitative mRNA analysis of transcription factors in precursors derived from the hGFAPeGFP and WT E14 cortex and the precursors sorted on the basis of their GFP content from the cortex of E14 hGFAPeGFP mice (+ and ++) (b); and on undifferentiated neurosphere cultures from E14 cortex or GE or the adult SEZ exposed for 1 or 3 days to differentiating conditions (a). Note, that the region specific differences in gene expression between cells from cortex and GE are severely reduced in neurosphere cultures

<i>Relative expression levels (GAPDH=1)</i>	<i>CTX neurospheres</i>	<i>CTX neurospheres differentiated for 1day</i>	<i>hGFAPeGFP++</i>	<i>hGFAPeGFP+</i>
tweety	7.7E-01	2.1E-01	3.0E-03	3.0E-03
sirt2	2.2E-01	5.1E-02	5.3E-04	2.6E-03
Sox4	2.3E-04	2.0E-04	8.5E-04	9.8E-03
Sox9	1.3E-02	7.9E-02	7.3E-02	5.0E-03
FABP7	3.9E-01	1.1E-01	2.9E-03	2.9E-03
KLf9	2.2E-01	1.1E-01	2.2E-02	3.5E-03
LMO1	2.9E-04	4.6E-04	3.4E-03	2.0E-02

Table 3. Quantitative mRNA analysis of the selected genes of the microarray experiments on the precursors sorted on the basis of their GFP content from the cortex of E14 hGFAPeGFP mice (+ and ++) and on the precursors on undifferentiated neurosphere cultures from E14 cortex and on undifferentiated neurosphere cultures from E14 cortex exposed for 1 day to differentiating conditions.

PLEASE SEE ATTACHED CD

Table 4. Thresholded genes of the microarray experiment performed on the precursors sorted on the basis of their GFP content from the cortex of E14 hGFAPeGFP mice (+ and ++)

PLEASE SEE ATTACHED CD

Table 5. Thresholded genes of the microarray experiment performed on the precursors on undifferentiated neurosphere cultures from E14 cortex and on undifferentiated neurosphere cultures from E14 cortex exposed for 1 day to differentiating conditions.

9 REFERENCES

- Aguirre, A. A., Chittajallu, R., Belachew, S. and Gallo, V.** (2004). NG2-expressing cells in the subventricular zone are type C-like cells and contribute to interneuron generation in the postnatal hippocampus. *J Cell Biol* **165**, 575-89.
- Altman, J.** (1969). Autoradiographic and histological studies of postnatal neurogenesis. IV. Cell proliferation and migration in the anterior forebrain, with special reference to persisting neurogenesis in the olfactory bulb. *J Comp Neurol* **137**, 433-57.
- Alvarez-Buylla, A. and Nottebohm, F.** (1988). Migration of young neurons in adult avian brain. *Nature* **335**, 353-4.
- Anderson, S., Mione, M., Yun, K. and Rubenstein, J. L.** (1999). Differential origins of neocortical projection and local circuit neurons: role of *Dlx* genes in neocortical interneuronogenesis. *Cereb Cortex* **9**, 646-54.
- Anderson, S. A., Eisenstat, D. D., Shi, L. and Rubenstein, J. L.** (1997a). Interneuron migration from basal forebrain to neocortex: dependence on *Dlx* genes. *Science* **278**, 474-6.
- Anderson, S. A., Qiu, M., Bulfone, A., Eisenstat, D. D., Meneses, J., Pedersen, R. and Rubenstein, J. L.** (1997b). Mutations of the homeobox genes *Dlx-1* and *Dlx-2* disrupt the striatal subventricular zone and differentiation of late born striatal neurons. *Neuron* **19**, 27-37.
- Anthony, T. E., Klein, C., Fishell, G. and Heintz, N.** (2004). Radial glia serve as neuronal progenitors in all regions of the central nervous system. *Neuron* **41**, 881-90.
- Arvidsson, A., Collin, T., Kirik, D., Kokaia, Z. and Lindvall, O.** (2002). Neuronal replacement from endogenous precursors in the adult brain after stroke. *Nat Med* **8**, 963-70.
- Ashery-Padan, R., Marquardt, T., Zhou, X. and Gruss, P.** (2000). Pax6 activity in the lens primordium is required for lens formation and for correct placement of a single retina in the eye. *Genes Dev* **14**, 2701-11.
- Ashery-Padan, R., Zhou, X., Marquardt, T., Herrera, P., Toubé, L., Berry, A. and Gruss, P.** (2004). Conditional inactivation of Pax6 in the pancreas causes early onset of diabetes. *Dev Biol* **269**, 479-88.
- Aubert, J., Dunstan, H., Chambers, I. and Smith, A.** (2002). Functional gene screening in embryonic stem cells implicates Wnt antagonism in neural differentiation. *Nat Biotechnol* **20**, 1240-5.
- Bamji, S. X. and Miller, F. D.** (1996). Comparison of the expression of a T alpha 1:nlacZ transgene and T alpha 1 alpha-tubulin mRNA in the mature central nervous system. *J Comp Neurol* **374**, 52-69.
- Barbin, G., Katz, D. M., Chamak, B., Glowinski, J. and Prochiantz, A.** (1988). Brain astrocytes express region-specific surface glycoproteins in culture. *Glia* **1**, 96-103.
- Bedard, A. and Parent, A.** (2004). Evidence of newly generated neurons in the human olfactory bulb. *Brain Res Dev Brain Res* **151**, 159-68.
- Belachew, S., Chittajallu, R., Aguirre, A. A., Yuan, X., Kirby, M., Anderson, S. and Gallo, V.** (2003). Postnatal NG2 proteoglycan-expressing progenitor cells are intrinsically multipotent and generate functional neurons. *J Cell Biol* **161**, 169-86.

- Belluzzi, O., Benedusi, M., Ackman, J. and LoTurco, J. J.** (2003). Electrophysiological differentiation of new neurons in the olfactory bulb. *J Neurosci* **23**, 10411-8.
- Bertrand, N., Castro, D. S. and Guillemot, F.** (2002). Proneural genes and the specification of neural cell types. *Nat Rev Neurosci* **3**, 517-30.
- Bertrand, N., Medevielle, F. and Pituello, F.** (2000). FGF signalling controls the timing of Pax6 activation in the neural tube. *Development* **127**, 4837-43.
- Bibel, M., Richter, J., Schrenk, K., Tucker, K. L., Staiger, V., Korte, M., Goetz, M. and Barde, Y. A.** (2004). Differentiation of mouse embryonic stem cells into a defined neuronal lineage. *Nat Neurosci* **7**, 1003-9.
- Blass-Kampmann, S., Reinhardt-Maelicke, S., Kindler-Rohrborn, A., Cleeves, V. and Rajewsky, M. F.** (1994). In vitro differentiation of E-N-CAM expressing rat neural precursor cells isolated by FACS during prenatal development. *J Neurosci Res* **37**, 359-73.
- Briata, P., Di Blas, E., Gulisano, M., Mallamaci, A., Iannone, R., Boncinelli, E. and Corte, G.** (1996). EMX1 homeoprotein is expressed in cell nuclei of the developing cerebral cortex and in the axons of the olfactory sensory neurons. *Mech Dev* **57**, 169-80.
- Brunjes, P. C.** (1994). Unilateral naris closure and olfactory system development. *Brain Res Brain Res Rev* **19**, 146-60.
- Byrom, M., Pallotta, V., Brown, D. and Ford, L. P.** (2002). RNAi in mammalian cells: visualizing siRNA and analyzing induction of RNAi. *Ambion Tech Notes* **9**, 6-8.
- Cai, L., Morrow, E. M. and Cepko, C. L.** (2000). Misexpression of basic helix-loop-helix genes in the murine cerebral cortex affects cell fate choices and neuronal survival. *Development* **127**, 3021-30.
- Campbell, K. and Götz, M.** (2002). Radial glia: multi-purpose cells for vertebrate brain development. *Trends Neurosci* **25**, 235-8.
- Capela, A. and Temple, S.** (2002). LeX/ssea-1 is expressed by adult mouse CNS stem cells, identifying them as nonependymal. *Neuron* **35**, 865-75.
- Carleton, A., Petreanu, L. T., Lansford, R., Alvarez-Buylla, A. and Lledo, P. M.** (2003). Becoming a new neuron in the adult olfactory bulb. *Nat Neurosci* **6**, 507-18.
- Casarosa, S., Fode, C. and Guillemot, F.** (1999). Mash1 regulates neurogenesis in the ventral telencephalon. *Development* **126**, 525-34.
- Chen, J., Magavi, S. S. and Macklis, J. D.** (2004). Neurogenesis of corticospinal motor neurons extending spinal projections in adult mice. *Proc Natl Acad Sci U S A* **101**, 16357-62.
- Cheung, M., Abu-Elmagd, M., Clevers, H. and Scotting, P. J.** (2000). Roles of Sox4 in central nervous system development. *Brain Res Mol Brain Res* **79**, 180-91.
- Chojnacki, A., Shimazaki, T., Gregg, C., Weinmaster, G. and Weiss, S.** (2003). Glycoprotein 130 signaling regulates Notch1 expression and activation in the self-renewal of mammalian forebrain neural stem cells. *J Neurosci* **23**, 1730-41.
- Ciccolini, F., Collins, T. J., Sudhoelter, J., Lipp, P., Berridge, M. J. and Bootman, M. D.** (2003). Local and global spontaneous calcium events regulate neurite outgrowth and onset of GABAergic phenotype during neural precursor differentiation. *J Neurosci* **23**, 103-11.
- Committee, B.** (1970). Embryonic vertebrate central nervous system: revised terminology. The Boulder Committee. *Anat Rec* **166**, 257-61.

Corbin, J. G., Gaiano, N., Machold, R. P., Langston, A. and Fishell, G. (2000). The Gsh2 homeodomain gene controls multiple aspects of telencephalic development. *Development* **127**, 5007-5020.

Davenne, M., Custody, C., Charneau, P. and Lledo, P. (2004). In vivo imaging of migrating neurons in the mammalian forebrain. *Chem. Senses* **in press**.

Decker, L., Durbec, P., Rougon, G. and Evercooren, A. B. (2002). Loss of polysialic residues accelerates CNS neural precursor differentiation in pathological conditions. *Mol Cell Neurosci* **19**, 225-38.

Dellovade, T. L., Pfaff, D. W. and Schwanzel-Fukuda, M. (1998). Olfactory bulb development is altered in small-eye (Sey) mice. *J Comp Neurol* **402**, 402-18.

Denis-Donini, S., Glowinski, J. and Prochiantz, A. (1984). Glial heterogeneity may define the three-dimensional shape of mouse mesencephalic dopaminergic neurones. *Nature* **307**, 641-3.

Diez del Corral, R., Olivera-Martinez, I., Goriely, A., Gale, E., Maden, M. and Storey, K. (2003). Opposing FGF and retinoid pathways control ventral neural pattern, neuronal differentiation, and segmentation during body axis extension. *Neuron* **40**, 65-79.

Doetsch, F., Caille, I., Lim, D. A., Garcia-Verdugo, J. M. and Alvarez-Buylla, A. (1999). Subventricular zone astrocytes are neural stem cells in the adult mammalian brain. *Cell* **97**, 703-16.

Doetsch, F., Petreanu, L., Caille, I., Garcia-Verdugo, J. M. and Alvarez-Buylla, A. (2002). EGF converts transit-amplifying neurogenic precursors in the adult brain into multipotent stem cells. *Neuron* **36**, 1021-34.

Dymecki, S. M. and Tomasiewicz, H. (1998). Using Flp-recombinase to characterize expansion of Wnt1-expressing neural progenitors in the mouse. *Dev Biol* **201**, 57-65.

Edlund, T. and Jessell, T. M. (1999). Progression from extrinsic to intrinsic signaling in cell fate specification: a view from the nervous system. *Cell* **96**, 211-24.

Eisenstat, D. D., Liu, J. K., Mione, M., Zhong, W., Yu, G., Anderson, S. A., Ghattas, I., Puelles, L. and Rubenstein, J. L. (1999). DLX-1, DLX-2, and DLX-5 expression define distinct stages of basal forebrain differentiation. *J Comp Neurol* **414**, 217-37.

Ericson, J., Rashbass, P., Schedl, A., Brenner-Morton, S., Kawakami, A., van Heyningen, V., Jessell, T. M. and Briscoe, J. (1997). Pax6 controls progenitor cell identity and neuronal fate in response to graded Shh signaling. *Cell* **90**, 169-80.

Follenzi, A., Ailles, L. E., Bakovic, S., Geuna, M. and Naldini, L. (2000). Gene transfer by lentiviral vectors is limited by nuclear translocation and rescued by HIV-1 pol sequences. *Nat Genet* **25**, 217-22.

Fricke, R. A., Carpenter, M. K., Winkler, C., Greco, C., Gates, M. A. and Bjorklund, A. (1999). Site-specific migration and neuronal differentiation of human neural progenitor cells after transplantation in the adult rat brain. *J Neurosci* **19**, 5990-6005.

Fulco, M., Schiltz, R. L., Iezzi, S., King, M. T., Zhao, P., Kashiwaya, Y., Hoffman, E., Veech, R. L. and Sartorelli, V. (2003). Sir2 regulates skeletal muscle differentiation as a potential sensor of the redox state. *Mol Cell* **12**, 51-62.

Furukawa, T., Mukherjee, S., Bao, Z. Z., Morrow, E. M. and Cepko, C. L. (2000). rax, Hes1, and notch1 promote the formation of Muller glia by postnatal retinal progenitor cells. *Neuron* **26**, 383-94.

- Gabay, L., Lowell, S., Rubin, L. and Anderson, D.** (2003). Deregulation of dorsoventral patterning by FGF confers trilineage differentiation capacity on CNS stem cells in vitro. *Neuron* **40**, 485-499.
- Galipeau, J., Li, H., Paquin, A., Sicilia, F., Karpati, G. and Nalbantoglu, J.** (1999). Vesicular stomatitis virus G pseudotyped retrovector mediates effective in vivo suicide gene delivery in experimental brain cancer. *Cancer Res* **59**, 2384-94.
- Gall, C. M., Hendry, S. H., Seroogy, K. B., Jones, E. G. and Haycock, J. W.** (1987). Evidence for coexistence of GABA and dopamine in neurons of the rat olfactory bulb. *J Comp Neurol* **266**, 307-18.
- Gangemi, R. M., Daga, A., Marubbi, D., Rosatto, N., Capra, M. C. and Corte, G.** (2001). Emx2 in adult neural precursor cells. *Mech Dev* **109**, 323-9.
- Garcia, A. D., Doan, N. B., Imura, T., Bush, T. G. and Sofroniew, M. V.** (2004). GFAP-expressing progenitors are the principal source of constitutive neurogenesis in adult mouse forebrain. *Nat Neurosci* **7**, 1233-41.
- Garel, S., Marin, F., Grosschedl, R. and Charnay, P.** (1999). Ebf1 controls early cell differentiation in the embryonic striatum. *Development* **126**, 5285-94.
- Geschwind, D. H., Ou, J., Easterday, M. C., Dougherty, J. D., Jackson, R. L., Chen, Z., Antoine, H., Terskikh, A., Weissman, I. L., Nelson, S. F. et al.** (2001). A genetic analysis of neural progenitor differentiation. *Neuron* **29**, 325-39.
- Ghattas, I. R., Sanes, J. R. and Majors, J. E.** (1991). The encephalomyocarditis virus internal ribosome entry site allows efficient coexpression of two genes from a recombinant provirus in cultured cells and in embryos. *Mol Cell Biol* **11**, 5848-59.
- Götz, M.** (1995). Getting there and being there in the cerebral cortex. *Experientia* **51**, 301-16.
- Götz, M., Hartfuss, E. and Malatesta, P.** (2002). Radial glial cells as neuronal precursors: a new perspective on the correlation of morphology and lineage restriction in the developing cerebral cortex of mice. *Brain Res Bull* **57**, 777-88.
- Götz, M., Stoykova, A. and Gruss, P.** (1998). Pax6 controls radial glia differentiation in the cerebral cortex. *Neuron* **21**, 1031-44.
- Grandbarbe, L., Bouissac, J., Rand, M., Hrabe de Angelis, M., Artavanis-Tsakonas, S. and Mohier, E.** (2003). Delta-Notch signaling controls the generation of neurons/glia from neural stem cells in a stepwise process. *Development* **130**, 1391-402.
- Gritti, A., Bonfanti, L., Doetsch, F., Caille, I., Alvarez-Buylla, A., Lim, D. A., Galli, R., Verdugo, J. M., Herrera, D. G. and Vescovi, A. L.** (2002). Multipotent neural stem cells reside into the rostral extension and olfactory bulb of adult rodents. *J Neurosci* **22**, 437-45.
- Gross, R. E., Mehler, M. F., Mabie, P. C., Zang, Z., Santschi, L. and Kessler, J. A.** (1996). Bone morphogenetic proteins promote astroglial lineage commitment by mammalian subventricular zone progenitor cells. *Neuron* **17**, 595-606.
- Grove, E. A., Williams, B. P., Li, D. Q., Hajihosseini, M., Friedrich, A. and Price, J.** (1993). Multiple restricted lineages in the embryonic rat cerebral cortex. *Development* **117**, 553-61.
- Gulisano, M., Broccoli, V., Pardini, C. and Boncinelli, E.** (1996). Emx1 and Emx2 show different patterns of expression during proliferation and differentiation of the developing cerebral cortex in the mouse. *Eur J Neurosci* **8**, 1037-50.

- Hack, M. A., Saghatelian, A., Chevigny, A., Pfeifer, A., Ashery-Padan, R., Lledo, P. M. and Götz, M.** (2005). Neuronal fate determinants of adult olfactory bulb neurogenesis. *Nat Neurosci* **under revision**.
- Hack, M. A., Sugimori, M., Lundberg, C., Nakafuku, M. and Götz, M.** (2004). Regionalization and fate specification in neurospheres: the role of Olig2 and Pax6. *Mol Cell Neurosci* **25**, 664-78.
- Hajhosseini, M. K. and Dickson, C.** (1999). A subset of fibroblast growth factors (Fgfs) promote survival, but Fgf-8b specifically promotes astroglial differentiation of rat cortical precursor cells. *Mol Cell Neurosci* **14**, 468-85.
- Hartfuss, E., Forster, E., Bock, H. H., Hack, M. A., LePrince, P., Luque, J. M., Herz, J., Frotscher, M. and Götz, M.** (2003). Reelin signaling directly affects radial glia morphology and biochemical maturation. *Development* **130**, 4597-609.
- Hartfuss, E., Galli, R., Heins, N. and Götz, M.** (2001). Characterization of CNS precursor subtypes and radial glia. *Dev Biol* **229**, 15-30.
- Hashimoto, M. and Mikoshiba, K.** (2004). Neuronal birthdate-specific gene transfer with adenoviral vectors. *J Neurosci* **24**, 286-96.
- Hattori, M., Fujiyama, A., Taylor, T. D., Watanabe, H., Yada, T., Park, H. S., Toyoda, A., Ishii, K., Totoki, Y., Choi, D. K. et al.** (2000). The DNA sequence of human chromosome 21. *Nature* **405**, 311-9.
- Haubensak, W., Attardo, A., Denk, W. and Huttner, W. B.** (2004). Neurons arise in the basal neuroepithelium of the early mammalian telencephalon: a major site of neurogenesis. *Proc Natl Acad Sci U S A* **101**, 3196-201.
- Haubst, N., Berger, J., Radjendirane, V., Graw, J., Favor, J., Saunders, G. F., Stoykova, A. and Götz, M.** (2004). Molecular dissection of Pax6 function: the specific roles of the paired domain and homeodomain in brain development. *Development* **131**, 6131-40.
- Heins, N., Cremisi, F., Malatesta, P., Gangemi, R. M., Corte, G., Price, J., Goudreau, G., Gruss, P. and Götz, M.** (2001). Emx2 promotes symmetric cell divisions and a multipotential fate in precursors from the cerebral cortex. *Mol Cell Neurosci* **18**, 485-502.
- Heins, N., Malatesta, P., Cecconi, F., Nakafuku, M., Tucker, K. L., Hack, M. A., Chappouton, P., Barde, Y. A. and Götz, M.** (2002). Glial cells generate neurons: the role of the transcription factor Pax6. *Nat Neurosci* **5**, 308-15.
- Herrera, D. G., Garcia-Verdugo, J. M. and Alvarez-Buylla, A.** (1999). Adult-derived neural precursors transplanted into multiple regions in the adult brain. *Ann Neurol* **46**, 867-77.
- Hevner, R. F., Neogi, T., Englund, C., Daza, R. A. and Fink, A.** (2003). Cajal-Retzius cells in the mouse: transcription factors, neurotransmitters, and birthdays suggest a pallial origin. *Brain Res Dev Brain Res* **141**, 39-53.
- Hill, R. E., Favor, J., Hogan, B. L., Ton, C. C., Saunders, G. F., Hanson, I. M., Prosser, J., Jordan, T., Hastie, N. D. and van Heyningen, V.** (1991). Mouse small eye results from mutations in a paired-like homeobox-containing gene. *Nature* **354**, 522-5.
- Hinks, G. L., Shah, B., French, S. J., Campos, L. S., Staley, K., Hughes, J. and Sofroniew, M. V.** (1997). Expression of LIM protein genes Lmo1, Lmo2, and Lmo3 in adult mouse hippocampus and other forebrain regions: differential regulation by seizure activity. *J Neurosci* **17**, 5549-59.

- Hitoshi, S., Alexson, T., Tropepe, V., Donoviel, D., Elia, A. J., Nye, J. S., Conlon, R. A., Mak, T. W., Bernstein, A. and van der Kooy, D.** (2002a). Notch pathway molecules are essential for the maintenance, but not the generation, of mammalian neural stem cells. *Genes Dev* **16**, 846-58.
- Hitoshi, S., Tropepe, V., Ekker, M. and van der Kooy, D.** (2002b). Neural stem cell lineages are regionally specified, but not committed, within distinct compartments of the developing brain. *Development* **129**, 233-44.
- Hojo, M., Ohtsuka, T., Hashimoto, N., Gradwohl, G., Guillemot, F. and Kageyama, R.** (2000). Glial cell fate specification modulated by the bHLH gene *Hes5* in mouse retina. *Development* **127**, 2515-22.
- Holtzman, D. M., Santucci, D., Kilbridge, J., Chua-Couzens, J., Fontana, D. J., Daniels, S. E., Johnson, R. M., Chen, K., Sun, Y., Carlson, E. et al.** (1996). Developmental abnormalities and age-related neurodegeneration in a mouse model of Down syndrome. *Proc Natl Acad Sci U S A* **93**, 13333-8.
- Huisman, E., Uylings, H. B. and Hoogland, P. V.** (2004). A 100% increase of dopaminergic cells in the olfactory bulb may explain hyposmia in Parkinson's disease. *Mov Disord* **19**, 687-92.
- Imura, T., Kornblum, H. I. and Sofroniew, M. V.** (2003). The predominant neural stem cell isolated from postnatal and adult forebrain but not early embryonic forebrain expresses GFAP. *J Neurosci* **23**, 2824-32.
- Ivanova, N. B., Dimos, J. T., Schaniel, C., Hackney, J. A., Moore, K. A. and Lemischka, I. R.** (2002). A stem cell molecular signature. *Science* **298**, 601-4.
- Jimenez, D., Garcia, C., de Castro, F., Chedotal, A., Sotelo, C., de Carlos, J. A., Valverde, F. and Lopez-Mascaraque, L.** (2000). Evidence for intrinsic development of olfactory structures in Pax-6 mutant mice. *J Comp Neurol* **428**, 511-26.
- Kalyani, A., Hobson, K. and Rao, M. S.** (1997). Neuroepithelial stem cells from the embryonic spinal cord: isolation, characterization, and clonal analysis. *Dev Biol* **186**, 202-23.
- Kalyani, A. J., Piper, D., Mujtaba, T., Lucero, M. T. and Rao, M. S.** (1998). Spinal cord neuronal precursors generate multiple neuronal phenotypes in culture. *J Neurosci* **18**, 7856-68.
- Kaneko, Y., Sakakibara, S., Imai, T., Suzuki, A., Nakamura, Y., Sawamoto, K., Ogawa, Y., Toyama, Y., Miyata, T. and Okano, H.** (2000). Musashi1: an evolutionally conserved marker for CNS progenitor cells including neural stem cells. *Dev Neurosci* **22**, 139-53.
- Keyoung, H. M., Roy, N. S., Benraiss, A., Louissaint, A., Jr., Suzuki, A., Hashimoto, M., Rashbaum, W. K., Okano, H. and Goldman, S. A.** (2001). High-yield selection and extraction of two promoter-defined phenotypes of neural stem cells from the fetal human brain. *Nat Biotechnol* **19**, 843-50.
- Kilpatrick, T. J. and Bartlett, P. F.** (1995). Cloned multipotential precursors from the mouse cerebrum require FGF-2, whereas glial restricted precursors are stimulated with either FGF-2 or EGF. *J Neurosci* **15**, 3653-61.
- Kirschenbaum, B., Doetsch, F., Lois, C. and Alvarez-Buylla, A.** (1999). Adult subventricular zone neuronal precursors continue to proliferate and migrate in the absence of the olfactory bulb. *J Neurosci* **19**, 2171-80.

- Klein, C., Bueler, H. and Mulligan, R. C.** (2000). Comparative analysis of genetically modified dendritic cells and tumor cells as therapeutic cancer vaccines. *J Exp Med* **191**, 1699-708.
- Korenberg, J. R.** (1991). Down syndrome phenotypic mapping. *Prog Clin Biol Res* **373**, 43-52.
- Kosaka, K., Toida, K., Aika, Y. and Kosaka, T.** (1998). How simple is the organization of the olfactory glomerulus?: the heterogeneity of so-called periglomerular cells. *Neurosci Res* **30**, 101-10.
- Kosaka, T., Hataguchi, Y., Hama, K., Nagatsu, I. and Wu, J. Y.** (1985). Coexistence of immunoreactivities for glutamate decarboxylase and tyrosine hydroxylase in some neurons in the periglomerular region of the rat main olfactory bulb: possible coexistence of gamma-aminobutyric acid (GABA) and dopamine. *Brain Res* **343**, 166-71.
- Laird, P. W., Zijderveld, A., Linders, K., Rudnicki, M. A., Jaenisch, R. and Berns, A.** (1991). Simplified mammalian DNA isolation procedure. *Nucleic Acids Res* **19**, 4293.
- Leavitt, B. R., Hearn-Grant, C. S. and Macklis, J. D.** (1999). Mature astrocytes transform into transitional radial glia within adult mouse neocortex that supports directed migration of transplanted immature neurons. *Exp Neurol* **157**, 43-57.
- Lee, S. K., Lee, B., Ruiz, E. C. and Pfaff, S. L.** (2005). Olig2 and Ngn2 function in opposition to modulate gene expression in motor neuron progenitor cells. *Genes Dev* **19**, 282-94.
- Levison, S. W. and Goldman, J. E.** (1993). Both oligodendrocytes and astrocytes develop from progenitors in the subventricular zone of postnatal rat forebrain. *Neuron* **10**, 201-12.
- Li, X. K., Guo, A. C. and Zuo, P. P.** (2003). Survival and differentiation of transplanted neural stem cells in mice brain with MPTP-induced Parkinson disease. *Acta Pharmacol Sin* **24**, 1192-8.
- Lillien, L.** (1997). Neural development: instructions for neural diversity. *Curr Biol* **7**, R168-71.
- Lim, D. A., Tramontin, A. D., Trevejo, J. M., Herrera, D. G., Garcia-Verdugo, J. M. and Alvarez-Buylla, A.** (2000). Noggin antagonizes BMP signaling to create a niche for adult neurogenesis. *Neuron* **28**, 713-26.
- Lo, L., Tiveron, M. C. and Anderson, D. J.** (1998). MASH1 activates expression of the paired homeodomain transcription factor Phox2a, and couples pan-neuronal and subtype-specific components of autonomic neuronal identity. *Development* **125**, 609-20.
- Lois, C. and Alvarez-Buylla, A.** (1994). Long-distance neuronal migration in the adult mammalian brain. *Science* **264**, 1145-8.
- Lu, Q. R., Cai, L., Rowitch, D., Cepko, C. L. and Stiles, C. D.** (2001). Ectopic expression of Olig1 promotes oligodendrocyte formation and reduces neuronal survival in developing mouse cortex. *Nat Neurosci* **4**, 973-4.
- Lu, Q. R., Sun, T., Zhu, Z., Ma, N., Garcia, M., Stiles, C. D. and Rowitch, D. H.** (2002). Common developmental requirement for Olig function indicates a motor neuron/oligodendrocyte connection. *Cell* **109**, 75-86.
- Luskin, M. B.** (1993). Restricted proliferation and migration of postnatally generated neurons derived from the forebrain subventricular zone. *Neuron* **11**, 173-89.

- Luskin, M. B., Parnavelas, J. G. and Barfield, J. A.** (1993). Neurons, astrocytes, and oligodendrocytes of the rat cerebral cortex originate from separate progenitor cells: an ultrastructural analysis of clonally related cells. *J Neurosci* **13**, 1730-50.
- Luskin, M. B., Pearlman, A. L. and Sanes, J. R.** (1988). Cell lineage in the cerebral cortex of the mouse studied in vivo and in vitro with a recombinant retrovirus. *Neuron* **1**, 635-47.
- Mabie, P. C., Mehler, M. F., Marmur, R., Papavasiliou, A., Song, Q. and Kessler, J. A.** (1997). Bone morphogenetic proteins induce astroglial differentiation of oligodendroglial-astroglial progenitor cells. *J Neurosci* **17**, 4112-20.
- Magavi, S. S., Leavitt, B. R. and Macklis, J. D.** (2000). Induction of neurogenesis in the neocortex of adult mice. *Nature* **405**, 951-5.
- Malatesta, P., Hack, M. A., Hartfuss, E., Kettenmann, H., Klinkert, W., Kirchhoff, F. and Götz, M.** (2003). Neuronal or glial progeny: regional differences in radial glia fate. *Neuron* **37**, 751-64.
- Malatesta, P., Hartfuss, E. and Götz, M.** (2000). Isolation of radial glial cells by fluorescent-activated cell sorting reveals a neuronal lineage. *Development* **127**, 5253-63.
- Mallamaci, A., Muzio, L., Chan, C. H., Parnavelas, J. and Boncinelli, E.** (2000). Area identity shifts in the early cerebral cortex of *Emx2*^{-/-} mutant mice. *Nat Neurosci* **3**, 679-86.
- Maric, D., Maric, I., Chang, Y. H. and Barker, J. L.** (2000). Stereotypical physiological properties emerge during early neuronal and glial lineage development in the embryonic rat neocortex. *Cereb Cortex* **10**, 729-47.
- Maric, D., Maric, I., Chang, Y. H. and Barker, J. L.** (2003). Prospective cell sorting of embryonic rat neural stem cells and neuronal and glial progenitors reveals selective effects of basic fibroblast growth factor and epidermal growth factor on self-renewal and differentiation. *J Neurosci* **23**, 240-51.
- Marshall, C. A., Suzuki, S. O. and Goldman, J. E.** (2003). Gliogenic and neurogenic progenitors of the subventricular zone: who are they, where did they come from, and where are they going? *Glia* **43**, 52-61.
- Martha, A., Strong, L. C., Ferrell, R. E. and Saunders, G. F.** (1995). Three novel aniridia mutations in the human PAX6 gene. *Hum Mutat* **6**, 44-9.
- Mayer-Proschel, M., Kalyani, A. J., Mujtaba, T. and Rao, M. S.** (1997). Isolation of lineage-restricted neuronal precursors from multipotent neuroepithelial stem cells. *Neuron* **19**, 773-85.
- McCarthy, M., Auger, D. and Whitemore, S. R.** (2000). Human cytomegalovirus causes productive infection and neuronal injury in differentiating fetal human central nervous system neuroepithelial precursor cells. *J Hum Virol* **3**, 215-28.
- McConnell, S. K. and Kaznowski, C. E.** (1991). Cell cycle dependence of laminar determination in developing neocortex. *Science* **254**, 282-5.
- McMahon, S. S. and McDermott, K. W.** (2001). Proliferation and migration of glial precursor cells in the developing rat spinal cord. *J Neurocytol* **30**, 821-8.
- Mehler, M. F., Mabie, P. C., Zhu, G., Gokhan, S. and Kessler, J. A.** (2000). Developmental changes in progenitor cell responsiveness to bone morphogenetic proteins differentially modulate progressive CNS lineage fate. *Dev Neurosci* **22**, 74-85.

- Menezes, J. R., Smith, C. M., Nelson, K. C. and Luskin, M. B.** (1995). The division of neuronal progenitor cells during migration in the neonatal mammalian forebrain. *Mol Cell Neurosci* **6**, 496-508.
- Merkle, F. T., Tramontin, A. D., Garcia-Verdugo, J. M. and Alvarez-Buylla, A.** (2004). Radial glia give rise to adult neural stem cells in the subventricular zone. *Proc Natl Acad Sci U S A*.
- Meyers, E. N., Lewandoski, M. and Martin, G. R.** (1998). An Fgf8 mutant allelic series generated by Cre- and Flp-mediated recombination. *Nat Genet* **18**, 136-41.
- Miyata, T., Kawaguchi, A., Okano, H. and Ogawa, M.** (2001). Asymmetric inheritance of radial glial fibers by cortical neurons. *Neuron* **31**, 727-41.
- Miyata, T., Kawaguchi, A., Saito, K., Kawano, M., Muto, T. and Ogawa, M.** (2004). Asymmetric production of surface-dividing and non-surface-dividing cortical progenitor cells. *Development* **131**, 3133-45.
- Mizuguchi, R., Sugimori, M., Takebayashi, H., Kosako, H., Nagao, M., Yoshida, S., Nabeshima, Y., Shimamura, K. and Nakafuku, M.** (2001). Combinatorial roles of olig2 and neurogenin2 in the coordinated induction of pan-neuronal and subtype-specific properties of motoneurons. *Neuron* **31**, 757-71.
- Molofsky, A. V., Pardal, R., Iwashita, T., Park, I. K., Clarke, M. F. and Morrison, S. J.** (2003). Bmi-1 dependence distinguishes neural stem cell self-renewal from progenitor proliferation. *Nature* **425**, 962-7.
- Morrison, S. J., Perez, S. E., Qiao, Z., Verdi, J. M., Hicks, C., Weinmaster, G. and Anderson, D. J.** (2000). Transient Notch activation initiates an irreversible switch from neurogenesis to gliogenesis by neural crest stem cells. *Cell* **101**, 499-510.
- Morshead, C. M., Garcia, A. D., Sofroniew, M. V. and Van Der Kooy, D.** (2003). The ablation of glial fibrillary acidic protein-positive cells from the adult central nervous system results in the loss of forebrain neural stem cells but not retinal stem cells. *Eur J Neurosci* **18**, 76-84.
- Murray, K., Calaora, V., Rottkamp, C., Guicherit, O. and Dubois-Dalcq, M.** (2002). Sonic hedgehog is a potent inducer of rat oligodendrocyte development from cortical precursors in vitro. *Mol Cell Neurosci* **19**, 320-32.
- Muzio, L., DiBenedetto, B., Stoykova, A., Boncinelli, E., Gruss, P. and Mallamaci, A.** (2002). Emx2 and Pax6 control regionalization of the pre-neuronogenic cortical primordium. *Cereb Cortex* **12**, 129-39.
- Nakamura, Y., Sakakibara, S., Miyata, T., Ogawa, M., Shimazaki, T., Weiss, S., Kageyama, R. and Okano, H.** (2000). The bHLH gene *hes1* as a repressor of the neuronal commitment of CNS stem cells. *J Neurosci* **20**, 283-93.
- Nakashima, K., Takizawa, T., Ochiai, W., Yanagisawa, M., Hisatsune, T., Nakafuku, M., Miyazono, K., Kishimoto, T., Kageyama, R. and Taga, T.** (2001). BMP2-mediated alteration in the developmental pathway of fetal mouse brain cells from neurogenesis to astrocytogenesis. *Proc Natl Acad Sci U S A* **98**, 5868-73.
- Noctor, S. C., Flint, A. C., Weissman, T. A., Dammerman, R. S. and Kriegstein, A. R.** (2001). Neurons derived from radial glial cells establish radial units in neocortex. *Nature* **409**, 714-20.
- Noctor, S. C., Flint, A. C., Weissman, T. A., Wong, W. S., Clinton, B. K. and Kriegstein, A. R.** (2002). Dividing precursor cells of the embryonic cortical ventricular

zone have morphological and molecular characteristics of radial glia. *J Neurosci* **22**, 3161-73.

Noctor, S. C., Martinez-Cerdeno, V., Ivic, L. and Kriegstein, A. R. (2004). Cortical neurons arise in symmetric and asymmetric division zones and migrate through specific phases. *Nat Neurosci* **7**, 136-44.

Nolte, C., Matyash, M., Pivneva, T., Schipke, C. G., Ohlemeyer, C., Hanisch, U. K., Kirchhoff, F. and Kettenmann, H. (2001). GFAP promoter-controlled EGFP-expressing transgenic mice: a tool to visualize astrocytes and astrogliosis in living brain tissue. *Glia* **33**, 72-86.

Nosaka, T., Kawashima, T., Misawa, K., Ikuta, K., Mui, A. L. and Kitamura, T. (1999). STAT5 as a molecular regulator of proliferation, differentiation and apoptosis in hematopoietic cells. *Embo J* **18**, 4754-65.

Novitch, B. G., Chen, A. I. and Jessell, T. M. (2001). Coordinate regulation of motor neuron subtype identity and pan-neuronal properties by the bHLH repressor Olig2. *Neuron* **31**, 773-89.

Novitch, B. G., Wichterle, H., Jessell, T. M. and Sockanathan, S. (2003). A requirement for retinoic acid-mediated transcriptional activation in ventral neural patterning and motor neuron specification. *Neuron* **40**, 81-95.

Nowakowski, R. S., Lewin, S. B. and Miller, M. W. (1989). Bromodeoxyuridine immunohistochemical determination of the lengths of the cell cycle and the DNA-synthetic phase for an anatomically defined population. *J Neurocytol* **18**, 311-8.

Olsson, M., Bjorklund, A. and Campbell, K. (1998). Early specification of striatal projection neurons and interneuronal subtypes in the lateral and medial ganglionic eminence. *Neuroscience* **84**, 867-876.

Olsson, M., Campbell, K., Wictorin, K. and Bjorklund, A. (1995). Projection neurons in fetal striatal transplants are predominantly derived from the lateral ganglionic eminence. *Neuroscience* **69**, 1169-82.

Ory, D. S., Neugeboren, B. A. and Mulligan, R. C. (1996). A stable human-derived packaging cell line for production of high titer retrovirus/vesicular stomatitis virus G pseudotypes. *Proc Natl Acad Sci U S A* **93**, 11400-6.

Ostenfeld, T., Joly, E., Tai, Y. T., Peters, A., Caldwell, M., Jauniaux, E. and Svendsen, C. N. (2002). Regional specification of rodent and human neurospheres. *Brain Res Dev Brain Res* **134**, 43-55.

Park, H. C. and Appel, B. (2003). Delta-Notch signaling regulates oligodendrocyte specification. *Development* **130**, 3747-55.

Parmar, M., Skogh, C., Bjorklund, A. and Campbell, K. (2002). Regional specification of neurosphere cultures derived from subregions of the embryonic telencephalon. *Mol Cell Neurosci* **21**, 645-56.

Parnavelas, J. G. (1999). Glial cell lineages in the rat cerebral cortex. *Exp Neurol* **156**, 418-29.

Parras, C. M., Galli, R., Britz, O., Soares, S., Galichet, C., Battiste, J., Johnson, J. E., Nakafuku, M., Vescovi, A. and Guillemot, F. (2004). Mash1 specifies neurons and oligodendrocytes in the postnatal brain. *Embo J* **23**, 4495-505.

Pear, W. S., Nolan, G. P., Scott, M. L. and Baltimore, D. (1993). Production of high-titer helper-free retroviruses by transient transfection. *Proc Natl Acad Sci U S A* **90**, 8392-6.

- Peterson, A. J., Kyba, M., Bornemann, D., Morgan, K., Brock, H. W. and Simon, J.** (1997). A domain shared by the Polycomb group proteins Scm and ph mediates heterotypic and homotypic interactions. *Mol Cell Biol* **17**, 6683-92.
- Petreanu, L. and Alvarez-Buylla, A.** (2002). Maturation and death of adult-born olfactory bulb granule neurons: role of olfaction. *J Neurosci* **22**, 6106-13.
- Pfeifer, A., Ikawa, M., Dayn, Y. and Verma, I. M.** (2002). Transgenesis by lentiviral vectors: lack of gene silencing in mammalian embryonic stem cells and preimplantation embryos. *Proc Natl Acad Sci U S A* **99**, 2140-5.
- Picard-Riera, N., Decker, L., Delarasse, C., Goude, K., Nait-Oumesmar, B., Liblau, R., Pham-Dinh, D. and Evercooren, A. B.** (2002). Experimental autoimmune encephalomyelitis mobilizes neural progenitors from the subventricular zone to undergo oligodendrogenesis in adult mice. *Proc Natl Acad Sci U S A* **99**, 13211-6.
- Plachta, N., Bibel, M., Tucker, K. L. and Barde, Y. A.** (2004). Developmental potential of defined neural progenitors derived from mouse embryonic stem cells. *Development* **131**, 5449-56.
- Porteus, M. H., Bulfone, A., Liu, J. K., Puelles, L., Lo, L. C. and Rubenstein, J. L.** (1994). DLX-2, MASH-1, and MAP-2 expression and bromodeoxyuridine incorporation define molecularly distinct cell populations in the embryonic mouse forebrain. *J Neurosci* **14**, 6370-83.
- Price, J.** (1987). Retroviruses and the study of cell lineage. *Development* **101**, 409-19.
- Price, J. and Thurlow, L.** (1988). Cell lineage in the rat cerebral cortex: a study using retroviral-mediated gene transfer. *Development* **104**, 473-82.
- Qian, X., Davis, A. A., Goderie, S. K. and Temple, S.** (1997). FGF2 concentration regulates the generation of neurons and glia from multipotent cortical stem cells. *Neuron* **18**, 81-93.
- Qian, X., Goderie, S. K., Shen, Q., Stern, J. H. and Temple, S.** (1998). Intrinsic programs of patterned cell lineages in isolated vertebrate CNS ventricular zone cells. *Development* **125**, 3143-52.
- Rakic, P.** (1985). Limits of neurogenesis in primates. *Science* **227**, 1054-6.
- Ramalho-Santos, M., Yoon, S., Matsuzaki, Y., Mulligan, R. C. and Melton, D. A.** (2002). "Stemness": transcriptional profiling of embryonic and adult stem cells. *Science* **298**, 597-600.
- Rao, M. S. and Mayer-Proschel, M.** (1997). Glial-restricted precursors are derived from multipotent neuroepithelial stem cells. *Dev Biol* **188**, 48-63.
- Reid, C. B. and Walsh, C. A.** (2002). Evidence of common progenitors and patterns of dispersion in rat striatum and cerebral cortex. *J Neurosci* **22**, 4002-14.
- Reynolds, B. A., Tetzlaff, W. and Weiss, S.** (1992). A multipotent EGF-responsive striatal embryonic progenitor cell produces neurons and astrocytes. *J Neurosci* **12**, 4565-74.
- Reynolds, B. A. and Weiss, S.** (1992). Generation of neurons and astrocytes from isolated cells of the adult mammalian central nervous system. *Science* **255**, 1707-10.
- Reynolds, B. A. and Weiss, S.** (1996). Clonal and population analyses demonstrate that an EGF-responsive mammalian embryonic CNS precursor is a stem cell. *Dev Biol* **175**, 1-13.

- Richardson, W. D., Pringle, N. P., Yu, W. P. and Hall, A. C.** (1997). Origins of spinal cord oligodendrocytes: possible developmental and evolutionary relationships with motor neurons. *Dev Neurosci* **19**, 58-68.
- Richardson, W. D., Smith, H. K., Sun, T., Pringle, N. P., Hall, A. and Woodruff, R.** (2000). Oligodendrocyte lineage and the motor neuron connection. *Glia* **29**, 136-42.
- Rowitch, D. H., Lu, Q. R., Kessler, N. and Richardson, W. D.** (2002). An 'oligarchy' rules neural development. *Trends Neurosci* **25**, 417-22.
- Rubenstein, J. L. and Puelles, L.** (1994). Homeobox gene expression during development of the vertebrate brain. *Curr Top Dev Biol* **29**, 1-63.
- Sadowski, I., Ma, J., Triezenberg, S. and Ptashne, M.** (1988). GAL4-VP16 is an unusually potent transcriptional activator. *Nature* **335**, 563-4.
- Saghatelian, A., de Chevigny, A., Schachner, M. and Lledo, P. M.** (2004). Tenascin-R mediates activity-dependent recruitment of neuroblasts in the adult mouse forebrain. *Nat Neurosci* **7**, 347-56.
- Sanai, N., Tramontin, A. D., Quinones-Hinojosa, A., Barbaro, N. M., Gupta, N., Kunwar, S., Lawton, M. T., McDermott, M. W., Parsa, A. T., Manuel-Garcia Verdugo, J. et al.** (2004). Unique astrocyte ribbon in adult human brain contains neural stem cells but lacks chain migration. *Nature* **427**, 740-4.
- Santa-Olalla, J., Baizabal, J. M., Fregoso, M., del Carmen Cardenas, M. and Covarrubias, L.** (2003). The in vivo positional identity gene expression code is not preserved in neural stem cells grown in culture. *Eur J Neurosci* **18**, 1073-84.
- Sawamoto, K., Nakao, N., Kakishita, K., Ogawa, Y., Toyama, Y., Yamamoto, A., Yamaguchi, M., Mori, K., Goldman, S. A., Itakura, T. et al.** (2001). Generation of dopaminergic neurons in the adult brain from mesencephalic precursor cells labeled with a nestin-GFP transgene. *J Neurosci* **21**, 3895-903.
- Scardigli, R., Baumer, N., Gruss, P., Guillemot, F. and Le Roux, I.** (2003). Direct and concentration-dependent regulation of the proneural gene Neurogenin2 by Pax6. *Development* **130**, 3269-81.
- Schmahl, W., Knoedlseder, M., Favor, J. and Davidson, D.** (1993). Defects of neuronal migration and the pathogenesis of cortical malformations are associated with Small eye (Sey) in the mouse, a point mutation at the Pax-6-locus. *Acta Neuropathol (Berl)* **86**, 126-35.
- Seri, B., Garcia-Verdugo, J. M., Collado-Morente, L., McEwen, B. S. and Alvarez-Buylla, A.** (2004). Cell types, lineage, and architecture of the germinal zone in the adult dentate gyrus. *J Comp Neurol* **478**, 359-78.
- Seri, B., Garcia-Verdugo, J. M., McEwen, B. S. and Alvarez-Buylla, A.** (2001). Astrocytes give rise to new neurons in the adult mammalian hippocampus. *J Neurosci* **21**, 7153-60.
- Shi, Y., Chichung Lie, D., Taupin, P., Nakashima, K., Ray, J., Yu, R. T., Gage, F. H. and Evans, R. M.** (2004). Expression and function of orphan nuclear receptor TLX in adult neural stem cells. *Nature* **427**, 78-83.
- Smart, I. H.** (1976). A pilot study of cell production by the ganglionic eminences of the developing mouse brain. *J Anat* **121**, 71-84.
- Smith, C. M. and Luskin, M. B.** (1998). Cell cycle length of olfactory bulb neuronal progenitors in the rostral migratory stream. *Dev Dyn* **213**, 220-7.

- Sockanathan, S., Perlmann, T. and Jessell, T. M.** (2003). Retinoid receptor signaling in postmitotic motor neurons regulates rostrocaudal positional identity and axonal projection pattern. *Neuron* **40**, 97-111.
- Song, H., Stevens, C. F. and Gage, F. H.** (2002). Astroglia induce neurogenesis from adult neural stem cells. *Nature* **417**, 39-44.
- Stenman, J., Toresson, H. and Campbell, K.** (2003). Identification of two distinct progenitor populations in the lateral ganglionic eminence: implications for striatal and olfactory bulb neurogenesis. *J Neurosci* **23**, 167-74.
- Stolt, C. C., Lommes, P., Sock, E., Chaboissier, M. C., Schedl, A. and Wegner, M.** (2003). The Sox9 transcription factor determines glial fate choice in the developing spinal cord. *Genes Dev* **17**, 1677-89.
- Stoykova, A., Götz, M., Gruss, P. and Price, J.** (1997). Pax6-dependent regulation of adhesive patterning, R-cadherin expression and boundary formation in developing forebrain. *Development* **124**, 3765-77.
- Stoykova, A., Hatano, O., Gruss, P. and Götz, M.** (2003). Increase in reelin-positive cells in the marginal zone of Pax6 mutant mouse cortex. *Cereb Cortex* **13**, 560-71.
- Stoykova, A., Treichel, D., Hallonet, M. and Gruss, P.** (2000). Pax6 modulates the dorsoventral patterning of the mammalian telencephalon. *J Neurosci* **20**, 8042-50.
- Stump, G., Durrer, A., Klein, A. L., Lutolf, S., Suter, U. and Taylor, V.** (2002). Notch1 and its ligands Delta-like and Jagged are expressed and active in distinct cell populations in the postnatal mouse brain. *Mech Dev* **114**, 153-9.
- Suzuki, M. and Mizuno, A.** (2004). A novel human Cl(-) channel family related to Drosophila flightless locus. *J Biol Chem* **279**, 22461-8.
- Swartz, M., Eberhart, J., Mastick, G. S. and Krull, C. E.** (2001a). Sparking new frontiers: using in vivo electroporation for genetic manipulations. *Dev Biol* **233**, 13-21.
- Swartz, M. E., Eberhart, J., Pasquale, E. B. and Krull, C. E.** (2001b). EphA4/ephrin-A5 interactions in muscle precursor cell migration in the avian forelimb. *Development* **128**, 4669-80.
- Takebayashi, H., Yoshida, S., Sugimori, M., Kosako, H., Kominami, R., Nakafuku, M. and Nabeshima, Y.** (2000). Dynamic expression of basic helix-loop-helix Olig family members: implication of Olig2 in neuron and oligodendrocyte differentiation and identification of a new member, Olig3. *Mech Dev* **99**, 143-8.
- Tamamaki, N., Nakamura, K., Okamoto, K. and Kaneko, T.** (2001). Radial glia is a progenitor of neocortical neurons in the developing cerebral cortex. *Neurosci Res* **41**, 51-60.
- Tanigaki, K., Nogaki, F., Takahashi, J., Tashiro, K., Kurooka, H. and Honjo, T.** (2001). Notch1 and Notch3 instructively restrict bFGF-responsive multipotent neural progenitor cells to an astroglial fate. *Neuron* **29**, 45-55.
- Tekki-Kessarlis, N., Woodruff, R., Hall, A. C., Gaffield, W., Kimura, S., Stiles, C. D., Rowitch, D. H. and Richardson, W. D.** (2001). Hedgehog-dependent oligodendrocyte lineage specification in the telencephalon. *Development* **128**, 2545-54.
- Toresson, H. and Campbell, K.** (2001). A role for Gsh1 in the developing striatum and olfactory bulb of Gsh2 mutant mice. *Development* **128**, 4769-4780.
- Toresson, H., Mata de Urquiza, A., Fagerstrom, C., Perlmann, T. and Campbell, K.** (1999). Retinoids are produced by glia in the lateral ganglionic eminence and regulate striatal neuron differentiation. *Development* **126**, 1317-1326.

- Toresson, H., Potter, S. S. and Campbell, K.** (2000). Genetic control of dorsal-ventral identity in the telencephalon: opposing roles for Pax6 and Gsh2. *Development* **127**, 4361-71.
- Tramontin, A. D., Garcia-Verdugo, J. M., Lim, D. A. and Alvarez-Buylla, A.** (2003). Postnatal development of radial glia and the ventricular zone (VZ): a continuum of the neural stem cell compartment. *Cereb Cortex* **13**, 580-7.
- Turner, D. L. and Cepko, C. L.** (1987). A common progenitor for neurons and glia persists in rat retina late in development. *Nature* **328**, 131-6.
- Veerkamp, J. H. and Zimmerman, A. W.** (2001). Fatty acid-binding proteins of nervous tissue. *J Mol Neurosci* **16**, 133-42; discussion 151-7.
- Vitalis, T., Cases, O., Engelkamp, D., Verney, C. and Price, D. J.** (2000). Defect of tyrosine hydroxylase-immunoreactive neurons in the brains of mice lacking the transcription factor Pax6. *J Neurosci* **20**, 6501-16.
- Wagner, J., Akerud, P., Castro, D. S., Holm, P. C., Canals, J. M., Snyder, E. Y., Perlmann, T. and Arenas, E.** (1999). Induction of a midbrain dopaminergic phenotype in Nurr1-overexpressing neural stem cells by type 1 astrocytes. *Nat Biotechnol* **17**, 653-9.
- Walsh, C. and Cepko, C. L.** (1993). Clonal dispersion in proliferative layers of developing cerebral cortex. *Nature* **362**, 632-5.
- Wang, S., Sdrulla, A. D., diSibio, G., Bush, G., Nofziger, D., Hicks, C., Weinmaster, G. and Barres, B. A.** (1998a). Notch receptor activation inhibits oligodendrocyte differentiation. *Neuron* **21**, 63-75.
- Wang, S., Wu, H., Jiang, J., Delohery, T. M., Isdell, F. and Goldman, S. A.** (1998b). Isolation of neuronal precursors by sorting embryonic forebrain transfected with GFP regulated by the T alpha 1 tubulin promoter. *Nat Biotechnol* **16**, 196-201.
- Wichterle, H., Garcia-Verdugo, J. M. and Alvarez-Buylla, A.** (1997). Direct evidence for homotypic, glia-independent neuronal migration. *Neuron* **18**, 779-91.
- Williams, B. P. and Price, J.** (1995). Evidence for multiple precursor cell types in the embryonic rat cerebral cortex. *Neuron* **14**, 1181-8.
- Williams, B. P., Read, J. and Price, J.** (1991). The generation of neurons and oligodendrocytes from a common precursor cell. *Neuron* **7**, 685-93.
- Winkler, C., Fricker, R. A., Gates, M. A., Olsson, M., Hammang, J. P., Carpenter, M. K. and Bjorklund, A.** (1998). Incorporation and glial differentiation of mouse EGF-responsive neural progenitor cells after transplantation into the embryonic rat brain. *Mol Cell Neurosci* **11**, 99-116.
- Winner, B., Cooper-Kuhn, C. M., Aigner, R., Winkler, J. and Kuhn, H. G.** (2002). Long-term survival and cell death of newly generated neurons in the adult rat olfactory bulb. *Eur J Neurosci* **16**, 1681-9.
- Xu, Q., de la Cruz, E. and Anderson, S. A.** (2003). Cortical interneuron fate determination: diverse sources for distinct subtypes? *Cereb Cortex* **13**, 670-6.
- Yamamoto, S., Nagao, M., Sugimori, M., Kosako, H., Nakatomi, H., Yamamoto, N., Takebayashi, H., Nabeshima, Y., Kitamura, T., Weinmaster, G. et al.** (2001). Transcription factor expression and Notch-dependent regulation of neural progenitors in the adult rat spinal cord. *J Neurosci* **21**, 9814-23.
- Yamasaki, T., Kawaji, K., Ono, K., Bito, H., Hirano, T., Osumi, N. and Kengaku, M.** (2001). Pax6 regulates granule cell polarization during parallel fiber formation in the developing cerebellum. *Development* **128**, 3133-44.

- Yan, J., Studer, L. and McKay, R. D.** (2001). Ascorbic acid increases the yield of dopaminergic neurons derived from basic fibroblast growth factor expanded mesencephalic precursors. *J Neurochem* **76**, 307-11.
- Yee, J. K., Friedmann, T. and Burns, J. C.** (1994). Generation of high-titer pseudotyped retroviral vectors with very broad host range. *Methods Cell Biol* **43 Pt A**, 99-112.
- Yu, R. T., Chiang, M. Y., Tanabe, T., Kobayashi, M., Yasuda, K., Evans, R. M. and Umesono, K.** (2000). The orphan nuclear receptor Tlx regulates Pax2 and is essential for vision. *Proc Natl Acad Sci U S A* **97**, 2621-5.
- Yun, K., Potter, S. and Rubenstein, J. L.** (2001). Gsh2 and Pax6 play complementary roles in dorsoventral patterning of the mammalian telencephalon. *Development* **128**, 193-205.
- Yung, S. Y., Gokhan, S., Jurcsak, J., Molero, A. E., Abrajano, J. J. and Mehler, M. F.** (2002). Differential modulation of BMP signaling promotes the elaboration of cerebral cortical GABAergic neurons or oligodendrocytes from a common sonic hedgehog-responsive ventral forebrain progenitor species. *Proc Natl Acad Sci U S A* **99**, 16273-8.
- Zerlin, M., Levison, S. W. and Goldman, J. E.** (1995). Early patterns of migration, morphogenesis, and intermediate filament expression of subventricular zone cells in the postnatal rat forebrain. *J Neurosci* **15**, 7238-49.
- Zhang, X. L., Zhang, D., Michel, F. J., Blum, J. L., Simmen, F. A. and Simmen, R. C.** (2003). Selective interactions of Kruppel-like factor 9/basic transcription element-binding protein with progesterone receptor isoforms A and B determine transcriptional activity of progesterone-responsive genes in endometrial epithelial cells. *J Biol Chem* **278**, 21474-82.
- Zhou, Q. and Anderson, D. J.** (2002). The bHLH transcription factors OLIG2 and OLIG1 couple neuronal and glial subtype specification. *Cell* **109**, 61-73.
- Zhou, Q., Choi, G. and Anderson, D. J.** (2001). The bHLH transcription factor Olig2 promotes oligodendrocyte differentiation in collaboration with Nkx2.2. *Neuron* **31**, 791-807.
- Zhuo, L., Sun, B., Zhang, C. L., Fine, A., Chiu, S. Y. and Messing, A.** (1997). Live astrocytes visualized by green fluorescent protein in transgenic mice. *Dev Biol* **187**, 36-42.
- Zinyk, D. L., Mercer, E. H., Harris, E., Anderson, D. J. and Joyner, A. L.** (1998). Fate mapping of the mouse midbrain-hindbrain constriction using a site-specific recombination system. *Curr Biol* **8**, 665-8.

10 ACKNOWLEDGMENTS

I would like to thank to

Magdalena Götz, for supervising me. She made me curious and encouraged me. I thank her for sharing her knowledge, creativity and open ears all the time and for creating a great research environment.

Romy Müller the best HIWI on this planet.

Mucella Öcallan, Annette Bust and Marianne Schellenberger for great technique assistance.

Paolo Malatesta, Julia von Frowein, Nicole Haubst, Eva Hartfuss, Marie-Theres Schmidt, Tetsuji Mori, Luisa Pinto, Dilek Ertürk, Benedikt Berninger, Prathiba Tripathi, and Andrea Wizenmann, Stefan Stricker and for creating a fruitful lab environment.

Richard Lu, Nic Tekki-Kessarlis and Bill Richardson, Dave Owanoghu and Jack Price, Armen Sagathelyan and Pierre-Marie Lledo for the perfect collaboration

Nico Heins for MFF4all, primer design and neurosphere splitting. Philip Grote and Ravi Jagasia for being great roommates.

Silvia Cappello for critical reading of the manuscript and much more

My parents for supporting me during my studies.

11 CURRICULUM VITAE

PERSONAL DETAILS

Name: Michael Anton Hack
Date of birth: 02/06/1975
Place of birth: Rothenburg ob der Tauber, Germany

RESEARCH EXPERIENCE

2001 – present **Ph.D. thesis** in the laboratory of Dr. Magdalena Götz at the Max-Planck-Institute for Neurobiology and at the Institute for Stem Cell Research. *Neuronal fate determinants of adult olfactory bulb neurogenesis*
Ludwig-Maximilian Universität München, Germany

2000 **Diploma thesis** laboratory of Dr. Evan Y. Snyder, at the Children's Hospital, Division of Neuroscience, Department of Neurology, *Differential Gene Expression in Neural Stem Cells under the Influence of Chronic and Acute Brain Lesions*
Harvard Medical School, Boston, MA

EDUCATION

1997-2000 **Diploma in Biotechnology**, Ecole Supérieure Biotechnologie de Strasbourg, Strasbourg, France

1995-1997 **Vordiplom in Biotechnology**,
Technische Universität Stuttgart, Germany

1994 **Abitur**, Goethe Gymnasium, Gaggenau, Germany

PUBLICATIONS

- 1) **Hack, M. A.**, Saghatelyan, A., de Chevigny, A., Lledo, P. M., Götz, M. (2005). Neuronal fate determinants of adult olfactory bulb neurogenesis. (*under revision Nat Neurosci*)
- 2) Koutmani, Y., Hurel, C., Patsavoudi, E., **Hack, M.**, Götz, M., Thomaidou, D. and Matsas, R. (2004). BM88 is an early marker of proliferating precursor cells that will differentiate into the neuronal lineage. *Eur J Neurosci* **20**, 2509-23.
- 3) **Hack, M. A.**, Sugimori, M., Lundberg, C., Nakafuku, M. and Götz, M. (2004). Regionalization and fate specification in neurospheres: the role of Olig2 and Pax6. *Mol Cell Neurosci* **25**, 664-78.
- 4) Hartfuss, E., Forster, E., Bock, H. H., **Hack, M. A.**, LePrince, P., Luque, J. M., Herz, J., Frotscher, M. and Götz, M. (2003). Reelin signaling directly affects radial glia morphology and biochemical maturation. *Development* **130**, 4597-609.
- 5) Malatesta, P., **Hack, M. A.**, Hartfuss, E., Kettenmann, H., Klinkert, W., Kirchhoff, F. and Götz, M. (2003). Neuronal or glial progeny: regional differences in radial glia fate. *Neuron* **37**, 751-64.
- 6) Heins, N., Malatesta, P., Cecconi, F., Nakafuku, M., Tucker, K. L., **Hack, M. A.**, Chapouton, P., Barde, Y. A. and Götz, M. (2002). Glial cells generate neurons: the role of the transcription factor Pax6. *Nat Neurosci* **5**, 308-15.